

# Maternal estrogen controls retinoic acid metabolism and signaling in early vertebrate development

Masanori Nishinaga, Yuh-ichi Onizuka, Takahiro Hanafusa, Kei-ichi Nomiyama, Daisuke Watanabe, Toshifumi Kinashi, Toshiaki Murashige, Munehiro Kunishi, Ryota Hori-e, Yasufumi Hayashida, and Ichiro Yamashita\*

Center for Gene Science, Hiroshima University, Kagamiyama 1-4-2, Higashihiroshima 739-8527, Japan

\*Corresponding author: E-mail: [iyama@hiroshima-u.ac.jp](mailto:iyama@hiroshima-u.ac.jp)

## SUMMARY

Fertilized eggs of lower vertebrates contain substantial amounts of steroidal hormones such as estrogen transferred from mother during oogenesis. However, molecular roles for maternal estrogen in the early embryonic development are largely unknown. Here we show that maternal estrogen and estrogen receptor- $\alpha$  modulate retinoic acid (RA) metabolism and RA-responsive gene expression in medaka embryos. Treatments with excess estradiol, an anti-estrogen (tamoxifen), overexpression or knockdown of estrogen receptor- $\alpha$  (ER $\alpha$ ) resulted in misregulation of RA-related gene expression such as *raldh2* (retinalaldehyde dehydrogenase), *cyp26a1* (RA hydroxylase), *fgf8* (fibroblast growth factor), *rara* (RA receptor- $\alpha$ ), and *ahr1* (aryl hydrocarbon receptor). We propose that maternal estrogen/ER $\alpha$  plays a critical role in the feedback control of *in vivo* level of RA and that it also activates RA signaling for the development of hindbrain and vasculatures. This is the first report demonstrating that maternal estrogen supports successful embryonic development by controlling RA metabolism and signaling in early vertebrate embryos.

**KEY WORD:** maternal estrogen, estrogen receptor, retinoic acid, hindbrain, anterior-posterior axis, vasculogenesis, medakafish

## INTRODUCTION

The early development of all animals must rely on maternal products such as RNA and protein that are loaded into the developing oocyte by the mother and present in the egg at the time of fertilization (Pelegri, 2003). These factors are

encoded by maternal-effect genes which enable the embryonic development including animal-vegetal polarity, egg activation, cleavage, body plan formation, and tissue morphogenesis during early and late embryonic stages and the transition from maternal to zygotic gene expression and translation (Abrams and Mullins, 2009; Li *et al.*, 2010). In addition to the regulatory mRNA and protein, several types of cargo are loaded into oocytes. These include lipoprotein yolk, fat soluble vitamins A and E, retinoids, carotenoids, inorganic phosphate, iron, calcium, magnesium, and other minerals, thyroid hormones, cortisol, and sex hormones such as testosterone and estrogen (Lubzens *et al.*, 2017). The bulk molecular cargo is used as a source of cellular energy and structural components for formation of embryos and larvae. Vitellogenin is the major yolk protein precursor, produced by the liver under regulation by estrogen in maturing females. Vitamin A (retinol), retinoids, and carotenoids are maternal sources of retinoic acid (RA) *de novo* synthesized in the embryos. RA is a well-known morphogen that binds to nuclear receptors for transcription and is essential for many aspects of animal development (Duester, 2008; Maden, 2002; Theodosiou *et al.*, 2010). Maternally derived thyroid hormones and cortisol are deposited in fish egg yolk and accelerate larval organ system differentiation until larvae become capable of endogenous endocrine function (Brown *et al.*, 2014). Absence of maternal thyroid hormones did not affect early specification of the neural epithelia but profoundly modified later dorsal specification of the brain and spinal cord as well as specific neuron differentiation (Camphino *et al.*, 2014).

Estrogen is synthesized in eumetazoan animals from cnidarians (Tarrant, 2005) to vertebrates, and its nuclear receptor acts as a transcriptional regulator in bilaterians (Bertrand *et al.*, 2011; Keay & Thornton, 2009). Estrogen receptor (ER) is widely expressed in different tissue types and is important in vertebrate endocrine systems such as sexual maturation, gestation, and oogonial proliferation and primary growth (Senthilkumaran *et al.*, 2004). Eggs of vertebrate oviparous species such as birds (Groothuis *et al.*, 2005), reptiles (Elf, 2003), amphibians (Fortune, 1983), and fish (Iwamatsu *et al.*, 2005) contain substantial amounts of steroidal hormones such as androgen and estrogen. These steroids are synthesized in the ovary by steroidogenic cells (Senthilkumaran *et al.*, 2004) and are lipophilic, thus, probably deposited in the egg yolk during oogenesis. Fully grown oocytes of medakafish also contain substantial amounts of 17 $\beta$ -estradiol (E2) equivalent to the level in the fluid of the ovarian cavity (Iwamatsu *et al.*, 2005). Although the concentration of E2

declines from the initial level to one-fourth after ovulation, fertilized eggs at one-day post-fertilization (dpf) contain half of the E2 level at fertilization, with the level further decreasing to a basal level by 2 dpf (Iwamatsu *et al.*, 2005) when medaka embryos have organized most of fundamental body architectures (Iwamatsu, 2004). Similar kinetics of the developmental change in yolk steroids have been reported in teleost fish (Paitz *et al.*, 2015) and reptiles (Elf, 2003; Paitz & Bowden, 2009). Recently, there has been increasing interest in the possibility that steroidal hormones deposited in the egg may comprise a major pathway by which mothers influence the embryonic development of their offspring (Elf, 2003; Groothuis *et al.*, 2005). Although exogenous application of gonadal steroids to eggs have been reported to influence a wide range of traits such as sex determination, behavior, growth, morphology, immune function, and survival, physiological significance of maternal steroids in early development remains largely unclear.

We have searched for chemical reagents that induce vascular damages in medaka embryos. We have shown that excess estrogen inhibits vascular formation in wild-type embryos (Kawahara *et al.*, 2000) and that ER $\alpha$ -overproducing transgenic embryos are hyper-sensitive to estrogen, indicating that activation of ER $\alpha$  causes the estrogen-induced vascular defects (Kawamura *et al.*, 2002). We also reported that treatments with the following reagents inhibit the development of common cardinal veins (CCV) on the yolk: excess RA, RA synthesis inhibitor (diethylamino-benzaldehyde, DEAB), retinoid receptor antagonists, agonist ( $\beta$ -naphthoflavone and dioxin) and antagonist ( $\alpha$ -naphthoflavone) for aryl hydrocarbon receptor (AHR) (Hayashida *et al.*, 2004). AHR is a ligand-activated nuclear receptor conserved among vertebrates and commonly known for its role in the adaptive metabolism of xenobiotics and in the toxic events that follow exposure to dioxin (Carney *et al.*, 2006; F.-Salguero *et al.*, 1996; Mimura *et al.*, 1997). On the other hand, AHR is also required for normal mammalian development of liver, peripheral immune system, heart, ovary, and vascular system (McMillan & Bradfield, 2007). We reported in medaka embryos that RA is required for transcriptional activation of a gene (*ahr1*) for AHR (Hayashida *et al.*, 2004; Kawamura & Yamashita, 2002) and that the RA-mediated transcriptional activation of *ahr1* plays a key role in the development of yolk veins (Sada *et al.*, 2019). These studies indicate that accurate regulation of retinoic acid (RA) level and signaling is crucial for normal development of blood vessels.

In this study, we made a new finding that PD98059, a potent and selective inhibitor of MAP kinase kinases, inhibits CCV formation. MAP kinase pathway is a major constituent in FGF (fibroblast growth factor) and VEGF (vascular endothelial growth factor) signaling. FGF signaling plays important roles in many aspects of early vertebrate development (Böttcher & Niehrs, 2005; Dorey & Amaya, 2010), and is known to activate expression of *raldh2* encoding RA-synthesizing enzyme, retinaldehyde dehydrogenase in *Xenopus* (Shiotsugu *et al.*, 2004). VEGF binds to and activates VEGF receptor in angioblasts, and stimulates their proliferation, migration, and survival during vasculogenesis (the formation of blood vessels from *de novo* generation of endothelial cells) and angiogenesis (the process of new blood vessel formation from the pre-existing vessels) (Apte *et al.*, 2019; Olsson *et al.*, 2006). We also found that cyclopamine, an antagonist of hedgehog pathway, inhibits formation of CCV and axial vessels. It has been reported in zebrafish that Sonic hedgehog expression in the notochord triggers expression of VEGF in the somites, high levels of which promote arterial cell fate in endothelial cells (Herbert *et al.* 2009; Lawson, 2002). Williams *et al.* (2010) also reported that *shh* signaling-deficient zebrafish embryos fail to form dorsal aorta. In avian and murine embryos, Sonic hedgehog promotes the assembly of angioblasts into vessel tubes (Byrd and Gabel, 2004; Kolesová *et al.* 2008; Moran *et al.* 2011; Vokes *et al.*, 2004). In the myogenesis of zebrafish embryos, *shh* plays a crucial role for the expression of *myoD* together with *fgf8* and RA (Hamade *et al.*, 2006).

To explore the significance of maternal estrogen in early development, we next investigated synergistic or suppressive effects among estrogen, estrogen antagonist (tamoxifen), RA, RA synthesis inhibitor (DEAB), and MAP kinase pathway inhibitor (PD98059), and also used knockdown of *era1* (ER $\alpha$ ) and *fgf8* (fibroblast growth factor). We conclude that maternal estrogen/ER $\alpha$  is important for feedback control of RA level by modulating expression of *raldh2* (retinaldehyde dehydrogenase), *cyp26a1* (RA hydroxylase), and *fgf8*. The RA-induced feedback mechanism is crucial to successful embryonic development in zebrafish (D.-McAuliffea *et al.*, 2004; White *et al.*, 2007). We also propose that maternal estrogen/ER $\alpha$  in turn acts positively for transcriptional activation of RA-responsive genes such as anterior-posterior hindbrain patterning genes (Campo-Paysaa *et al.*, 2008) and *ahr1* that is essential for vascular formation (Sada *et al.*, 2019).

## **MATERIALS AND METHODS**

### **Fish, embryo, and exposure to reagent.**

We used the d-rR strain of medaka fish, *Oryzias latipes* (Kawahara and Yamashita, 2000). The fish were maintained at 25 – 26°C under artificial photo-period of 14L:10D, and fed by powdered Tetramin (Tetra). Fertilized eggs were collected before 10 hpf, rinsed and immersed in Yamamoto's salt solution (Sada *et al.*, 2019; Yamamoto, 1969). Embryos were treated with reagents starting from 10 hpf unless otherwise indicated, incubated at 25 – 26°C under shading with aluminum foil, and inspected for vascular development under a dissecting microscope at 3 dpf as described (Hayashida *et al.*, 2004) or processed for analysis of mRNA. All reagents were purchased from Sigma-Aldrich except for Ro41-5253 (kindly provided by E.-M. Gutknecht, F. Hoffmann-La Roche Ltd, Basel), PD98059 (Promega or CalBiochem), R115866 (Lieven Meerpoel or Johnson & Johnson), and 4-oxo all-*trans*-RA (Tront Research Chemicals). Reagents were dissolved in dimethyl sulfoxide or ethanol, and stored at –80°C. Stock solutions were diluted over 1,000-fold with Yamamoto's solution before use. The solvents were added to the mock-treated eggs as controls. Experiments were done at least 3 times in which unit samples contained more than 30 or approximately 50 eggs for observation of vascular development or extraction of total RNA, respectively. Percent embryos with vascular damages were presented as average  $\pm$  SD. Statistical significance between values of control and experiment was assessed by Student's *t*-test or *chi*-square test.

### **DAPI staining.**

Embryos were fixed with 4% paraformaldehyde at 4°C for 24 h, transferred into PBS, and dechorionated by forceps. The dechorionated embryos were rinsed twice with PBS, and stained for DNA with 4', 6-diamidino-2-phenylindole (DAPI) (0.5  $\mu$ g/ml) for 5 min under shading with aluminum foil. After washing twice with PBS, the embryos were removed from the yolk and examined under fluorescence microscope.

### **RT-PCR.**

Total RNA was extracted using NucleoSpin kit (Macherey-Nagel) after homogenization of embryos with pellet mixers. RT-PCR analysis was done using Ready-To-Go RT-PCR beads (GE Healthcare) or by two-step reactions, first

with reverse transcriptase (ReverTra Ace, Toyobo) using oligo-dT as a primer and then with DNA polymerase (Ex Taq, Takara). For specific detection of *era1* and antisense-*era1* RNAs, reverse transcription was done with the following primers:

*era1*, 5'-GTAGGAGGTCATAAAGAGGG-3';

antisense-*era1*, 5'-CTTCCGTGTGCTCAAACCTCA-3'.

PCR was done at least 5 times for each RNA sample at optimal and suboptimal cycle numbers with gene-specific primers as follows:

***era1* and antisense-*era1*,**

F 5'-CTTCCGTGTGCTCAAACCTCA-3',

R 5'-GTAGGAGGTCATAAAGAGGG-3'.

Annealing at 60°C for 30 sec, extension at 72°C for 1 min, 320-bp amplified DNA.

Nested PCR for *era1*,

F 5'-CTTCCGTGTGCTCAAACCTCA-3',

R 5'-GAGGGACTTTGTTCTTGAC-3'.

Annealing at 60°C for 30 sec, extension at 72°C for 1 min, 305-bp amplified DNA.

**Choriogenin H,**

F 5'-CGCCATCTACTACTTTCCCG-3',

R 5'-AATTTTGACCCATGATGAAA-3'.

Annealing at 61°C for 1.5 min, extension at 72°C for 1 min, 830-bp amplified DNA.

**Choriogenin L,**

F 5'-ACAATGATGAAGTTCACTGCG-3',

R 5'-CTGCTCCACTGACCTCCTTC-3'.

Annealing at 61°C for 1.5 min, extension at 72°C for 1 min, 1050-bp amplified DNA.

PCR primers for amplification of *ahr1* and  $\beta$ -actin were described previously (Sada *et al.*, 2019). After electrophoresis in agarose gel, amplified DNAs were stained with ethidium bromide and photographed. DNA bands were scanned with GT-9700F scanner (Epson), adjusted using software (Adobe Photoshop Elements 3.0), and analyzed for intensity with Scion Image software. Statistical significance was assessed by Student's *t*-test.

### **Whole-mount *in situ* hybridization.**

Whole-mount *in situ* hybridization was performed essentially as described (Inohaya, 1997). Embryos were treated with cycloheximide (50 or 100 mg/l) for 5

h before fixation in order to enhance *ahr1*, *rara* (at gastrula stage), *raldh2*, and *cyp26a1* mRNAs. If necessary, gastrula-stage embryos were fixed with paraformaldehyde in diluted (x 0.2 or x 0.4) Yamamoto's solution or PBS in order to dissolve yolk material and avoid hybridization background. The resulting transparent embryos need to be handled with care. The cDNAs used as a template for preparation of probes were cloned in the following plasmids: *ahr1* (pOL97 or pOL100); *cyp26a1* (pTM1); *fgf3* (pKN5, provided by T. Czerny); *fgf8* (pKN6, provided by T. Czerny); *hoxa3a* (pOL145); *krox20* (pOL150); *myoD* (pKN1); *no tail* (pKN3, provided by K. Araki); *raldh2* (pOL155); *rara* (pOL151); *rarg1* (pOL167); *shh* (pKN4, provided by K. Araki); *sprouty4* (pKN2, provided by H. Takeda); and *vegfr1* (pOL121 for sense, pOL122 for antisense).

### **Introduction of plasmid DNA and morpholino into embryos.**

Plasmid DNA was introduced into one- to four-cell stage embryos by electroporation as described (Sada *et al.*, 2019) or injected into 1-cell stage embryos as described (Yokoi *et al.*, 2007). Plasmids pOL21 and pOL22 are used for expression of green fluorescent protein (GFP-S65T) and ER $\alpha$  (Kawamura *et al.*, 2002), respectively. Plasmid pOL23 is used for expression of antisense-*era1* RNA from the entire sequence of the *era1* cDNA (Kawahara *et al.*, 2000). Every expression is driven by the medaka  $\beta$ -actin promoter (Hamada *et al.*, 1998). Control morpholino (5'-CCTCTTACCTCAGTTACAATTTATA-3') and *fgf8*-MO (5'-ATAGCTGCATGGCACGGGTCTCATC-3') targeted to the 1st methionine of the medaka *fgf8* gene were obtained from GeneTools (Corvallis, OR) and injected as described previously (Yokoi *et al.*, 2007).

## **RESULTS**

### **Search for chemical reagents that inhibit vascular formation.**

Previously, we reported that exogenously added 17 $\beta$ -estradiol (E2) but not 17 $\alpha$ -estradiol at 10 hpf causes blood aggregates at the blood island, loss of CCV, and edema under the head field at 3 dpf (Kawahara *et al.*, 2000; Kawamura *et al.*, 2002). To analyze when E2 is responsible for these vascular damages during the development, staged embryos were treated with E2 and examined at 3 dpf. Half of the embryos became insensitive to E2 around 15 hpf (Fig. 1A), indicating that E2 affects vascular formation at an early gastrula stage (Iwamatsu, 2004). We also found that E2 causes curved tail at 6 dpf with the same sensitive period as that for vascular damages (Fig. 1A).

To follow the development of CCVs, we visualized angioblasts by *in situ* hybridization using as a probe the medaka cDNA (*vegfr1*) (Hayashida *et al.*, 2004) encoding vascular endothelial growth factor receptor (VEGFR) (Fig. 1B). We observed that E2 inhibited CCV formation on the yolk at 48 hpf in wild-type embryos at high concentration (4 mg/l) but did not at concentrations less than 2 mg/l (not shown). However, CCV did not form in ER $\alpha$ -overproducing transgenic embryos in the presence of an extremely lower concentration of E2 (1  $\mu$ g/l), indicating that hyperactivation of ER $\alpha$  causes loss of CCV. Next, to investigate whether E2 affects the accumulation of angioblasts at the prospective brachial arch (PBA), the earliest known event essential for CCV formation (Sada *et al.*, 2019), we examined angioblasts at both 36 and 48 hpf. E2 did not affect an early appearance of angioblasts at PBA at 36 hpf, but inhibited further accumulation at 48 hpf (Fig. 1C). These results indicate that E2/ER $\alpha$  damages CCV formation by inhibiting accumulation of angioblasts at PBA.

We also reported previously that excess RA causes vascular damages (Hayashida *et al.*, 2004) and loss of CCV, however, does not inhibit the accumulation of angioblasts at PBA (Sada *et al.*, 2019). We here examined the sensitive period to excess RA by treating staged embryos with 9 nM RA followed by *in situ* hybridization of 48-hpf embryos with the *vegfr1* probe. The embryos to which RA was added at or before 25 hpf accumulated angioblasts at PBA but did not form CCV, while they became insensitive to RA around 30 hpf after entering into somite stage (Fig. 2A).

Although exogenously added RA inhibited CCV formation, it is uncertain whether the concentration of excess RA is physiologically relevant. To test this, we used R115866, a specific inhibitor of RA-metabolizing enzyme CYP26 (Hernandez *et al.*, 2007). This drug showed the same defective traits as exogenously added RA such as vascular damages including loss of CCV and malformation of head and body (Fig. 2B). These damages were recovered by co-treatment with the RA synthesis inhibitor DEAB (Fig. 2B). These results indicate that proper control of RA level is essential for early development of medaka embryos.

We newly examined the effect of the MAP kinase pathway inhibitor, PD98059. We investigated the effect of the drug beforehand by analyzing expression of *sprouty4*, a well-known downstream target of FGF signaling (Fürthauer *et al.*, 2001; Yokoi *et al.*, 2007). As expected, the drug well inhibited *sprouty4* expression (Fig. 3A). We then examined the effect of the drug on vessel

formation. The drug caused vascular damages and inhibited CCV formation (Fig. 3B). However, the treated embryos accumulated angioblasts at PBA as in the presence of excess RA (Fig. 3B). The drug also caused curved tails (Fig. 3C), the same developmental defect as that caused by the treatments with E2 (Fig. 1A) and DEAB (Hayashida *et al.*, 2004). In the time-lapse experiment, embryos became insensitive to the drug after entering into the somite stage (Fig. 3D), showing the same sensitive period as that for excess RA.

Finally, we tested whether cyclopamine is effective in medaka embryos. The drug caused vascular damages (Fig. 4A), loss of CCV (Fig. 4B), and curved tails (Fig. 4C), however, did not affect the accumulation of angioblasts at PBA (Fig. 4D). These results suggest that *shh* signaling originating from notochord is important for angioblasts to form CCV on the surface of the yolk.

Next we investigated whether E2 would affect myogenesis, because the curved tail caused by E2 is the same trait as observed in the treatments with DEAB (Hayashida *et al.*, 2004), PD98059, and cyclopamine. These drugs are expected to inhibit *myoD* expression because RA, *fgf8*, and *shh* are required for *myoD* expression in the zebrafish myogenesis (Hamada *et al.*, 2006). We observed that *myoD* is expressed only in somites (Fig. 5A) as reported previously (Yokoi *et al.*, 2007), while, in zebrafish, expressed in both somites and adaxial cells. As expected, RA was required for and activated *myoD* expression (Fig. 5A). PD98059 inhibited *myoD* expression (Fig. 5B) as expected that FGF signaling would be inhibited by the MAP kinase inhibitor. Unexpectedly, cyclopamine also inhibited somitic *myoD* expression (Fig. 5B), while in zebrafish *shh* is required for *myoD* expression in adaxial cells but not in somites. These results represent an additional example of the evolutionary difference in the regulation of myogenesis between medaka and zebrafish. As expected on the basis of defective traits in body axis, E2 inhibited *myoD* expression (Fig. 5C). Furthermore, co-treatment with E2 and DEAB showed a synergistic effect (Fig. 5D), suggesting that the action of E2 is closely related to RA signaling. Another possibility is that E2 affects FGF or *shh* signaling. We then investigated whether E2 affects expressions of *shh* and *no tail*, markers for midline mesoderm or notochord. We observed no effect of E2 on the expression of *shh* during 25 to 48 hpf (Fig. 6A) or of *no tail* during 19 to 48 hpf (Fig. 6B). We also observed no effects of PD98059 and DEAB on *shh* expression at 36 hpf (Fig. 6C). These results indicate that *shh* expression is not a target of these drugs.

### **Synergistic effects.**

To investigate whether E2 affects CCV formation in association with RA and FGF signaling, embryos were treated with every pair of E2, RA, DEAB (RA synthesis inhibitor), and PD98059 (MAP kinase pathway inhibitor). First, we examined the effect of co-treatment with E2 and DEAB at a low concentration that alone show minor effect, resulting in synergistic elevation of per cent embryos with vascular damages (Fig. 7A) including loss of CCV (not shown). These damages persisted during the gastrula stage well beyond the E2-effective blastula stage (Fig. 7B). These results suggest that E2 acts negatively on RA activity. We further examined whether E2 acts through binding to ER $\alpha$ . To test this, we used ER $\alpha$ -overproducing transgenic embryos (Kawamura *et al.*, 2002). The embryos showed significant increase in vascular damages after treating with E2 and DEAB, either alone or together, at concentrations ineffective to wild-type embryos (Fig. 7C). Introduction into wild-type embryos of plasmid DNA expressing ER $\alpha$  under control of  $\beta$ -actin promoter also increased vascular damages in the presence of DEAB (Fig. 7D). These results indicate that hyperactivation of ER $\alpha$  is responsible to the vascular damages.

Next we investigated synergism between PD98059 and DEAB, resulting in gross elevation of vascular damages (Fig. 7E) including loss of CCV (Fig. 7F). Embryos became insensitive to the cotreatment after entering into late gastrula stage (Fig. 7G). The sensitive period was the same as that for the cotreatment of E2 and DEAB, well before the sensitive period for the treatment with PD98059 alone. These results suggest that MAP Kinase acts positively both on RA activity (or signaling) at gastrula stage and for CCV formation at early somite stage.

We also examined the effect of co-treatment of E2 with PD98059, because each alone caused the same developmental defects such as vascular damages and curved tails, resulting in synergistic effects on both traits (Fig. 7H). This result is consistent with the notion that E2 inhibits MAP Kinase pathway. We also speculate that E2 and PD98059 synergistically inhibit RA activity, because both drugs increased the vascular damages in the presence of DEAB, as described above. We then examined whether both drugs would lower the inhibitory activity of ectopic RA. Contrary to our speculation, we observed that both drugs increased vascular damages synergistically with RA (Figs. 7I, K). Embryos co-treated with ineffective concentrations of RA and PD98059 lost CCV but accumulated angioblasts at PBA (Fig. 7J) like those treated alone with excess RA or PD98059. Embryos co-treated with RA and E2 also showed vascular

damages during the gastrula stage (Fig. 7L) like those treated alone with excess RA and PD98059. These results suggest that RA and E2 inhibit MAP kinase pathway.

Finally, we investigated the effect of co-treatment of E2 (2 mg/l) with cyclopamine (2 or 4 mg/l), resulting in no synergistic effect on vascular formation (data not shown), suggesting no functional link between E2 and cyclopamine.

### **Effects of E2 on RA metabolism and signaling.**

We investigated whether E2 affects anterior-posterior patterning of hindbrain that is well known to be controlled by RA in chordate (Campo-Paysaa *et al.*, 2008). As expected for negative control of RA activity, E2-treated embryos showed wider rhombomeres than controls like DEAB-treated ones at 58 hpf (Fig. 8A). Furthermore, we observed synergistic effect on rhombomere width of co-treatment of E2 with DEAB that alone showed no effect (Fig. 8B). E2 (17 $\beta$ -estradiol) but not 17 $\alpha$ -estradiol also caused moderate shift of rhombomere to posterior direction as evident from *krox20* expression in rhombomere (r)-3 and r-5 (Fig. 9A). These results support our conclusion that E2 acts negatively on RA activity.

To verify this, we examined whether E2 affects RA-responsible gene expression such as *rara* (inducible), *raldh2* (repressible), and *rarg1* as a constitutive control (Sada *et al.*, 2019) (Fig. 9A). The regulatory pattern of *rara* and *raldh2* by RA was evident from results of treatment with a RAR antagonist, Ro41-5253: posterior shift of r-3 and r-5; decrease in *rara* expression; and increase in *raldh2* expression. We observed that E2 inhibited *rara* expression but showed no effect on *rarg1*, suggesting that E2 represses *rara* expression directly or indirectly by lowering RA level. Consistent with the latter possibility, E2 repressed expression of *raldh2* encoding RA-synthesizing enzyme. The E2-induced regulation was apparently caused by estrogenic activity of E2 (17 $\beta$ -estradiol), because a chiral isomer, 17 $\alpha$ -estradiol, showed no effect. We also observed synergistic inhibition with E2 and DEAB of *rara* expression and of r-7 to r-8 expression of *hoxa3a* that is RA-inducible (Sada *et al.*, 2019) (marked by open triangle) (Fig. 9B), confirming the inhibitory activity of E2 against RA activity.

To further clarify the suppressive effect of E2 against RA level, staged embryos were treated with E2 and examined at 36 hpf for *rara* expression. Embryos to which E2 was added at or before 19 hpf showed reduced expression

in a slightly posterior region, while there was no effect of E2 after 20 hpf (Fig. 9C). Considering the previous observation (Sada *et al.*, 2019) that expressions of *rara* and *raldh2* increase grossly after 19 hpf (about 60% epiboly), results of the time-lapse experiment suggest that loss of E2 inhibition would be due to increase in *de novo* synthesis of RA. Consistent with this, E2 was effective even at 20 hpf in the presence of minimum concentration of DEAB (Fig. 9B). Furthermore, addition of E2 at 10 hpf reduced expression levels of *rara* in 18-hpf embryos in a concentration-dependent manner (Fig. 9D). Together, these results suggest that E2 inhibits RA synthesis.

Next we investigated whether E2 affects RA metabolism during the gastrula stage by analyzing expression of genes, *raldh2* and *cyp26a1*, encoding RA synthesizing and metabolizing enzymes, respectively. To investigate the effect of E2 on *raldh2* expression, embryos were first treated with E2 or mock-treated at 10 hpf, to which cycloheximide (CHX) was added at 18 hpf to enhance hybridization signal, and fixed at 23 hpf. We observed that E2 reduced *raldh2* expression at the edge of the blastoderm (Fig. 10A) as observed at the somite stage (Fig. 9A). Next, to investigate whether this repression is direct or whether translation of intermediate signals is required, embryos were first treated with CHX at 17 hpf, to which E2 or mock solvent was added at 18 hpf, and fixed at 23 hpf. As shown in Fig. 10B, E2 repressed *raldh2* expression even in the presence of CHX, indicating a direct effect. We also investigated the effect of E2 on *cyp26a1* expression. We observed that E2 increased *cyp26a1* expression at presumptive anterior head (Fig. 10C), while did not in the presence of CHX (Fig. 10D). Therefore, E2 appears to require translation of downstream factors to mediate its effect on *cyp26a1*. Together, these results suggest that addition of excess E2 lowers *in vivo* levels of RA by inhibiting *raldh2* and activating *cyp26a1*, consistent with the observations that E2 caused posterior shift of the rhombomere and reduction in expression of RA-inducible genes such as *rara* and *hoxa3a*.

### **MAP kinase modulates RA metabolism and signaling.**

To investigate whether MAP kinase modulates RA signaling, embryos were treated with increasing concentrations of PD98059 (MEK inhibitor) and analyzed for expressions at 36 hpf of RA-controlled genes, *rara*, *hoxa3a*, and *krox20*. The drug was ineffective at 2 and 5  $\mu$ M, but inhibited *rara* expression moderately at 10  $\mu$ M and to a greater extent at 20  $\mu$ M (Fig. 11A). The highest concentration

caused posterior shift of *krox20* signal and moderate reduction in *hoxa3a* expression at r7 to r8 (Fig. 11A). The drug inhibited *rara* expression synergistically with DEAB (RA synthesis inhibitor) (Fig. 11B). The synergistic inhibition of *rara* expression was evident at an early gastrula stage but reduced at late gastrula stage (Fig. 11C) as observed when vascular damage was examined (Fig. 7G). We also observed that expression of *rara* was inhibited by PD98059 alone at a middle gastrula stage (Fig. 11D). These results support again that MAP Kinase acts positively on RA signaling at gastrula stage.

Next we investigated whether PD98059 affects RA metabolism during the gastrula stage by analyzing expression of *raldh2* and *cyp26a1* after treatment with PD98059 from 10 hpf to 18 or 24 hpf. In the 18-hpf embryos, the drug inhibited *raldh2* expression (Fig. 12A) while activated *cyp26a1* expression with enlarged area of expression but no effect on density (Fig. 12B). We also observed in 24-hpf embryos that the drug expanded *cyp26a1* expression at anterior head and caused delayed gastrulation at tail region (Fig. 12C), consistent with the previous notion that MAP kinases are involved in cell migration during gastrulation (Krens *et al.*, 2008). Together, these results suggest that MAP kinase is required for *in vivo* levels of RA by activating *raldh2* and repressing *cyp26a1*.

Treatment with PD98059 alone caused vascular damages during somite stage (Fig. 3D), while the drug was effective during gastrula stage in the co-treatment with DEAB (Fig. 7G). Previously, we reported that RA is required for CCV formation at gastrula stage by activating expression of *ahr1* at PBA (Sada *et al.*, 2019). Accordingly, we speculated that co-treatment of PD98059 with DEAB caused loss of CCV through inhibition of *ahr1* expression at PBA while PD98059 alone affected CCV formation through another pathway. To test this, *ahr1* expression was investigated after treating embryos with PD98059 in the presence or absence of DEAB. As expected, PD98059 inhibited *ahr1* expression at PBA in the presence of DEAB (Fig. 13A) while alone had no effect (Fig. 13B), further supporting the significance of MAP kinase in the RA signaling.

### **Effects of E2 on FGF expression.**

We first analyzed expression patterns of *fgf3* and *fgf8* during the somite stage when PD98059 causes loss of CCV (Fig. 14A). *fgf3* was expressed at midbrain-hindbrain boundary (MHB) and r-4 throughout the somite stage. During late neurula to 2-somite stage, *fgf8* was mostly expressed at r-2, r-4, and tail bud,

and faintly in adaxial mesoderm at the level of r-2 and r-4. At 4-somite stage and later, *fgf8* was expressed at telencephalon, MHB, and tail bud. These results were essentially the same as those reported previously (Hochmann *et al.*, 2007; Ishikawa *et al.*, 2008).

To investigate whether FGF plays a role in the regulatory pathway of CCV formation that is inhibited by ectopic E2, embryos were treated with E2 and analyzed for *fgf3* and *fgf8* expression (Fig. 14B). There was no effect of E2 on *fgf3* expression except a slight posterior shift at 30 and 36 hpf. Expression level of *fgf8* was not affected by E2 during 19 to 30 hpf, however, clearly diminished specifically in MHB at 36 hpf. To confirm the effect of E2 on *fgf8* expression, we analyzed expression of *sprouty4*, a downstream target of *fgf8*, during 19 to 48 hpf (Fig. 14C). We observed specific inhibition of *sprouty4* at MHB and its posterior adaxial mesoderm (bracket) at 36 hpf. While this inhibition was recovered later at 48 hpf, we observed unexpectedly somitic expression of *sprouty4* (bracket) in the control embryos and its inhibition by E2. Furthermore, we observed that *sprouty4* expression at MHB and posteriorly neighboring adaxial mesoderm was inhibited by E2 in a concentration-dependent manner (Fig. 14D). To investigate whether the negative regulation is mediated by ER $\alpha$ , embryos were injected with plasmid DNA expressing ER $\alpha$ , and analyzed for expressions of *fgf8* at 36 hpf and *myoD* at 44 hpf. Embryos overproducing ER $\alpha$  appeared shorter in body length and showed inhibition of *fgf8* expression at MHB and of *myoD* expression in the somites (Fig. 15). Collectively, these results suggest a role for E2/ER $\alpha$  in the negative regulation of *fgf8* and *myoD*.

### ***fgf8* is required for CCV formation independently of RA signaling.**

Considering that ectopic RA inhibits CCV formation synergistically with either PD98059 or E2, we assumed that excess RA would act through FGF signaling. To investigate this, staged embryos were treated with RA and analyzed for *fgf8* and *sprouty4* expressions at 36 hpf (Fig. 16A). *fgf8* expression was specifically inhibited at MHB in the 10-hpf embryos but not in later embryos. Expression of *sprouty4* was also inhibited at MHB exclusively at 10 hpf, while its expression at adaxial mesoderm and tail bud was inhibited in 10- to 25-hpf and 10- to 20-hpf embryos, respectively (Figs. 16A, B). These results indicate that RA has three target sites with different sensitive period: MHB at 10 hpf, adaxial mesoderm during 10 to 25 hpf, and tail bud during 10 to 20 hpf. The first and second sensitive periods are the same as those for E2 (Fig. 1A) and RA (Figs. 2A, 16B),

respectively, against vascular damages (Hayashida *et al.*, 2004). Collectively, these results suggest that both RA and E2 inhibit CCV formation by decreasing *fgf8* expression at MHB and adaxial mesoderm.

We also examined whether excess RA would affect specific expression of *ahr1* at PBA that is important for accumulation of angioblasts at PBA before CCV formation (Sada *et al.*, 2019). After addition of excess RA at 10 and 18 hpf, expression of *ahr1* was increased throughout the anterior head of malformed embryos, in which there was a mass of *ahr1* expression (gray triangle) at or near the otic vesicle (open triangle) (Fig. 17A). Malformation of head structure was evident from the shorter distance between top of head and otic vesicle (double arrowhead) (Figs. 17A, B). However, there was no effect on *ahr1* expression including the expression at PBA (closed triangle) after addition of RA at 24 hpf that is the time within the second sensitive period (Fig. 17A). These results suggest that *ahr1* is not involved at least quantitatively in vascular damages caused by excess RA.

To verify the significance of *fgf8* in CCV formation and in RA signaling and metabolism, embryos were injected with control-MO or *fgf8*-MO and analyzed by *in situ* hybridization. We first examined the effect of *fgf8*-MO on FGF signaling by analyzing *sprouty4* expression, resulting in moderate or severe reduction in half population each (Fig. 18A). Both type of embryos showed severe malformation of posterior structure, consistent with the somite-less phenotype reported previously (Yokoi *et al.*, 2007). These results suggest that most of the expression at telencephalon, MHB, adaxial mesoderm, and tail bud in the embryos injected with control-MO is under the control of *fgf8*. We next examined CCV formation by visualizing *vegfr1*<sup>+</sup> angioblasts. Embryos injected with *fgf8*-MO showed loss of the CCV with complete structure developing upward to head region, however, there was accumulation of angioblasts at PBA and short vessels formed near the PBA (Fig. 18A), indicating a critical role of *fgf8* in the extension of CCV from PBA to heart lying beneath the head. To investigate the importance of *fgf8* in the RA signaling, expression of RA-inducible genes, *rara* and *ahr1*, was analyzed. Expression of *rara* was reduced in the morpholino-knockdown embryos at 18 and 36 hpf (Fig. 18A), which was lost synergistically by co-treatment with DEAB (Fig. 18B). These results suggest a role of *fgf8* in RA signaling. However, there was no change in *ahr1* expression at PBA (Fig. 18A), suggesting that *ahr1* is not involved in the morpholino-induced vascular damages. This is consistent with the observation that angioblasts accumulated at PBA in the knockdown embryos,

which is required for *ahr1* function (Sada *et al*, 2019). Next, to investigate whether *fgf8* controls RA metabolism, we analyzed expression of RA-synthesizing and -catabolizing genes, *raldh2* and *cyp26a1*, respectively. In the morpholino-knockdown embryos, expression of *raldh2* was reduced, while expression area of *cyp26a1* was expanded with no change in density (Fig. 18A) as reported previously that FGF signaling is necessary and sufficient for the suppression of the anterior gene *cyp26* during gastrulation in zebrafish (Kudoh *et al*, 2002). These results are the same as those in embryos treated with MAP kinase inhibitor PD98059 (Fig. 12), suggesting that *fgf8* raises concentration of RA by activating synthesis and repressing catabolism.

### **Maternal estrogen controls RA-responsive gene expression and vascular formation through binding to ER $\alpha$ .**

To analyze rhombomere formation, embryos were stained with DAPI and examined under fluorescent microscope. We observed that axial width of unit rhombomere was lengthened in DEAB-treated embryos while ectopic RA caused malformation of the brain with posteriorized hindbrain (Fig. 19A), consistent with the established notion that RA controls anterior-posterior (A-P) patterning of hindbrain. To investigate whether maternal estrogen is involved in the A-P patterning, embryos were co-treated with RA and an anti-estrogen, tamoxifen (TAM). The co-treated embryos formed normal size of rhombomere, however, again deformed like RA-treated ones by further addition of E2 that alone caused no effect (Fig. 19A). We further analyzed expression of *krox20*, a marker for r-3 and r-5, resulting in anterior shift by ectopic RA, which was recovered by co-treatment with TAM (Fig. 19B). These results indicate that maternal estrogen is required for posteriorizing activity of RA.

To investigate whether maternal estrogen plays a role in expression of RA-inducible genes, *rara* and *hoxa3a*, embryos were treated with RA in the presence or absence of TAM. We observed that excess RA could not activate expression of *rara* and *hoxa3a* at r-7 to r-8 in the presence of TAM (Fig. 19C), indicating a role for maternal estrogen in the RA-inducible activation. In the time-lapse experiment, embryos activated *rara* expression as estimated by both intensity and area of expression when RA was added before 18 hpf while could not in the presence of TAM (Figs. 19D, E). The short head caused by excess RA was also recovered by co-treatment with TAM (Fig. 19F). These results suggest that TAM was effective at early gastrula stage.

Next, we investigated whether TAM inhibits RA-activation of *rara* expression in the gastrula-stage embryos. Because of low expression, we could not detect a specific signal for *rara* expression in the gastrula-stage embryos according to the conventional method. To enhance signal intensity, embryos were first treated with CHX for 5 h before fixation. We also improved how to exclude background signal in the yolk by fixing embryos in the diluted saline buffer in order to dissolve yolk materials. In this way, we detected clear signal of *rara* expression at dorsal edge of blastoderm in the embryos treated with CHX at 13 and 16 hpf and at midline of the embryonic shield treated with CHX at 19 hpf (50% epiboly) (Fig. 20A). To test the significance of maternal estrogen, embryos were treated with RA in the presence or absence of TAM at 10 hpf, with CHX at 18 hpf, and fixed at 23 hpf. Excess RA activated *rara* expression, while co-treatment with TAM counteracted the effect of RA (Fig. 20B). These results confirm a role for maternal estrogen in the control of RA-inducible gene expression at gastrula stage. We also investigated whether maternal estrogen would directly activate *rara* expression. To test this, embryos were first treated with CHX at 14 or 18 hpf, then with RA in the presence or absence of TAM at 15 or 19 hpf, respectively. In this scheme, RA activated *rara* expression both in the presence and absence of TAM (Fig. 20C). These results suggest that RA activates *rara* expression directly and that maternal estrogen acts indirectly or serves as a specific stabilizer for *rara* mRNA which is exchangeable with CHX.

To confirm the significance of maternal estrogen in RA control of *ahr1* expression at PBA, embryos were treated with RA in the presence or absence of TAM at 18 hpf, with CHX at 48 hpf, and fixed at 53 hpf. Expression of *ahr1* at PBA was increased by RA concomitant with posteriorization of hindbrain (anterior shift of otic vesicle), while recovered to a control level by co-treatment with TAM (Fig. 21). Further addition of E2 again increased *ahr1* expression which occurred concurrently with posteriorization of hindbrain (Fig. 21). These results indicate that maternal estrogen is also required for RA-activation of *ahr1* expression and confirm the role of maternal estrogen in the RA-induced posteriorization of hindbrain.

We further investigated whether maternal estrogen is involved in inhibition of FGF signaling by ectopic RA. We observed that expression of *sprouty4* at MHB and adaxial mesoderm was recovered with TAM from the RA-induced inhibition in the 36-hpf embryos (Fig. 22A). In the time-lapse experiment, in which RA was added at 10 hpf with addition of TAM at the indicated time, *fgf8* expression at

MHB was restored with TAM before 20 hpf (Fig. 22B). These results suggest that maternal estrogen controls *fgf8* expression negatively in concert with RA at early gastrula stage.

Next we examined whether ectopic RA inhibits FGF signaling cooperatively with maternal estrogen in the gastrula-stage embryos. We first examined the effect of high RA concentration on *fgf8* expression by adding 9 nM RA at 10 hpf (Fig. 22C). At blastula/gastrula stage (13 hpf), RA showed no inhibition of *fgf8* expression at dorsal margin of blastoderm. At a middle gastrula stage (19 hpf), *fgf8* is strongly inhibited by RA in the dorsal marginal mesoderm fated to become the tailbud. At late gastrula stage (24 hpf), *fgf8* expression in the presumptive tailbud was separated (marked by arrowhead) because of delay in cell movement and gastrulation as reported previously in *Xenopus* (Sive *et al.*, 1990), while there was no effect in the anterior neural region. To investigate a role of maternal estrogen in the inhibition of *fgf8* expression, embryos were treated with TAM in the presence of RA, resulting in recovery from the RA-induced defects (Fig. 22C). We also observed the same results when *sprouty4* expression was examined (Fig. 22D), confirming that maternal estrogen controls *fgf8* expression negatively in concert with RA at gastrula stage. We also investigated whether the negative control of maternal estrogen is mediated through ER $\alpha$  by analyzing *fgf8* expression at 19 hpf in the ER $\alpha$ -KD embryos. We observed increased expression of *fgf8* (Fig. 22E), indicating that maternal estrogen binds to ER $\alpha$  and represses *fgf8*.

We also investigated whether ectopic RA would directly inhibit *fgf8* expression. To test this, embryos were first treated with CHX at 16 hpf, then with RA at 17 hpf. In this scheme, RA did not inhibit *fgf8* expression (Fig. 22F), indicating an indirect role of the inhibitory activity of RA. We also examined whether RA present in the normal development of embryos would repress *fgf8* expression. To test this, RA synthesis was inhibited by addition of DEAB, then *fgf8* expression was analyzed. We observed no effect of the RA deficiency on the expression of *fgf8* at 19 and 36 hpf (Fig. 22G), indicating that normal level of RA does not control *fgf8*. We further investigated whether increased concentration of endogenous RA would suppress *fgf8* by incubating embryos in the presence of the CYP26 inhibitor (R115866). We observed that the drug inhibited *fgf8* expression at 19 hpf (Fig. 22H). Considering the role of *fgf8* both in activation of *raldh2* and inhibition of *cyp26a1* shown in Fig. 18A, the result

indicates an important role of *fgf8* in the feedback control of *in vivo* RA concentration.

Next we investigated whether maternal estrogen is required for the effect of excess RA on vascular formation. We observed suppression of the RA-induced vascular damages by co-treatment with TAM, which was canceled by further addition of E2 (Fig. 23A). We also observed that the synergistic inhibition of vascular formation by RA and E2 was recovered by TAM (Fig. 23B). These results indicate that maternal estrogen is involved in the ectopic RA-induced inhibition of vascular formation. To investigate the sensitive period for TAM, embryos were incubated in the presence of RA starting from 10 hpf with time-lapse addition of TAM, and analyzed for vascular damages and body axis malformation such as dysgenesis of head and tail. As shown in Fig. 23C, TAM was effective before early gastrula stage, the same one for ectopic E2 (Fig. 1A).

Next, we investigated whether maternal estrogen is required for vascular formation. We found no discernible morphological defects in the embryos treated with TAM at concentrations up to 4 mg/l from 10 hpf to 6 dpf. However, we observed that TAM caused vascular damages including loss of CCV in the presence of low dose of DEAB that alone showed minor effect (Figs. 24A, B). The embryos with vascular damages were apparently normal in other aspects of developments, suggesting that vascular cells are most sensitive to these drugs. The synergistic inhibition was partially rescued by addition of low dose of either RA (Fig. 24C) or E2 (Fig. 24D). These results suggest that maternal estrogen plays a role cooperatively with RA in vascular formation. To investigate when maternal estrogen is required, staged embryos were co-treated with TAM and DEAB, and examined for vascular damages at 3 dpf or *vegfr1*<sup>+</sup> angioblasts at 48 hpf. We also investigated the sensitive period for TAM by incubating embryos in the presence of DEAB starting from 10 hpf with time-lapse addition of TAM (closed square). We observed that embryos passing through middle gastrula stage became insensitive to TAM (Figs. 24E, F), indicating that maternal estrogen is required for vascular formation including CCV before the middle gastrula stage.

To elucidate a role for maternal estrogen in the RA pathway in which RA activates transcription of *ahr1* that is essential for CCV formation (Sada *et al.*, 2019), we analyzed transcript level of *ahr1* by RT-PCR method under the conditions where E2 and TAM interact with RA and DEAB to cause vascular damage synergistically or suppressively. We first observed that co-treatment

with low dose of RA and E2 that alone showed no effect activated *ahr1* expression synergistically (Fig. 25A). Conversely, activation of *ahr1* by high concentration of RA was suppressed by co-treatment with TAM, which was recovered by further addition of E2 (Fig. 25B). We also observed that *ahr1* expression was inhibited synergistically by co-treatment with a low dose of DEAB and TAM (Fig. 25C), which was recovered by addition of RA (Fig. 25D). These results suggest that *ahr1* expression is activated cooperatively by RA and maternal estrogen. Specific expression of *ahr1* at PBA was also abolished synergistically by DEAB and TAM (Fig. 25E) whereas *rara* expression was not (Fig. 25F), indicating that the vascular damages caused by co-treatment with DEAB and TAM are due to loss of *ahr1* expression at PBA.

We then explored whether the action of maternal estrogen is mediated through ER $\alpha$ . We first analyzed transcript levels of ER $\alpha$ -encoding *era1* in RNA samples extracted previously from blastula to somite stage (Sada *et al.*, 2019). *era1* expression was essentially constant during the developmental period, and estimated to be very low because amplified signals were first detectable after the second amplification of the first PCR product (Fig. 26A), consistent with the previous observation that no positive *in situ* signals for *era1* RNA are detectable in the embryos before hatching (Kawamura *et al.*, 2002). Transcription of *era1* is not regulated by RA because RA synthesis inhibitor, DEAB, did not affect *era1* RNA level at the concentration (20  $\mu$ M) (not shown) that completely inhibits the development of vessel and body-axis (Hayashida *et al.*, 2004).

To investigate the effect of overexpression of ER $\alpha$  on *ahr1* expression, we introduced a series of increasing concentrations of a plasmid DNA expressing ER $\alpha$  (*era1* plasmid) (Kawamura *et al.*, 2002) into one- to four-cell stage embryos by the aid of electroporation, and analyzed transcript levels at 36 hpf from *ahr1* as well as genes encoding choriogenins H and L (Lee *et al.*, 2002) as positive controls and  $\beta$ -actin gene as a negative control (Fig. 26B). *ahr1* RNA became more abundant with increasing levels of *era1* RNA expressed from the introduced plasmid. Transcriptions from the choriogenin genes were also activated, while  $\beta$ -actin RNA levels were constant regardless of *era1* RNA levels. The ER $\alpha$ -induced transcriptional activation of *ahr1* and the choriogenin H gene was inhibited by the presence of the anti-estrogen TAM (Fig. 26C). These results indicate that ER $\alpha$  activates transcription of *ahr1* after binding to maternal estrogen present in fertilized eggs.

To investigate the physiological significance of ER $\alpha$  in the transcription of *ahr1* and embryonic development, we first examined whether an antisense-*era1* RNA could knock down the activity of ER $\alpha$  that induces transcriptional activation of the choriogenin gene. We introduced into embryos a dose of *era1* plasmid alone or simultaneously ten-fold dose of a plasmid DNA (antisense-*era1* plasmid) expressing antisense RNA from the entire *era1* cDNA sequence, and analyzed transcript levels of choriogenin H as well as those of  $\beta$ -actin, *era1*, and antisense-*era1* as controls at 36 hpf (Fig. 26D). The antisense RNA inhibited the ER $\alpha$ -induced activation of choriogenin H RNA but did not affect RNA levels of *era1* or  $\beta$ -actin, indicating the specific knockdown of the ER $\alpha$  activity by the antisense-*era1* RNA probably at a translational level.

We then examined whether the knockdown of ER $\alpha$  could affect transcription of *ahr1*. We observed that transcript level from *ahr1* was not altered by the treatment either with the antisense-*era1* plasmid or low dose of DEAB, but significantly reduced exclusively in the embryos treated with the antisense-*era1* plasmid followed by incubation in the presence of DEAB (Fig. 26E). The reduced level of *ahr1* RNA was restored to a control level by introduction of the same dose of *era1* plasmid as that of the antisense-*era1* plasmid (Fig. 26F). These results indicate that ER $\alpha$  is essential for transcription of *ahr1* in cooperation with RA.

We then explored whether the knockdown of ER $\alpha$  could affect vascular development (Fig. 26G). In the embryos into which antisense-*era1* plasmid was introduced followed by incubation in the absence of DEAB, vascular damages were temporarily observed at 3 dpf in small but significant percentage (24%, n=140). These damages were mostly dysgenesis of one of the Cuvierian ducts that crawl on the yolk from both sides of the base of the pectoral fin (Iwamatsu, 2004). The embryos with the vascular damage were almost normal in other aspects of the development including circulation, and regenerated a new Cuvierian duct with the blood clots remaining on the original location of the degenerated duct at 4 dpf (marked by arrow). However, in the presence of DEAB (2  $\mu$ M), the antisense-treated embryos had more severe defects in the vascular development at 3 dpf (50%, n=46) and thereafter. They failed to form yolk veins including the Cuvierian ducts and the vitellocaudal vein (Iwamatsu, 2004) with no circulation, and exhibited blood clots at the blood island (marked by arrowhead). *era1* plasmid suppressed the antisense-*era1*-induced vascular

defects, demonstrating that ER $\alpha$  is essential for vascular development coordinately with RA.

### **Maternal estrogen modulates RA metabolism through binding to ER $\alpha$ .**

Because ectopic E2 reduces *in vivo* level of RA by activating *cyp26a1* and repressing *raldh2*, we investigated a physiological role of maternal estrogen in the regulation of RA metabolism by analyzing the effect of TAM on expressions of *raldh2* and *cyp26a1*. We first examined whether RA controls *raldh2*. RA deficiency caused by DEAB activated *raldh2* while ectopic RA inhibited it (Fig. 27A), indicating a feedback control of *raldh2*. Next we investigated whether maternal estrogen is involved in the negative regulation. We observed that the RA-induced repression was cancelled by addition of TAM both in the 18- and 36-hpf embryos (Fig. 27B, C). Furthermore, DEAB and TAM synergistically relieved *raldh2* of its transcriptional burden (Fig. 27D). These results suggest that maternal estrogen is important for the feedback repression of *raldh2* and exclude the possibility that the TAM-induced derepression of *raldh2* occurs indirectly through *fgf8*, an activator for *raldh2* that is concurrently regulated by RA and maternal estrogen but is unresponsive to DEAB (Fig. 22G). We also examined whether intrinsic excess of RA caused by inhibition of CYP26 represses *raldh2* coordinately with maternal estrogen. As expected, we observed that R115866 repressed *raldh2* which was recovered by addition of TAM (Fig. 27E). To test direct role of RA, experiment was done after addition of CHX. We observed that excess RA repressed *raldh2* in the presence of CHX (Fig. 27F), indicating a direct role of RA. We also observed that the RA-induced repression remained unchanged after co-treatment with TAM (Fig. 27F), suggesting that maternal estrogen acts indirectly or that CHX serves as a specific stabilizer for RA signaling.

Next we examined whether RA controls *cyp26a1*. Ectopic RA as well as R115866-induced accumulation of RA activated *cyp26a1* judging from higher signal intensity and broad expression area, while RA deficiency caused by DEAB inhibited *cyp26a1* (Fig. 28A), indicating a feedback control of *cyp26a1*. We also observed excess RA activated *cyp26a1* in the presence of CHX, in this case, with increase in signal intensity not in expression area (Fig. 28B). These results indicate a direct role of RA and suggest that the broaden area of *cyp26a1* expression was due to reduced cell movement that was caused by RA inhibition of *fgf8*. We also observed that the RA-induced activation was cancelled by

co-treatment with TAM (Fig. 28C), indicating a role of maternal estrogen in the feedback control of *cyp26a1*.

We also investigated a physiological role of maternal estrogen in the regulation of RA metabolism by analyzing the effect of overproduction or knockdown of ER $\alpha$  on *raldh2* expression. We anticipated that overproduction and knockdown of ER $\alpha$  would decrease and increase *raldh2* expression, respectively. However, we observed that both activated *raldh2* (Fig. 29A). Because overproduction of ER $\alpha$  causes phenotypic traits like RA deficiency (Figs. 7C, D), the increase in *raldh2* expression by ER $\alpha$ -OP is considered due to derepression of *raldh2* from negative control by RA. The increase in *raldh2* expression by ER $\alpha$ -KD is consistent with the conclusion that ER $\alpha$  controls *raldh2* negatively. We also examined the effect of ER $\alpha$ -KD on RA-induced repression of *raldh2*. Unlike our expectation that it restores the expression of *raldh2*, it caused a further decline in *raldh2* expression (Fig. 29B). From this result, we speculated that ER $\alpha$ -KD caused an increase in RA level. To test this, we examined the effect of overproduction or knockdown of ER $\alpha$  on RA-inducible *rara* expression, resulting in activation of *rara* in both cases (Fig. 29C). The increase by ER $\alpha$ -OP is consistent with the conclusion that ER $\alpha$  activates *rara*. The increase by ER $\alpha$ -KD is considered due to activation of *rara* by an increase in RA level.

We also investigated the effect of overproduction or knockdown of ER $\alpha$  on *cyp26a1* expression. We anticipated that overproduction and knockdown of ER $\alpha$  would increase and decrease *cyp26a1* expression, respectively. As expected, ER $\alpha$ -OP considerably activated *cyp26a1* judging from increase in intensity but not in area of *cyp26a1* expression (Fig. 29D), suggesting that it causes RA deficiency. However, ER $\alpha$ -KD showed no significant effect (Fig. 29D). We then examined the effect of ER $\alpha$ -KD on RA-induced activation of *cyp26a1*. Expectedly, it impaired the activity of RA regarding both intensity and area of *cyp26a1* expression (Fig. 29E), indicating that ER $\alpha$  activates *cyp26a1* in coordination with RA. We speculate that ER $\alpha$  activates transcription of *cyp26a1* and controls expression area of *cyp26a1* by repressing *fgf8* coordinately with RA.

Our studies highlight a role of maternal estrogen/ER $\alpha$  in the regulatory mechanism for feedback control of RA level, which includes *raldh2*, *cyp26a1*, and *fgf8*. Elevated concentration of *in vivo* RA directs the expression of the regulatory genes toward lowering RA level in coordination with maternal estrogen through four routes: direct repression of *raldh2*, reduced activation of

*raldh2* caused by repression of *fgf8* that is a positive regulator of *raldh2*, direct activation of *cyp26a1*, and indirect activation of *cyp26a1* by repressing *fgf8* that is a negative regulator of *cyp26a1*. We observed that activation of ER $\alpha$  by either excess E2 or overproduction of ER $\alpha$  causes RA deficiency. On the contrary, we speculate that inactivation of ER $\alpha$  by either TAM or ER $\alpha$ -KD increases RA level. If our model was correct, treatment of CYP26-inactive embryos with TAM would further increase RA level. To test this, we investigated vascular damages and *rara* expression after co-treating embryos with R115866 (CYP26 inhibitor) and TAM. As expected, we observed synergistic inhibition of the development in vasculature, head, and tail which are characteristic to excess RA (Fig. 30A). Expressions of *rara* in the posterior hindbrain at 36 hpf (Fig. 30B) and in the prospective tail region at 18 hpf (Fig. 30C) were also synergistically activated by R115866 and TAM. Furthermore, we investigated whether TAM would increase vascular damages and *rara* expression in the presence of 4-oxo-RA, an active retinoic acid that is generated in the metabolic pathway downstream from the reaction of CYP26a1 (Pijnappel *et al.*, 1993; Topletz *et al.*, 2015). We observed synergistic inhibition of vascular formation (Fig. 30D). We also observed that 4-oxo-RA activated *rara* expression at 18 hpf and that TAM further increased its expression (Fig. 30E). Collectively, these results suggest that TAM increases RA level and that maternal estrogen plays a critical role in the feedback control of *in vivo* level of RA.

## DISCUSSION

Our data demonstrate the importance of maternal estrogen and its receptor ER $\alpha$  in the early embryonic development of medaka fish. Our findings reveal a functional cooperation between the two ubiquitous molecules, estrogen and RA, both in the feedback control of *in vivo* level of RA and in the transcriptional activation of RA-inducible genes. In our model (Fig. 31), activation of maternal estrogen/ER $\alpha$  leads to decreasing RA level and conversely upregulates RA-inducible gene expression. Thus, maternal estrogen/ER $\alpha$  acts as a buffer against developmental misregulation and environmental change in RA metabolism and signaling. Maternal estrogen/ER $\alpha$  may play a limited role in normal development but is vital in RA-deficient and -excess embryos. Indeed, we observed no effect of the antiestrogenic drug (TAM) in the normal development but clear effects in RA-deficient and -excess embryos. In a nutritional point of view, maternal estrogen may serve to moderate RA deficiency

that occurs from a shortage of maternally derived vitamin-A, a precursor of RA. Since RA plays fundamental roles in many aspects of animal development acting as a morphogen that forms a gradient of concentrations in developing embryos (Maden, 2002; Rhinn & Dollé, 2012), the synergistic activation of RA signaling by maternal estrogen may be important for spatial control of gene expression. Although molecular mechanisms for the cooperation between RAR and ER $\alpha$  are at present unknown in medaka, it is interesting to speculate a transcriptional control of target genes with binding sites for RAR and ER $\alpha$  at nearby or overlapping *cis*-regulatory elements. Hua *et al.* (2009) reported that binding sites for RAR and ER $\alpha$  are highly coincident throughout the human genome. They proposed a genome-wide crosstalk of RA and estrogen signaling to antagonistically regulate breast cancer-associated genes. The transcriptional linkage between RA and estrogen may be conserved in vertebrate. We also speculate that lower activity of RA signaling that activates Hox gene expression at 1  $\mu$ M concentration in basal chordata, amphioxus (*Branchiostoma floridae*) and ascidian (*Ciona intestinalis*), which is 100-fold higher concentration than in vertebrate, may be in part due to lack of estrogen-responsive ER in their genomes (Koop *et al.*, 2010; Nagatomo *et al.*, 2003; Paris *et al.*, 2008). Little has been learned about the developmental roles of ER genes in lower vertebrates (Celeghin *et al.*, 2011; Froehlicher *et al.*, 2009; Gamba *et al.*, 2010). In order to characterize the physiological roles of ER genes, it may be necessary to explore synergistic conditions or synthetic lethal relationship between *er* mutation and RA-related one.

## ACKNOWLEDGEMENTS

We thank K. Kitamura, N. Tanaka, and D. Hirata for discussions, T. Czerny, K. Araki, and H. Takeda for plasmid, and E.-M. Gutknecht for RA antagonist. Supported by grants from the Ministry of Education, Culture, Sports, Science and Technology of Japan.

## REFERENCES

- Abrams, E. W., & Mullins, M. C. Early zebrafish development: It's in the maternal genes. *Curr. Opin. Genet. Dev.* 19: 396-403 (2009).
- Apte, R. S., Chen, D. S., & Ferrara, N. VEGF in signaling and disease: Beyond discovery and development. *Cell* 176: 1248-1264 (2019).

Bertrand, S., Belgacem, M. R., & Escriva, H. Nuclear hormone receptors in chordates. *Mol. Cell. Endocrinol.* 334: 67-75 (2011).

Böttcher, R. T., & Niehrs, C. Fibroblast growth factor signaling during early vertebrate development. *Endoc. Rev.* 26: 63-77 (2005).

Brown, C. L., Urbinati, E. C., Zhang, W., Brown, S. B., & McComb-Kobza, M. Maternal thyroid and glucocorticoid hormone interactions in larval fish development, and their applications in aquaculture. *Rev. Fish Sci. Aquac.* 22: 207-220 (2014).

Byrd, N., & Grabel, L. Hedgehog signaling in murine vasculogenesis and angiogenesis. *Trends Cardiovasc. Med.* 14: 308-313 (2004).

Campinho, M. A., Saraiva, J., Florindo, C., & Power, D. M. Maternal thyroid hormones are essential for neural development in zebrafish. *Mol. Endocrinol.* 28: 1136-1149 (2014).

Campo-Paysaa, F., Marlétaz, F., Laudet, V., & Schubert, M. Retinoic acid signaling in development: Tissue-specific functions and evolutionary origins. *Genesis* 46: 640–656 (2008).

Carney, S. A., Prasch, A. L., Heideman, W., & Peterson, R. E. Understanding dioxin developmental toxicity using the zebrafish model. *Birth Defects Res. (Part A)* 76: 7-18 (2006).

Celeghin, A., Benato, F., Pikulkaew, S., Rabbane, M. G., Colombo, L., & Valle, L. D. The knockdown of the maternal estrogen receptor 2a (*esr2a*) mRNA affects embryo transcript contents and larval development in zebrafish. *Gen. Comp. Endocrinol.* 172: 120-129 (2011).

D.-McAuliffea, B., Zhaob, Q., & Linney, E. Feedback mechanisms regulate retinoic acid production and degradation in the zebrafish embryo. *Mech. Dev.* 121: 339-350 (2004).

- Dorey, K., & Amaya, E. FGF signalling: diverse roles during early vertebrate embryogenesis. *Development* 137: 3731-3742 (2010).
- Duester, G. Retinoic acid synthesis and signaling during early organogenesis. *Cell* 134: 921-931 (2008).
- Elf, P. K. Yolk steroid hormones and sex determination in reptiles with TSD. *Gen. Comp. Endocrinol.* 132: 349-355 (2003).
- Fortune, J. E. Steroid production by *Xenopus* ovarian follicles at different developmental stages. *Dev. Biol.* 99: 502-509 (1983).
- Froehlicher, M., Liedtke, A., Groh, K., López-Schier, H., Neuhauss, S. C. F., Segner, H., & Eggen, R. I. L. Estrogen receptor subtype  $\beta 2$  is involved in neuromast development in zebrafish (*Danio rerio*) larvae. *Dev. Biol.* 330: 32-43 (2009).
- F.-Salguero, P. M., Hilbert, D. M., Rudikoff, S., Ward, J. M., & Gonzalez, F. J. Aryl-hydrocarbon receptor-deficient mice are resistant to 2,3,7,8-tetrachlorodibenzo-*p*-dioxin-induced toxicity. *Toxicol. Appl. Pharmacol.* 140: 173-179 (1996).
- Fürthauer, M., Reifers, F., Brand, M., Thisse, B., & Thisse, C. *sprouty4* acts *in vivo* as a feedback-induced antagonist of FGF signaling in zebrafish. *Development* 128: 2175-2186 (2001).
- Gamba, L., Cubedo, N., Ghysen, A., Lutfalla, G., & Dambly-Chaudière, C. Estrogen receptor ESR1 controls cell migration by repressing chemokine receptor CXCR4 in the zebrafish posterior lateral line system. *Proc. Natl. Acad. Sci. U.S.A.* 107: 6358-6363 (2010).
- Groothuis, T. G. G., Müller, W., von Engelhardt, N., Carere, C., & Eising, C. Maternal hormones as a tool to adjust offspring phenotype in avian species. *Neurosci. Biobehav. Rev.* 29: 329-352 (2005).

Hamada, K., Tamaki, K., Sasado, T., Watai, Y., Kani, S., Wakamatsu, Y., Ozato, K., Kinoshita, M., Kohno, R., Takagi, S., & Kimura, M. Usefulness of the medaka  $\beta$ -actin promoter investigated using a mutant GFP reporter gene in transgenic medaka (*Oryzias latipes*). *Mol. Mar. Biol. Biotech.* 7: 173-180 (1998).

Hamade, A., Deries, M., Begemann, G., Bally-Cuif, L., Genêt, C., Sabatier, F., Bonnieu, A., & Cousin, X. Retinoic acid activates myogenesis *in vivo* through Fgf8 signalling. *Dev. Biol.* 289: 127-140 (2006).

Hayashida, Y., Kawamura, T., Hori-e, R., & Yamashita, I. Retinoic acid and its receptors are required for expression of aryl hydrocarbon receptor mRNA and embryonic development of blood vessel and bone in the medaka fish, *Oryzias latipes*. *Zool. Sci.* 21: 541-551 (2004).

Herbert, S. P., Huisken, J., Kim, T. N., Feldman, M. E., Houseman, B. T., Wang, R. A., Shokat, K. M., & Stainier, D. Y. R. Arterial-venous segregation by selective cell sprouting: An alternative mode of blood vessel formation. *Science* 326: 294-298 (2009).

Hernandez, R. E., Putzke, A. P., Myers, J. P., Margaretha, L., & Moens, C. B. Cyp26 enzymes generate the retinoic acid response pattern necessary for hindbrain development. *Development* 134: 177-187 (2007).

Hochmann, S., Aghaallaei, N., Bajoghli, B., Soroldoni, D., Carl, M., & Czerny, T. Expression of marker genes during early ear development in medaka. *Gene Expr. Patterns* 7: 355–362 (2007).

Hua, S., Kittler, R., & White, K. P. Genomic antagonism between retinoic acid and estrogen signaling in breast cancer. *Cell* 137: 1259-1271 (2009).

Inohaya, K., Yasumasu, S., Araki, K., Naruse, K., Yamazaki, K., Yasumasu, I., Iuchi, I., & Yamagami, K. Species-dependent migration of fish hatching gland cells that commonly express astacin-like proteases in common. *Dev. Growth Differ.* 39: 191-197 (1997).

Ishikawa, Y., Yasuda, T., Kage, T., Takashima, S., Yoshimoto, M., Yamamoto, N., Maruyama, K., Takeda, H., & Ito, H. Early development of the cerebellum in teleost fishes: A study based on gene expression patterns and histology in the medaka embryo. *Zool. Sci.* 25: 407-418 (2008).

Iwamatsu, T. Stages of normal development in the medaka *Oryzias latipes*. *Mech. Dev.* 121: 605-618 (2004).

Iwamatsu, T., Kobayashi, H., Hamaguchi, S., Sagegami, R., & Shuo, T. Estradiol-17 $\beta$  content in developing eggs and induced sex reversal of the medaka (*Oryzias latipes*). *J. Exp. Zool.* 303A: 161-167 (2005).

Kawahara, T., Okada, H., & Yamashita, I. Cloning and expression of genomic and complementary DNAs encoding an estrogen receptor in the medaka fish, *Oryzias latipes*. *Zool. Sci.* 17: 643-649 (2000).

Kawahara, T., & Yamashita, I. Estrogen-independent ovary formation in the medaka fish, *Oryzias latipes*. *Zool. Sci.* 17: 65-68 (2000).

Kawamura, T., Sakai, S., Omura, S., Hori-e, R., Kawahara, T., Kinoshita, M., & Yamashita, I. Estrogen inhibits development of yolk veins and causes blood clotting in transgenic medaka fish overexpressing estrogen receptor. *Zool. Sci.* 19: 1355-1361 (2002).

Kawamura, T., & Yamashita, I. Aryl hydrocarbon receptor is required for prevention of blood clotting and for the development of vasculature and bone in the embryos of medaka fish, *Oryzias latipes*. *Zool. Sci.* 19: 309-319 (2002).

Keay, J., & Thornton, J. W. Hormone-activated estrogen receptors in annelid invertebrates: Implications for evolution and endocrine disruption. *Endocrinol.* 150: 1731-1738 (2009).

Kolesová, H., Roelink, H., & Grim, M. Sonic hedgehog is required for the assembly and remodeling of branchial arch blood vessels. *Dev Dyn.* 237: 1923-1934 (2008).

Koop, D., Holland, N. D., Sémon, M., Alvarez, S., Rodriguez de Lera, A., Laudet, V., Holland, L. Z., & Schubert, M. Retinoic acid signaling targets Hox genes during the amphioxus gastrula stage: Insights into early anterior–posterior patterning of the chordate body plan. *Dev. Biol.* 338: 98-106 (2010).

Krens, S. F. G., He, S., Lamers, G. E. M., Meijer, A. H., Bakkers, J., Schmidt, T., Spaink, H. P., & Snaar-Jagalska, B. E. Distinct functions for ERK1 and ERK2 in cell migration processes during zebrafish gastrulation. *Dev. Biol.* 319: 370–383 (2008).

Kudoh, T., Wilson, S. W., & Dawid, I. B. Distinct roles for Fgf, Wnt and retinoic acid in posteriorizing the neural ectoderm. *Development* 129: 4335-4346 (2002).

Lawson, N. D., Vogel, A. M., & Weinstein, B. M. Sonic hedgehog and vascular endothelial growth factor act upstream of the notch pathway during arterial endothelial differentiation. *Dev. Cell* 3: 127-136 (2002).

Lee, C., Na, J. G., Lee, K.-C. & Park, K. Choriogenin mRNA induction in male medaka, *Oryzias latipes* as a biomarker of endocrine disruption. *Aqua. Toxicol.* 61: 233-241 (2002).

Li, L., Zheng, P., & Dean, J. Maternal control of early mouse development. *Development* 137: 859-870 (2010).

Lubzens, E., Bobe, J., Young, G., & Sullivan, C. V. Maternal investment in fish oocytes and eggs: The molecular cargo and its contributions to fertility and early development. *Aquaculture* 472: 107-143 (2017).

Maden, M. Retinoid signalling in the development of the central nervous system. *Nature Rev. Neurosci.* 3: 843-853 (2002).

McMillan, B. J., & Bradfield, C. A. The aryl hydrocarbon receptor sans xenobiotics: Endogenous function in genetic model systems. *Mol. Pharmacol.* 72: 487-498 (2007).

Mimura, J., Yamashita, K., Nakamura, K., Morita, M., Takagi, T. N., Nakao, K., Ema, M., Sogawa, K., Yasuda, M., Katsuki, M., & Fujii-Kuriyama, Y. Loss of teratogenic response to 2,3,7,8-tetrachlorodibenzo-*p*-dioxin (TCDD) in mice lacking the Ah (dioxin) receptor. *Genes Cells* 2: 645-654 (1997).

Moran, C. M., Salanga, M. C., & Krieg, P. A. Hedgehog signaling regulates size of the dorsal aortae and density of the plexus during avian vascular development. *Dev. Dyn.* 240: 1354-1364 (2011).

Nagatomo, K., Ishibashia, T., Satou, Y., Satoh, N., & Fujiwara, S. Retinoic acid affects gene expression and morphogenesis without upregulating the retinoic acid receptor in the ascidian *Ciona intestinalis*. *Mech. Dev.* 120: 363-372 (2003).

Olsson, A.-K., Dimberg, A., Kreuger, J., & Claesson-Welsh, L. VEGF receptor signalling — in control of vascular function. *Nature Rev. Mol. Cell Biol.* 7: 359-371 (2006).

Paitz, R. T. & Bowden, R. M. Rapid decline in the concentrations of three yolk steroids during development: Is it embryonic regulation? *Gen. Comp. Endocrinol.* 161: 246–251 (2009).

Paitz, R. T., Mommer, B. C., Suhr, E., & Bell, A. M. Changes in the concentrations of four maternal steroids during embryonic development in the threespined stickleback (*Gasterosteus aculeatus*). *J. Exp. Zool.* 323A: 422-429 (2015).

Paris, M., Pettersson, K., Schubert, M. Bertrand, S., Pongratz, I., Escriva, H., & Laudet, V. An amphioxus orthologue of the estrogen receptor that does not bind estradiol: Insights into estrogen receptor evolution. *BMC Evo. Biol.* 8: 219-238 (2008).

Pelegri, F. Maternal factors in zebrafish development. *Dev. Dyn.* 228: 535-554 (2003).

Pijnappel, W. W., Hendriks, H. F., Folkers, G. E., van den Brink, C. E., Dekker, E. J., Edelenbosch, C., van der Saag, P. T., & Durston, A. J. The retinoid ligand 4-oxo-retinoic acid is a highly active modulator of positional specification. *Nature* 366: 340-344 (1993).

Rhinn, M., & Dollé, P. Retinoic acid signalling during development. *Development* 139: 843-858 (2012).

Sada, N., Hanafusa, T., Onizuka, Y., Hayashida, Y., Kageyama, S., & Yamashita, I. Retinoic acid controls vascular formation by activating transcription of aryl hydrocarbon receptor gene in medakafish *Oryzias latipes*. Hiroshima University Institutional Repository ID 47694 (2019).

Senthilkumaran, B., Yoshikuni, M., & Nagahama, Y. A shift in steroidogenesis occurring in ovarian follicles prior to oocyte maturation. *Mol. Cell. Endocrinol.* 215: 11-18 (2004).

Shiotsugu, J., Katsuyama, Y., Arima, K., Baxter, A., Koide, T., Song, J., Chandraratna, R. A. S., & Blumberg, B. Multiple points of interaction between retinoic acid and FGF signaling during embryonic axis formation. *Development* 131: 2653-2667 (2004).

Sive, H. L., Draper, B. W., Harland, R. M., & Weintraub, H. Identification of a retinoic acid-sensitive period during primary axis formation in *Xenopus laevis*. *Genes Dev.* 4: 932-942 (1990).

Tarrant, A. M. Endocrine-like signaling in cnidarians: Current understanding and implications for ecophysiology. *Integr. Comp. Biol.* 45: 201–214 (2005).

Theodosiou, M., Laudet, V., & Schubert, M. From carrot to clinic: An overview of the retinoic acid signaling pathway. *Cell. Mol. Life Sci.* 67: 1423-1445 (2010).

Topletz, A. R., Tripathy, S., Foti, R. S., Shimshoni, J. A., Nelson, W. L., & Isoherranen, N. Induction of CYP26A1 by metabolites of retinoic acid: evidence that CYP26A1 is an important enzyme in the elimination of active retinoids. *Mol. Pharmacol.* 87: 430-441 (2015).

Vokes, S. A., Yatskievych, T. A., Heimark, R. L., McMahon, J., McMahon, A. P., Antin, P. B., & Krieg, P. A. Hedgehog signaling is essential for endothelial tube formation during vasculogenesis. *Development*. 131: 4371-4380 (2004).

White, R. J., Nie, Q., Lander, A. D., & Schilling, T. F. Complex regulation of *cyp26a1* creates a robust retinoic acid gradient in the zebrafish embryo. *PLoS Biol.* 5(11): e304 (2007).

Williams, C., Kim, S.-H., Ni, T. T., Mitchell, L., Ro, H., Penn, J. S., Baldwin, S. H., Solnica-Krezel, L., & Zhong, T. P. Hedgehog signaling induces arterial endothelial cell formation by repressing venous cell fate. *Dev. Biol.* 341: 196-204 (2010).

Yamamoto, T. Sex differentiation. In "Fish Physiology 3" Ed by W. S. Hoar, D. J. Randall, Academic Press, New York, pp 117-175. (1969).

Yokoi, H., Shimada, A., Carl, M., Takashima, S., Kobayashi, D., Narita, T., Jindo, T., Kimura, T., Kitagawa, T., Kage, T., Sawada, A., Naruse, K., Asakawa, S., Shimizu, N., Mitani, H., Shima, A., Tsutsumi, M., Hori, H., Wittbrodt, J., Saga, Y., Ishikawa, Y., Araki, K., & Takeda, H. Mutant analyses reveal different functions of *fgfr1* in medaka and zebrafish despite conserved ligand-receptor relationships. *Dev. Biol.* 304: 326-337 (2007).

**Figure 1. Hyperactivation of ER $\alpha$  causes loss of CCV.**

**(A)** Staged embryos were treated with E2 (4 mg/l) and examined at 3 dpf for vascular damages. % Embryos with vascular damages or curved tail (inset; blood aggregates marked by an arrow) were shown. **(B)** Wild-type embryos and transgenic ones overproducing ER $\alpha$  were treated with E2 at the indicated concentration and examined for *vegfr1*<sup>+</sup> angioblasts at 48 hpf. Arrows indicate CCV. **(C)** Wild-type embryos were treated with E2 (4 mg/l) and examined for *vegfr1*<sup>+</sup> angioblasts at PBA (bracket) at 36 and 48 hpf. Open arrowhead indicates otic vesicle.

**Figure 2. Excess RA causes loss of CCV.**

**(A)** Staged embryos were treated with RA (9 nM) and examined at 48 hpf for *vegfr1*<sup>+</sup> angioblasts. % Embryos without CCV were shown. **(B)** Embryos were treated with R115866 (a specific inhibitor of CYP26) (10  $\mu$ M) and DEAB (a RA synthesis inhibitor) (1  $\mu$ M) either alone or together as indicated, and photographed at 3 dpf. % Embryos with vascular damages were shown.

\*  $p < 0.002$ ; \*\*  $p < 0.00001$ .

**Figure 3. MAP kinase pathway inhibitor (PD98059) causes loss of CCV.**

**(A)** Embryos were treated with PD98059 (5  $\mu$ M) and examined at 36 hpf for expression of *sprouty4*. **(B)** Embryos were treated with PD98059 at the indicated concentration and examined at 3 dpf for vascular damages. % Embryos with vascular damages were shown. Embryos treated with the drug (20  $\mu$ M) were also examined for *vegfr1*<sup>+</sup> angioblasts at 48 hpf. **(C)** 5-dpf embryos with curved tail treated with the drug (20  $\mu$ M). **(D)** Staged embryos were treated with the drug (20  $\mu$ M) and examined for vascular damages at 3 dpf and for *vegfr1*<sup>+</sup> angioblasts at 48 hpf. \*  $p < 0.0001$ .

**Figure 4. Cyclopamine causes loss of CCV.**

**(A, B)** Embryos were treated with cyclopamine at the indicated concentration and examined for vascular damages at 3 dpf (A) and for *vegfr1*<sup>+</sup> angioblasts at 48 hpf (B). **(C)** Embryos were treated with the drug (10 mg/l) and photographed at the indicated time. **(D)** Embryos were treated with the drug (25 mg/l) and examined for *vegfr1*<sup>+</sup> angioblasts at 48 hpf. \*  $p < 0.0001$ .

**Figure 5. Effects on *myoD* expression of DEAB, RA, PD98059, cyclopamine, and E2.** *myoD* expression was examined at 44 hpf after treating embryos with the following drugs: **(A)** DEAB (10  $\mu$ M), or RA (10 nM), **(B)** PD98059 (20  $\mu$ M) or cyclopamine (40 mg/l), **(C)** E2 (4 mg/l), and **(D)** E2 (4 mg/l), DEAB (10  $\mu$ M), or E2 (4 mg/l) plus DEAB (10  $\mu$ M).

**Figure 6. Effects of E2, PD98059, and DEAB on expressions of *shh* and *no tail*.** **(A, B)** Embryos were treated with E2 (4 mg/l) and examined for expression of *shh* (A) or *no tail* (B) at the indicated time. **(C)** Embryos were treated with PD98059 (20  $\mu$ M) or DEAB (50  $\mu$ M) and examined for *shh* expression at 36 hpf.

**Figure 7. Synergistic effects.**

**(A)** Embryos were treated with E2 and DEAB at the indicated concentration and examined for vascular damages at 3 dpf. **(B)** Staged embryos were treated with E2 and DEAB at the indicated concentration and examined for vascular damages at 3 dpf. **(C)** Wild-type and ER $\alpha$ -overproducing transgenic embryos were treated with E2 and DEAB at the indicated concentration and examined for vascular damages at 3 dpf. **(D)** Wild-type embryos with the ER $\alpha$ -overproducing plasmid DNA (pOL22) introduced by electroporation were treated with DEAB and examined for vascular damages at 3 dpf. **(E, F)** Embryos were treated with PD98059 and DEAB at the indicated concentration and examined for vascular damages at 3 dpf (E) and for *vegfr1*<sup>+</sup> angioblasts at 48 hpf (F). **(G)** Embryos were treated with DEAB (2  $\mu$ M) at 10 hpf, added with PD98059 (5  $\mu$ M) at the indicated time, and examined for vascular damages at 3 dpf. **(H)** Embryos were treated with PD98059 and E2 at the indicated concentration and examined for vascular damages at 3 dpf and for curved tails at 5 dpf. **(I)** Embryos were treated with PD98059 and RA at the indicated concentration and examined for vascular damages at 3 dpf. **(J)** Embryos were treated with PD98059 and RA at the indicated concentration and examined for *vegfr1*<sup>+</sup> angioblasts at 48 hpf. **(K)** Embryos were treated with E2 and RA at the indicated concentration and examined for vascular damages at 3 dpf. **(L)** Staged embryos were treated with E2 and RA at the indicated concentration and examined for vascular damages at 3 dpf. \*  $p < 0.05$ ; \*\*  $p < 0.01$ ; \*\*\*  $p < 0.001$ .

**Figure 8. Effect of E2 on hindbrain formation.**

(A) Embryos were treated with E2 and DEAB at the indicated concentration and examined for rhombomere formation at 58 hpf. (B) Synergistic effect of E2 and DEAB on rhombomere formation. Arrows indicate boundary between rhombomeres. OV, otic vesicle.

**Figure 9. Effect of E2 on RA-inducible gene expression.**

(A) Embryos were treated with Ro41-5253 (5  $\mu$ M), 17 $\beta$ -E2 (4 mg/l), and 17 $\alpha$ -E2 (4 mg/l) and examined for expression of the genes indicated at 36 hpf. (B) Embryos were treated with E2 and/or DEAB at 10 or 20 hpf and examined for expression of *rara* and *hoxa3a* at 36 hpf. Open arrowhead indicates no expression of *hoxa3a* at r-7 to r-8. (C) Staged embryos were treated with E2 and examined for *rara* expression at 36 hpf. Embryos of 10, 16, and 19 hpf are at developmental stage of late blastula, mid-gastrula, and pre-late gastrula, respectively. (D) Embryos were treated with E2 at the indicated concentration and examined for *rara* expression (in circle) at 18 hpf. \*  $p < 0.01$ .

**Figure 10. Effect of E2 on *raldh2* and *cyp26a1* expression.**

(A) Embryos were treated with E2 at 10 hpf, added with cycloheximide at 18 hpf, fixed at 23 hpf, and examined for *raldh2* expression. (B) Embryos were treated with E2 at 18 hpf 1 h after addition of cycloheximide, and examined for *raldh2* expression. (C) Embryos were treated with E2 as indicated and examined for *cyp26a1* expression. (D) Embryos were treated with E2 after addition of cycloheximide as indicated, and examined for *cyp26a1* expression.

**Figure 11. Effect of PD98059 on RA-controlled gene expression.**

(A) Embryos were treated with PD98059 at the indicated concentration and examined for expression of the genes indicated at 36 hpf. (B) Embryos were treated with PD98059 and/or DEAB and examined for *rara* expression at 36 hpf. (C) Staged embryos were treated with PD98059 (5  $\mu$ M) and DEAB (2  $\mu$ M) and examined for *rara* expression at 36 hpf. % Embryos with no *rara* expression are shown. (D) Embryos were treated with PD98059 and examined for *rara* expression at 18 hpf. \*  $p < 0.01$ ; \*\*  $p < 0.001$ .

**Figure 12. Effect of PD98059 on *raldh2* and *cyp26a1* expression.**

(A) Embryos were treated with PD98059 at 10 hpf, added with cycloheximide at 18 hpf, fixed at 23 hpf, and examined for *raldh2* expression. (B, C) Embryos were treated with PD98059 at 10 hpf, added with cycloheximide at 18 hpf (B) or 24 hpf (C), fixed 5 h later, and examined for *cyp26a1* expression. \*  $p < 0.001$ .

**Figure 13. Effect of PD98059 on *ahr1* expression.**

(A) Embryos were treated with PD98059 and/or DEAB and examined for *ahr1* expression at 48 hpf. (B) Embryos were treated with PD98059 and examined for *ahr1* expression at 48 hpf. Closed arrowhead, *ahr1* expression at PBA; open arrowhead, otic vesicle; \*  $p < 0.005$ .

**Figure 14. Effect of E2 on FGF signaling.**

(A) Expression of *fgf3* and *fgf8* during somite stage. (B) Effect of E2 on *fgf3* and *fgf8* expression. (C) Effect of E2 on *sprouty4* expression. (D) Embryos were treated with increasing concentrations of E2 as indicated and examined for *sprouty4* expression at 36 hpf. MHB, midbrain-hindbrain boundary; TB, tail bud; TEL, telencephalome.

**Figure 15. Effect of ER $\alpha$  overproduction on *fgf8* and *myoD* expression.**

Expression of *fgf8* and *myoD* was examined at 36 and 44 hpf, respectively, in the embryos injected with plasmid DNA (pOL22) overproducing ER $\alpha$ .

**Figure 16. Effect of RA on *fgf8* and *sprouty4* expression.**

(A) Staged embryos were treated with RA (9 nM) and examined for *fgf8* and *sprouty4* expression at 36 hpf. (B) % Embryos with no *sprouty4* expression at MHB or adaxial mesoderm (AM) and relative length of *sprouty4* signal at tail bud (TB) are shown. % Embryos with vascular damages from Hayashida *et al.* (2004). Arrows indicate that embryos were affected before the time marked.

\*  $p < 0.001$ .

**Figure 17. Effect of RA on *ahr1* expression.**

**(A)** Staged embryos were treated with RA (10 nM) and examined for *ahr1* expression at 48 hpf. **(B)** Average length from top of head to otic vesicle marked by double arrowhead in (A). Open arrowhead, otic vesicle; closed arrowhead, *ahr1* expression at PBA; Grey arrowhead, *ahr1* expression at otic vesicle.

\*  $p < 0.0001$ .

**Figure 18. Effect of *fgf8* knockdown on CCV formation and RA metabolism and signaling.**

**(A)** Embryos were injected with control-MO or *fgf8*-MO and examined for the expression as follows: *ahr1* (48 hpf), *cyp26a1* (18 hpf), *raldh2* (18 hpf), *rara* (18 or 36 hpf), *sprouty4* (36 hpf), and *vegfr1* (48 hpf). **(B)** Embryos were injected with control-MO or *fgf8*-MO, incubated in the presence or absence of DEAB, and examined for *rara* expression at 36 hpf. Arrowhead, PBA; arrow, tail tip.

**Figure 19. Effect of antiestrogen on hindbrain formation.**

**(A)** 54-hpf DAPI-stained embryos treated with E2 (2 mg/l), DEAB (10  $\mu$ M), RA (10 nM), RA (10 nM) + TAM (4 mg/l), or RA (10 nM) + TAM (4 mg/l) + E2 (2 mg/l). Number, rhombomere; arrow, otic vesicle. **(B)** Embryos were treated with RA (10 nM) or RA (10 nM) + TAM (4 mg/l), and examined for *krox20* expression at 36 hpf. Arrows indicate RA-induced anterior shift of r-3 and r-5 and its recovery by TAM. **(C)** Embryos were treated as indicated and examined for expressions of *rara* and *hoxa3a* at 36 hpf. **(D)** Staged embryos were treated as indicated and examined for *rara* expression at 36 hpf. **(E)** Relative intensity and area of *rara* expression in (D). Broken line indicates control level. **(F)** Relative length from top of head to *rara* signal (bracket) in (D). \*  $p < 0.001$ ; \*\*  $p < 0.0001$ .

**Figure 20. Effect of antiestrogen on *rara* expression during gastrula stage.**

**(A)** Staged embryos were analyzed for *rara* expression by *in situ* hybridization using anti-sense and sense probes. **(B)** Embryos were treated with RA (10 nM) or RA (10 nM) + TAM (4 mg/l) as indicated and examined for *rara* expression. **(C)** Embryos were first treated with cycloheximide, then with RA (10 nM) or RA (10 nM) + TAM (4 mg/l) as indicated, and examined for *rara* expression.

\*  $p < 0.005$ ; \*\*  $p < 0.001$ ; n.s., not significant.

**Figure 21. Effect of antiestrogen on *ahr1* expression.**

Embryos were treated with RA (10 nM), RA (10 nM) + TAM (0.5 mg/l), or RA (10 nM) + TAM (0.5 mg/l) + E2 (2 mg/l) as indicated, and examined for *ahr1* expression. Open arrowhead, otic vesicle; closed arrowhead, *ahr1* expression at PBA. Average length from top of head to otic vesicle marked by double arrowhead is also shown. \*  $p < 0.05$ ; \*\*  $p < 0.0001$ .

**Figure 22. Effect of antiestrogen, ER $\alpha$ -KD, and RA on FGF signaling.**

**(A)** Embryos were treated with RA (9 nM) and/or TAM (4 mg/l) as indicated and examined for *sprouty4* expression at 36 hpf. Bracket indicates *sprouty4* expression at adaxial mesoderm. **(B)** Embryos were treated with RA (9 nM) at 10 hpf, added with TAM (4 mg/l) at the indicated time, and examined for *fgf8* expression at 36 hpf. **(C, D)** Embryos were treated as in (A) and examined for expressions of *fgf8* (C) and *sprouty4* (D) at the indicated time. Arrowhead indicates split of the signal caused by gastrulation delay. **(E)** *fgf8* expression in 19-hpf embryos injected with plasmid DNA expressing anti-sense ER $\alpha$  RNA. **(F)** Embryos were treated with cycloheximide at 16 hpf, added with RA (9 nM) at 17 hpf, fixed at 22 hpf, and examined for *fgf8* expression. **(G)** Embryos were treated with DEAB (50 or 10  $\mu$ M), and examined for *fgf8* expression at 19 or 36 hpf, respectively. **(H)** *fgf8* expression in 19-hpf embryos treated with R115866 (10  $\mu$ M).

**Figure 23. Effect of antiestrogen on vascular formation.**

**(A, B)** Embryos were treated as indicated and examined for vascular damages. % Embryos with vascular damages are shown. (A) Suppression of the RA-induced vascular damages by co-treatment with TAM, and its cancellation by further addition of E2. (B) TAM-induced recovery from the synergistic inhibition of vascular formation by RA and E2. \*  $p < 0.01$ . **(C)** Embryos were treated with RA (9 nM) at 10 hpf, added with TAM at the indicated time, and examined for vascular damages and body-axis malformation. Values for embryos treated with RA alone were marked by arrows (closed, vascular damages; open, body-axis malformation). 3-dpf embryos are also shown for control and the treatment with RA alone or with RA together with addition of TAM at 10 or 16 hpf.

**Figure 24. Synergistic inhibition of vascular formation by TAM and DEAB.** (A, B, C, D) Embryos were treated as indicated and examined for vascular damages (A, C, D) and *vegfr1*<sup>+</sup> CCV (B). (A) Synergistic inhibition of vascular formation. (B) Synergistic inhibition of CCV formation. (C) Rescue by addition of RA. (D) Rescue by addition of E2. (E) Staged embryos were treated with DEAB and TAM as indicated (gray diamond, circle, open square). Embryos were also treated with DEAB at 10 hpf and added with TAM at the indicated time (closed square). % Embryos with vascular damages are shown. (F) Staged embryos were treated with DEAB and TAM as indicated, and examined for *vegfr1*<sup>+</sup> CCV. \*  $p < 0.05$ ; \*\*  $p < 0.005$ .

**Figure 25. Control of *ahr1* transcript levels by RA and maternal estrogen.** (A, B, C, D) Embryos were treated as indicated and examined for *ahr1* transcript levels at 36 hpf by RT-PCR. rRNA is used as a control for the total RNA content used in RT-PCR. (A) Synergistic activation by RA and E2. (B) Suppression by TAM of RA-induced activation, and its cancellation by E2. (C) Synergistic inhibition by DEAB and TAM. (D) Rescue by RA from the synergistic inhibition by DEAB and TAM. (E, F) Embryos were treated as indicated and examined by *in situ* hybridization for *ahr1* expression at 48 hpf (E) and for *rara* expression at 36 hpf (F). Closed arrowhead, *ahr1* expression at PBA; open arrowhead, no expression.

**Figure 26. ER $\alpha$  is essential for *ahr1* expression and vascular formation.**

**(A)** Transcript levels from *era1* (ER $\alpha$ ) and  $\beta$ -actin genes at the indicated developmental period. **(B)** Activation of *ahr1* and genes for choriogenins (*chg*) H and L at 36 hpf after electroporation with increasing doses of the *era1*-plasmid (pOL22). **(C)** Inhibition of the *era1*-induced overexpression of *ahr1* and *chg*-H by the treatment with TAM. **(D)** Inhibition of the *era1*-induced overexpression of *chg*-H by the antisense-*era1*-plasmid (pOL23). Transcript levels of *chg*-H were normalized by  $\beta$ -actin RNA. **(E)** Inhibition of *ahr1* expression in the embryos treated with the antisense-*era1*-plasmid followed by incubation in the presence of DEAB. **(F)** Restoration from the antisense-*era1*-induced inhibition of *ahr1* by the *era1*-plasmid. **(G)** Embryos (upper, 4 dpf; lower, 3 dpf) treated with or without the antisense-*era1*-plasmid followed by incubation in the presence or absence of DEAB. Vascular damages represented by blood clots on the yolk (arrow) and at the blood island (arrowhead). % Embryos with vascular damages are shown. GFP-expressing embryos (approximately 20% of the treated embryos) were collected at 36 hpf for extraction of total RNA and at 2 dpf for observation of vascular damages at 3 dpf in (E) to (G). DNA concentrations ( $\mu\text{g}/\mu\text{l}$ ) of the plasmids in 10 x Yamamoto's solution were as follows: 0.01, 0.05, 0.1, and 0.5 for pOL22 in (B); 0.5 for pOL22 in (C); 0.05 for pOL22 and 0.5 for pOL23 in (D); 0.5 for pOL21 and pOL23 in (E); 0.5 for pOL21, pOL22, and pOL23 in (F, G).  
\*  $p < 0.01$ , \*\*  $p < 0.05$ .

**Figure 27. Control of *raldh2* expression by RA and maternal estrogen.**

Embryos were treated with DEAB (10  $\mu\text{M}$ ), RA (10 nM), TAM (4 mg/l), and R115866 (1.0  $\mu\text{M}$ ) as indicated and examined for *raldh2* expression. **(A)** Activation by DEAB and inhibition by RA. **(B, C)** Rescue by TAM from the RA-induced inhibition at 18 hpf (B) and 36 hpf (C). **(D)** Synergistic activation by co-treatment with DEAB and TAM. **(E)** Rescue by TAM from the inhibition by R115866-induced RA excess. **(F)** Inhibition by RA but no effect of TAM after pretreatment with cycloheximide. \*  $p < 0.01$ .

**Figure 28. Control of *cyp26a1* expression by RA and maternal estrogen.**

Embryos were treated with RA (10 nM), R115866 (1.0  $\mu$ M), DEAB (10  $\mu$ M), and TAM (4 mg/l) as indicated and examined for *cyp26a1* expression. **(A)** Activation by RA or R115866, and inhibition by DEAB. **(B)** Direct activation by RA. **(C)** Cancellation by TAM of the RA-induced activation.

**Figure 29. Effects of overproduction and knockdown of ER $\alpha$  on expressions of *raldh2*, *rara*, and *cyp26a1*.**

Embryos were injected with plasmid DNA (pOL21 for control; pOL22 for overproduction of ER $\alpha$ ; and pOL23 for knockdown of ER $\alpha$ ), added with cycloheximide at 18 hpf, and fixed at 23 hpf. RA was added at 10 hpf. **(A)** Activation of *raldh2* by overproduction or knockdown of ER $\alpha$ . **(B)** RA-induced repression of *raldh2* and its additional reduction by knockdown of ER $\alpha$ . **(C)** Activation of *rara* by overproduction or knockdown of ER $\alpha$ . **(D)** Activation of *cyp26a1* by overproduction of ER $\alpha$ . No effect of knockdown of ER $\alpha$  on *cyp26a1* expression. **(E)** RA-induced activation of *cyp26a1* and its reduction by knockdown of ER $\alpha$ .

**Figure 30. TAM advances RA-excess phenotypes.**

**(A)** Synergistic inhibition of vascular formation by TAM and R115866. 3-dpf embryos are also shown. \*  $p < 0.001$ ; \*\*  $p < 0.0002$ . **(B)** Synergistic activation of *rara* expression at 36 hpf by TAM and R115866. \*  $p < 0.0003$ ; \*\*  $p < 0.0001$ . **(C)** Synergistic activation of *rara* expression at 18 hpf by TAM and R115866. \*  $p < 0.05$ . **(D)** Synergistic inhibition of vascular formation by TAM and 4-oxo-RA. \*  $p < 0.01$ . **(E)** Synergistic activation of *rara* expression at 18 hpf by TAM and 4-oxo-RA. \*  $p = 0.00001$ ; \*\*  $p < 0.00001$ .

**Figure 31. A model for how maternal estrogen/ER $\alpha$  controls RA metabolism and signaling.** RA is produced by *Raldh2* from maternally deposited retinal. RA is converted to 4-OH-RA by *Cyp26a1* and led to the degradative pathway through an active retinoid, 4-oxo-RA. RA level is controlled by the feedback mechanisms. RA directly represses *raldh2* expression and activates *cyp26a1* expression in order to lower RA level. RA is also involved in the feedback regulation indirectly through inhibition of *fgf8* that is both an activator for *raldh2* and a negative regulator against *cyp26a1*. RA is required for expressions of *rara* and *ahr1* that are essential for the formation of CCV, prospective Cuvierian ducts. RA is also required for A-P patterning of hindbrain (not shown). Maternal estrogen/ER $\alpha$  (oval with a pen point) acts cooperatively with RA. Inhibition of its function with an anti-estrogen, TAM, or knockdown of ER $\alpha$  abolishes the feedback regulation of RA level, resulting in excess RA. On the contrary, excess estrogen or overproduction of ER $\alpha$  stimulates degradation of RA. Maternal estrogen/ER $\alpha$ , on the other hand, activates RA signaling and is essential for vascular and hindbrain formation. *Fgf8* is required for RA synthesis by activating *raldh2* and, independently of it, for CCV formation. Regional expression of *cyp26a1* in the anterior brain is regulated in part through *fgf8* function in the cell migration during epiboly/gastrulation. *Lower left*, expression patterns of *cyp26a1*, *fgf8*, and *raldh2* in the 50% epiboly, in which RA level is controlled by the regulatory circuit shown above. *Lower right*, expression patterns of *ahr1* (PBA), *fgf8* (MHB and adaxial mesoderm), *krox20* (r-3 and r-5), *rara* (r-7 to r-8), *shh* (midline), and *vegfr1* (precursor of CCV), and the expression of VEGF, which is proposed to be under control of *ahr1* and is required for accumulation of *vegfr1*<sup>+</sup> cells at PBA (Sada *et al.*, 2019).

**Figure 1. Hyperactivation of ER $\alpha$  causes loss of CCV.**

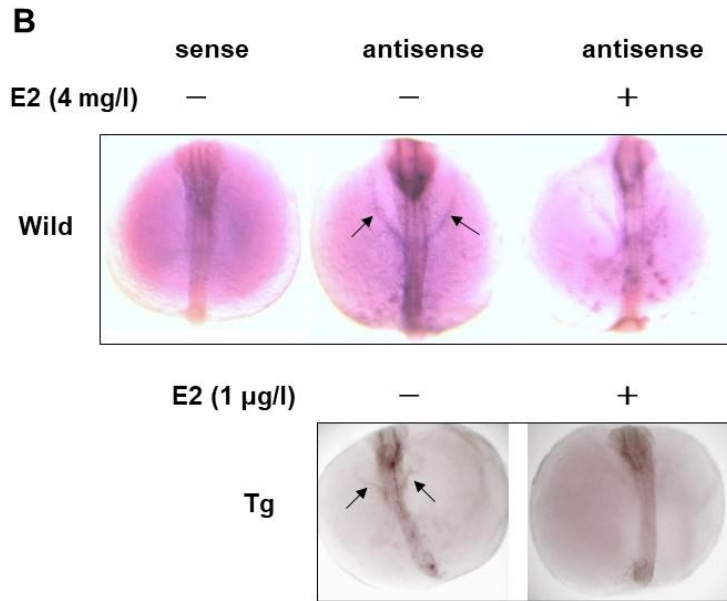
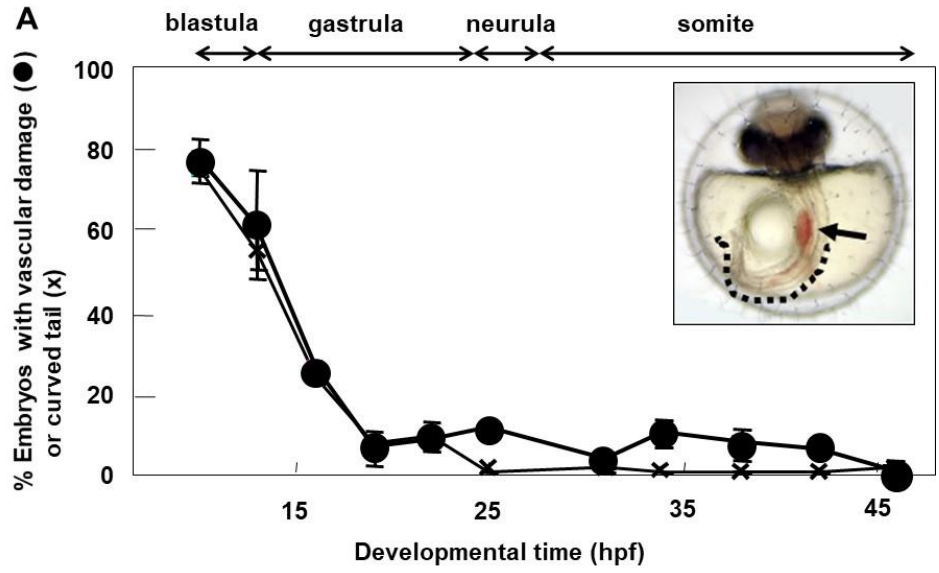


**Figure 2. Excess RA causes loss of CCV.**

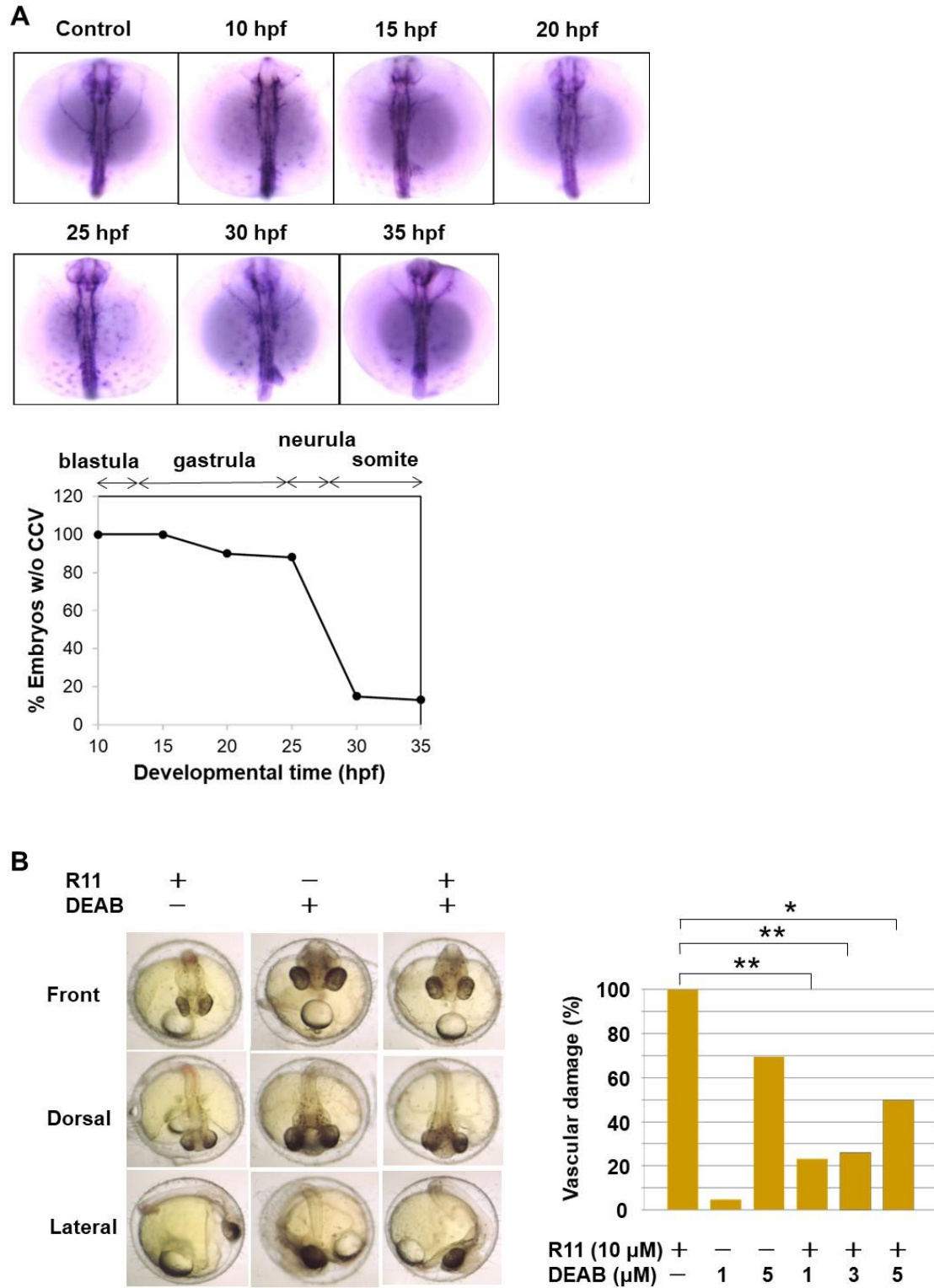


**Figure 3. MAP kinase pathway inhibitor (PD98059) causes loss of CCV.**

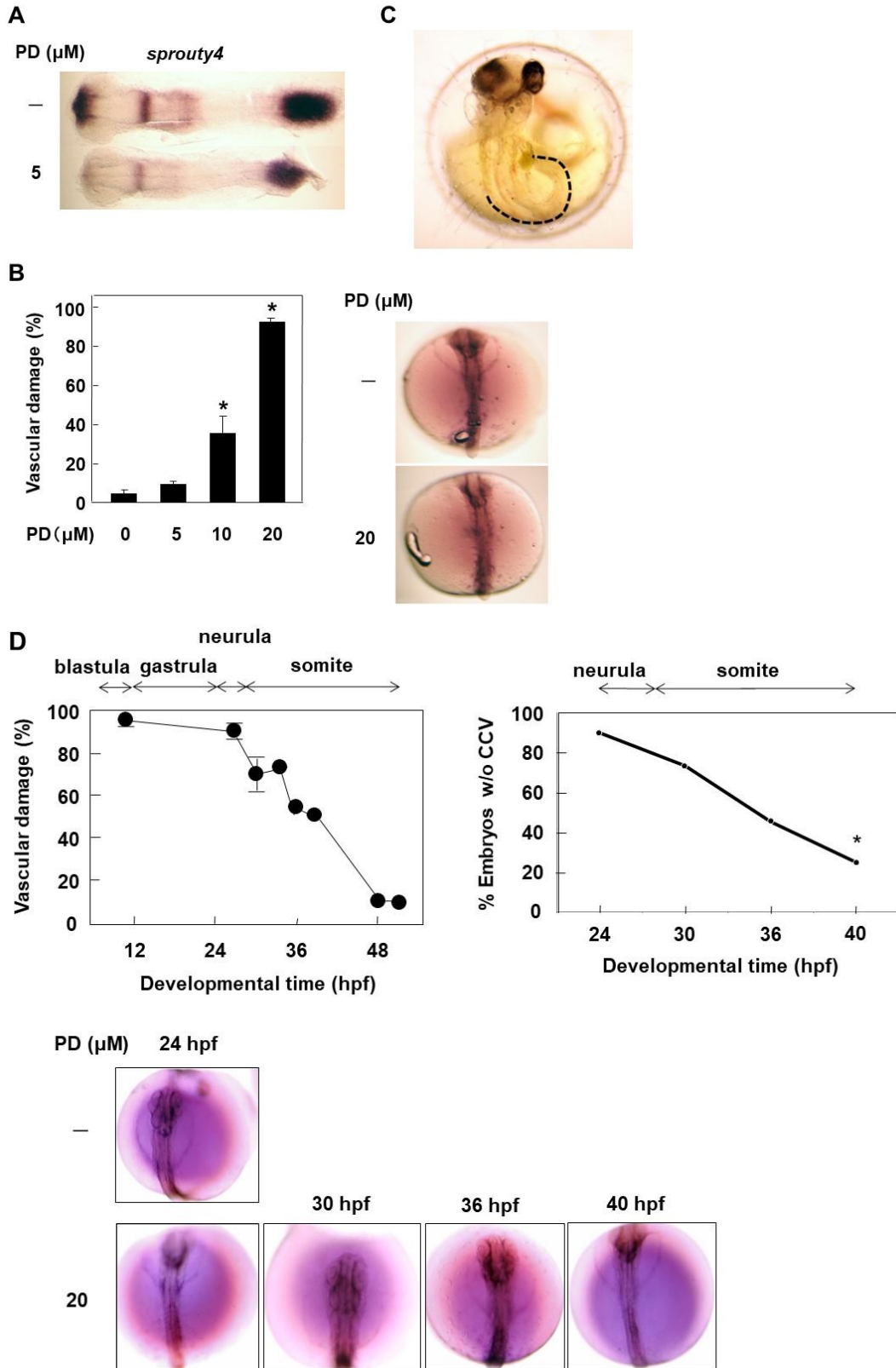
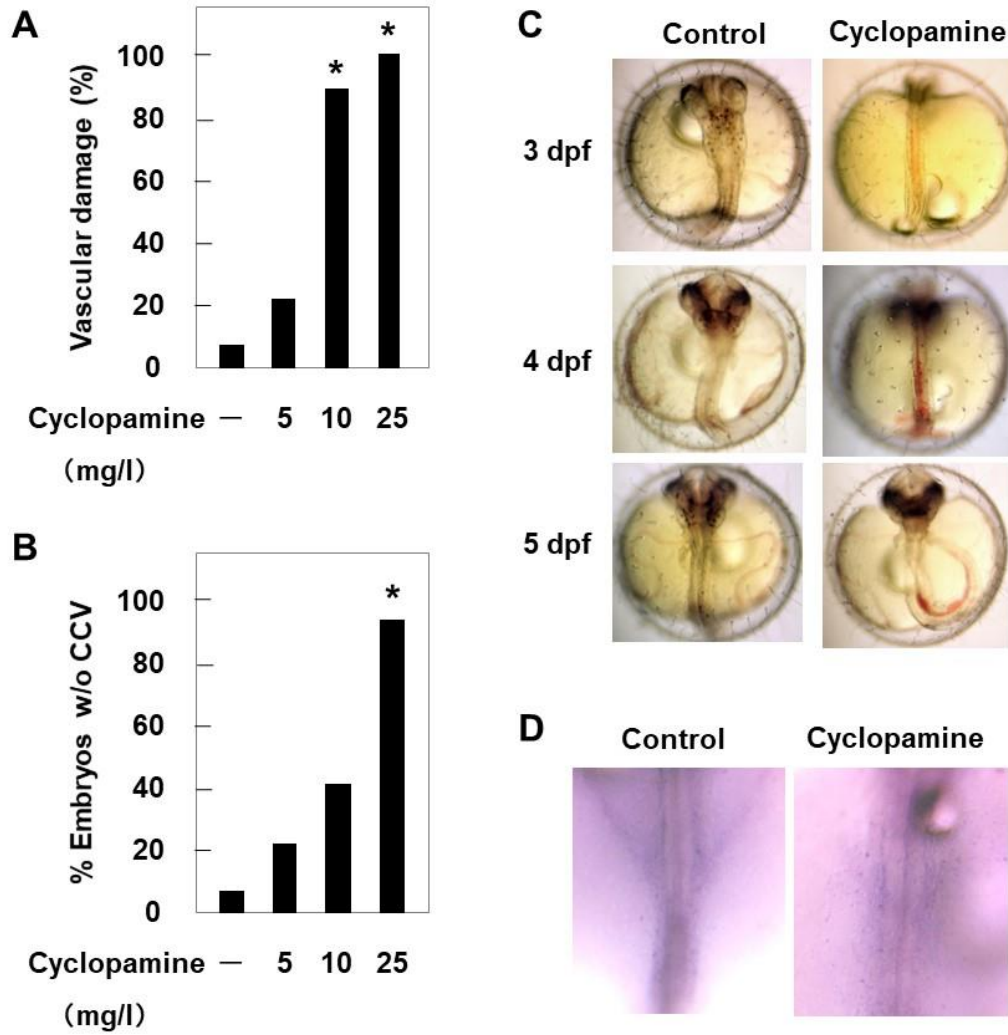
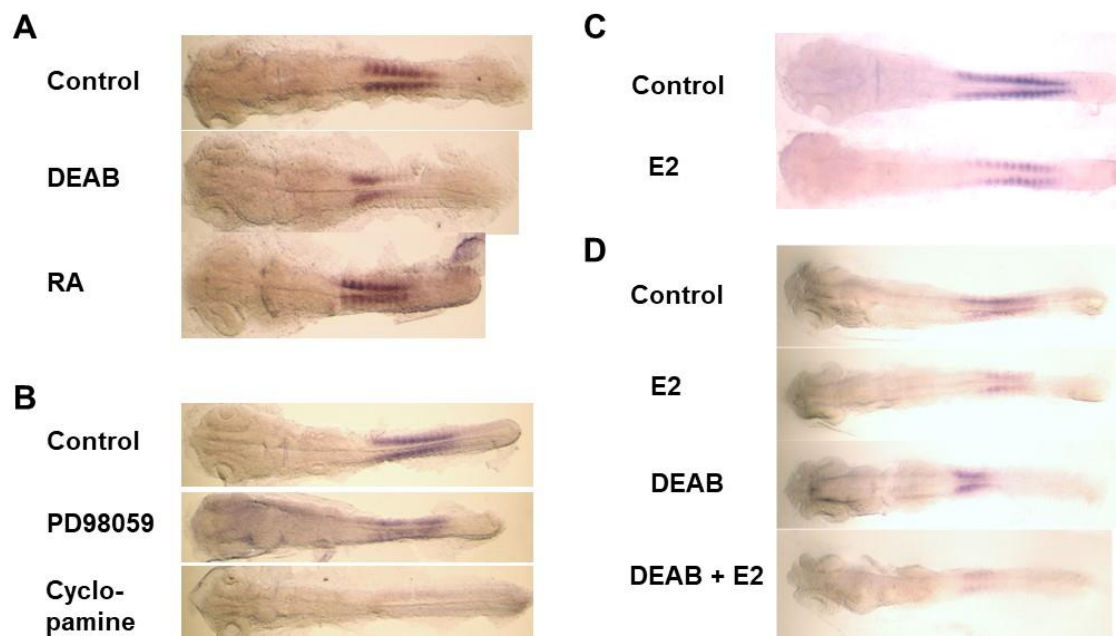


Figure 4. Cyclopamine causes loss of CCV.



**Figure 5. Effects on *myoD* expression of DEAB, RA, PD98059, cyclopamine, and E2.**



**Figure 6. Effects of E2, PD98059, and DEAB on expressions of *shh* and *no tail*.**

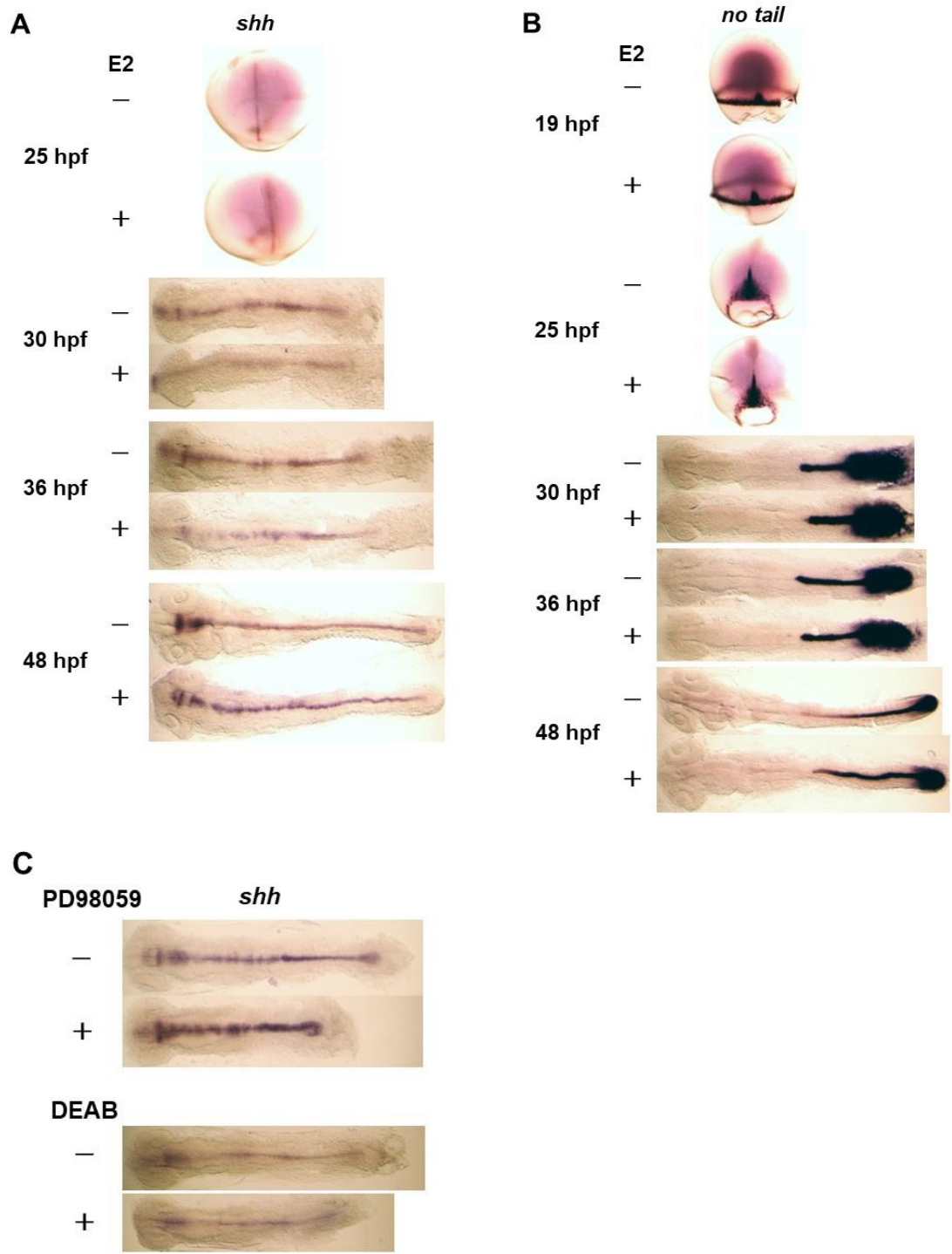


Figure 7. Synergistic effects.

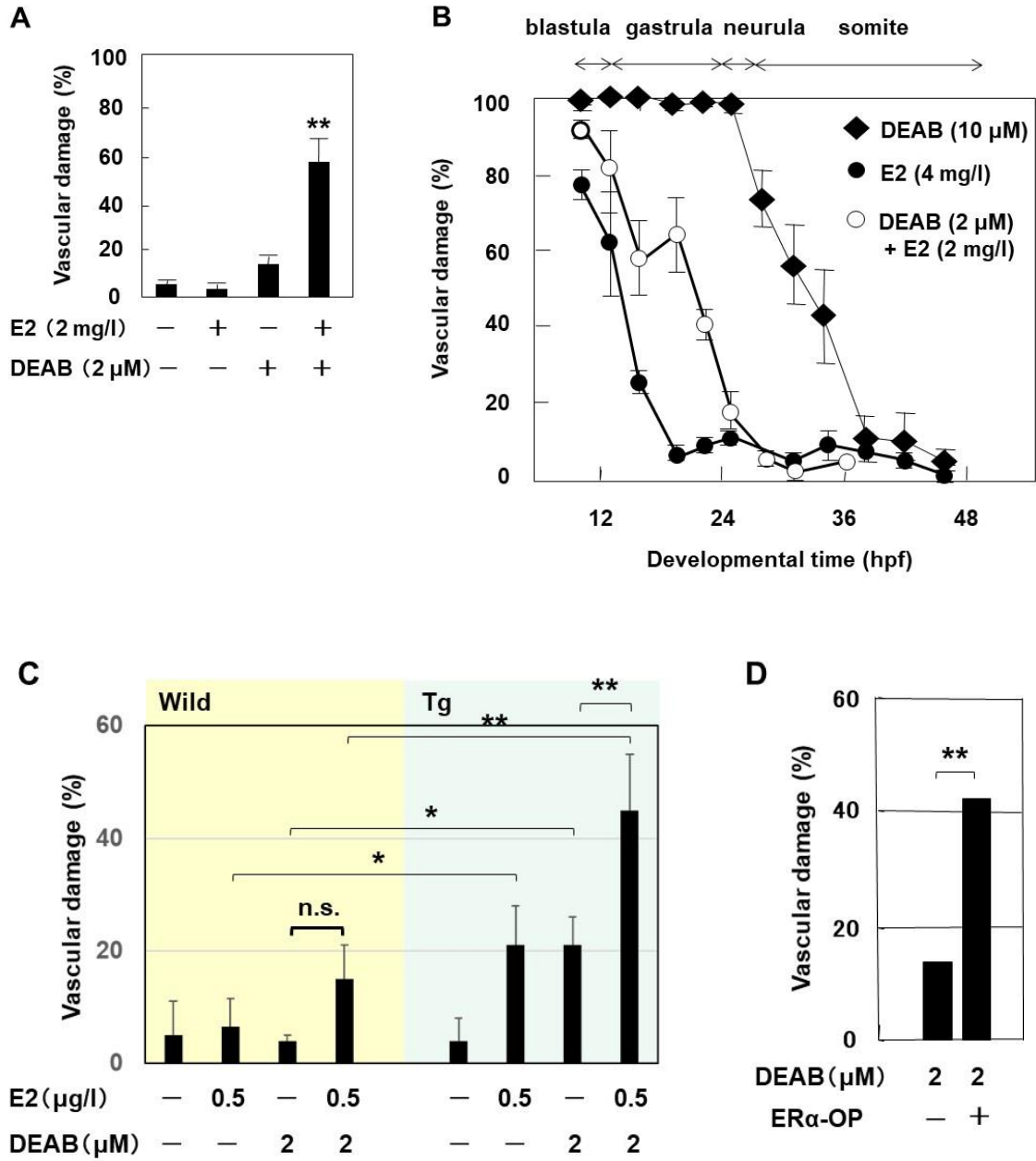


Figure 7. (continued)

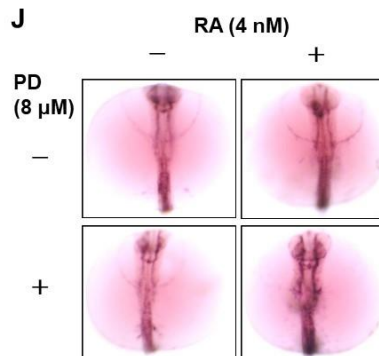
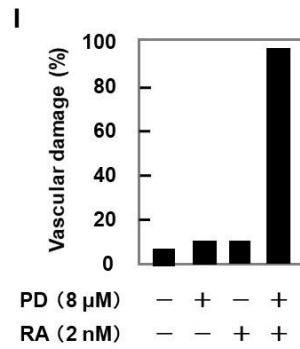
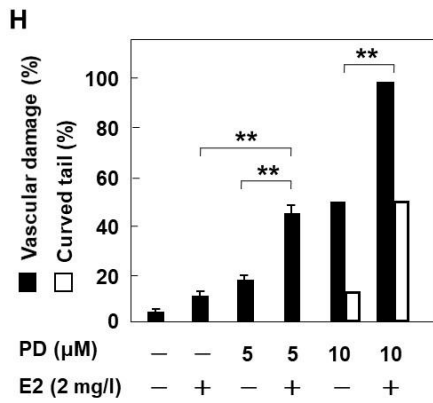
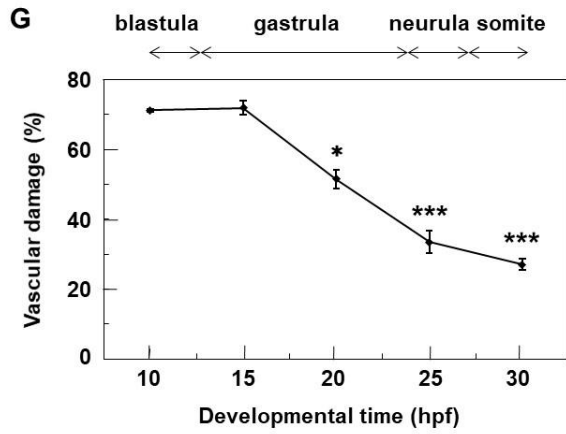
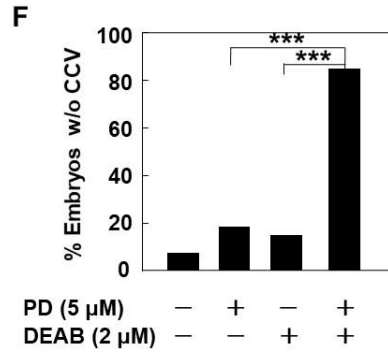
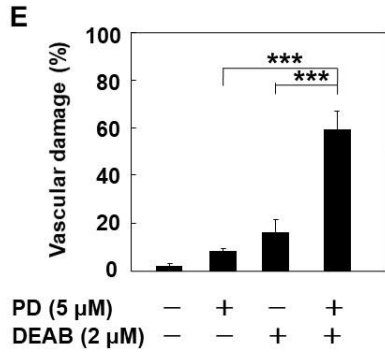
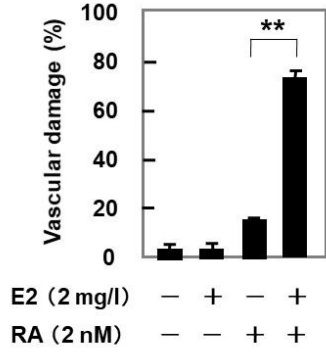
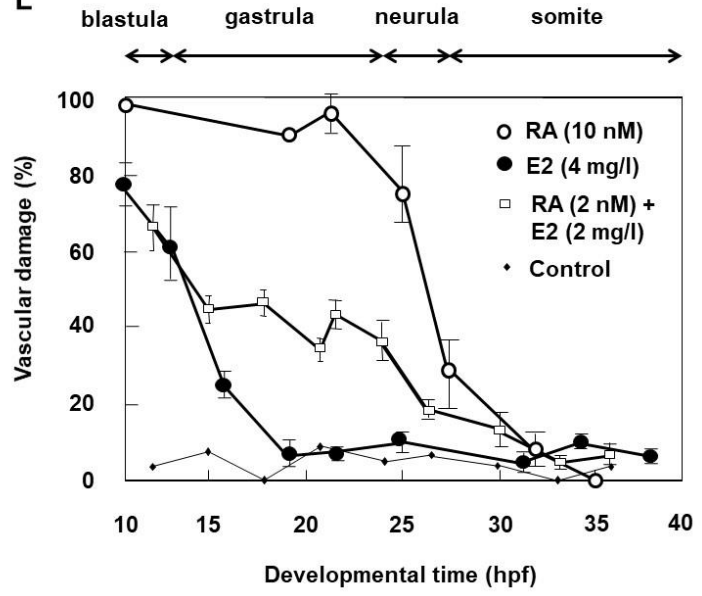


Figure 7. (continued)

K



L



**Figure 8. Effect of E2 on hindbrain formation.**

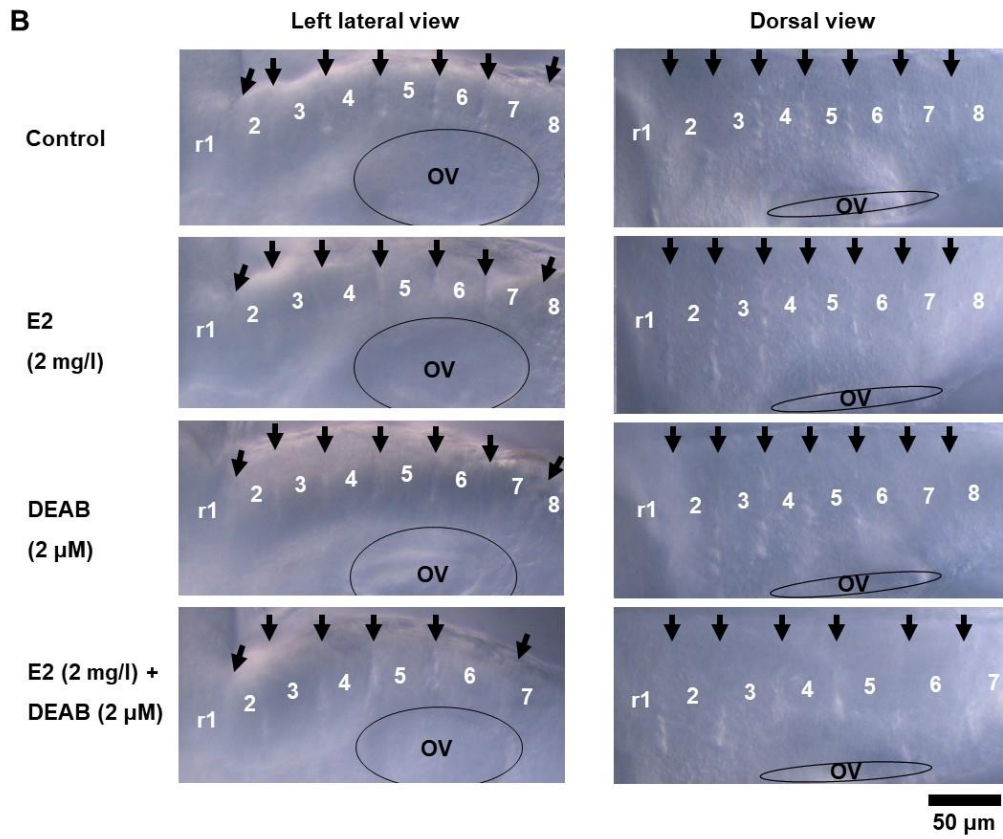
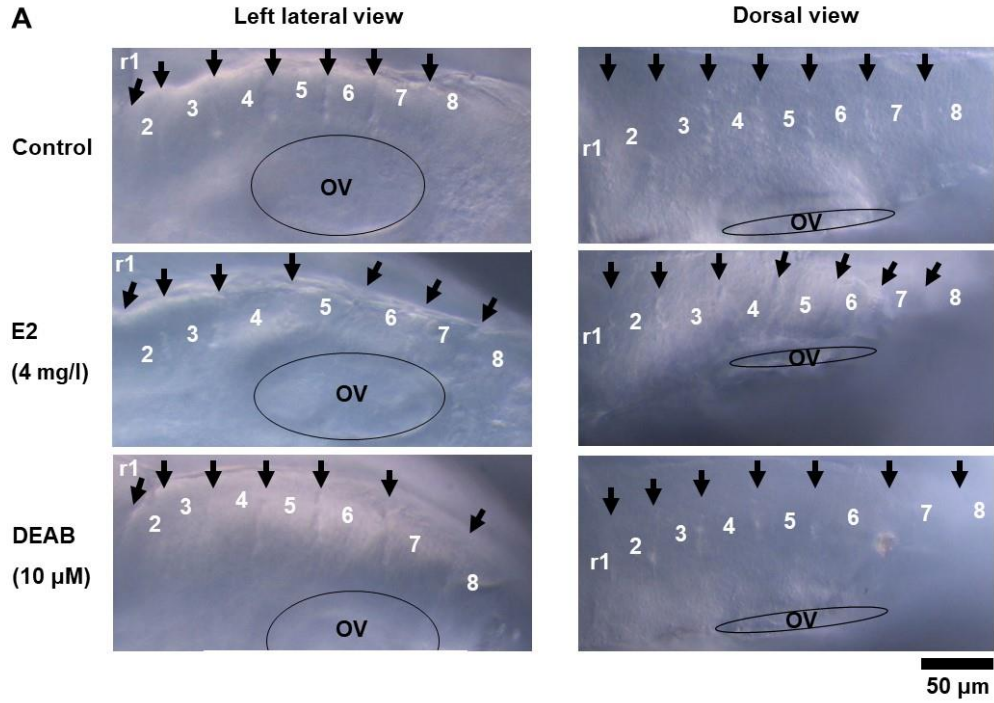


**Figure 9. Effect of E2 on RA-inducible gene expression.**

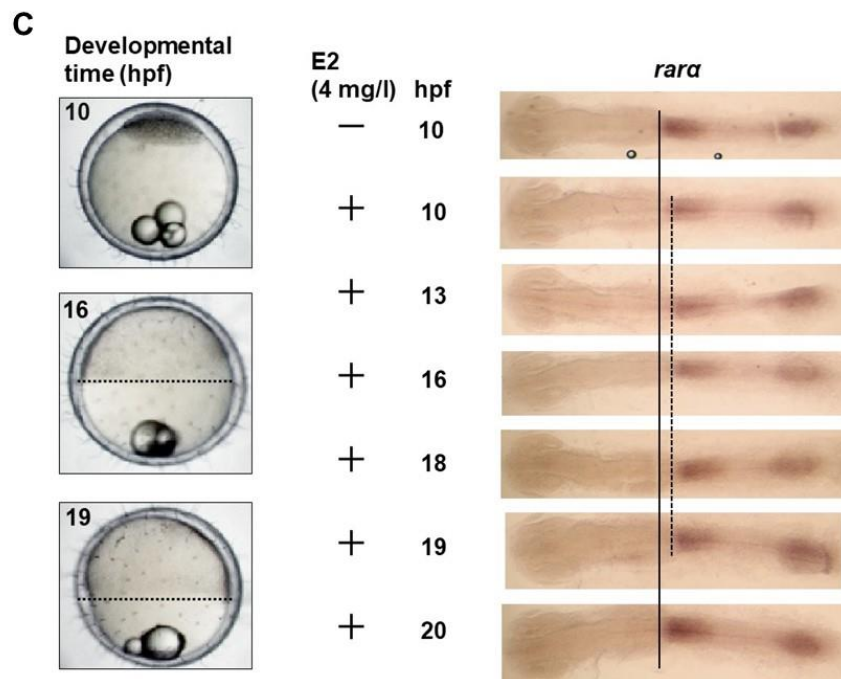
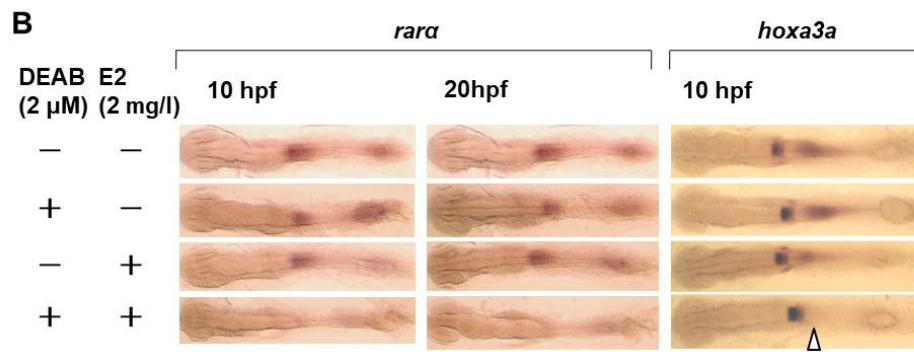
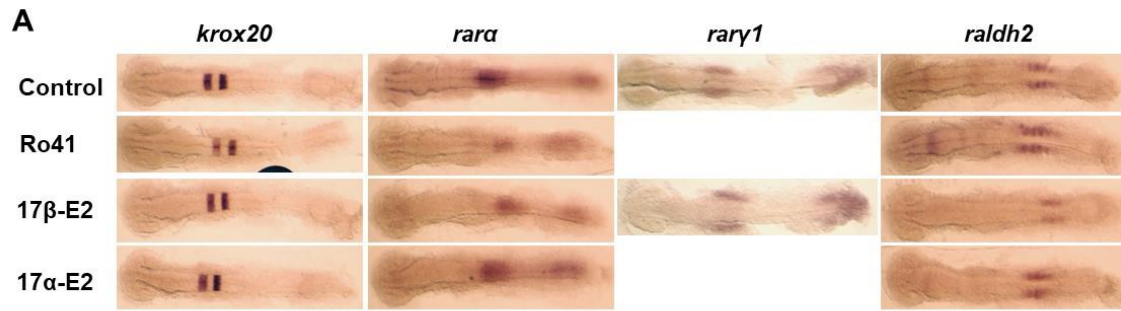


**Figure 9. (continued)**

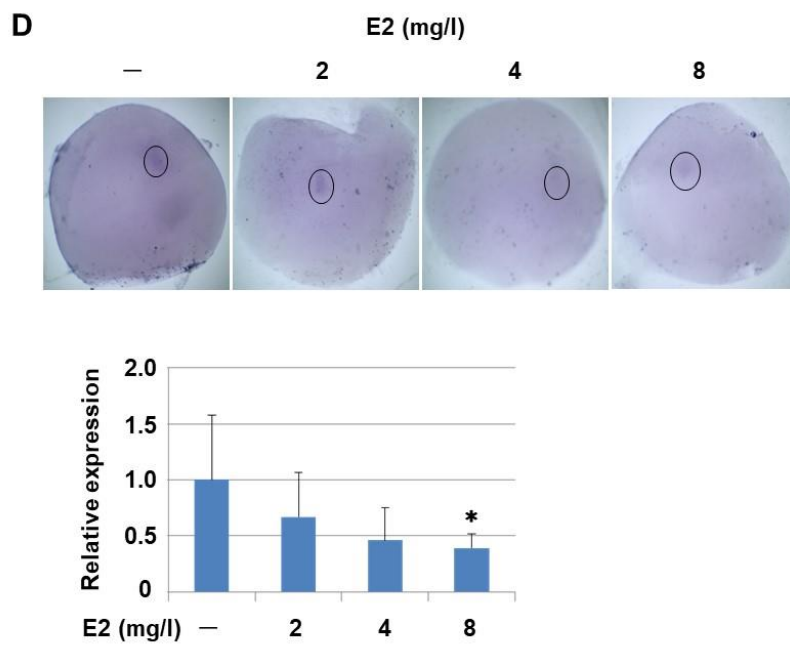


Figure 10. Effect of E2 on *raldh2* and *cyp26a1* expression.

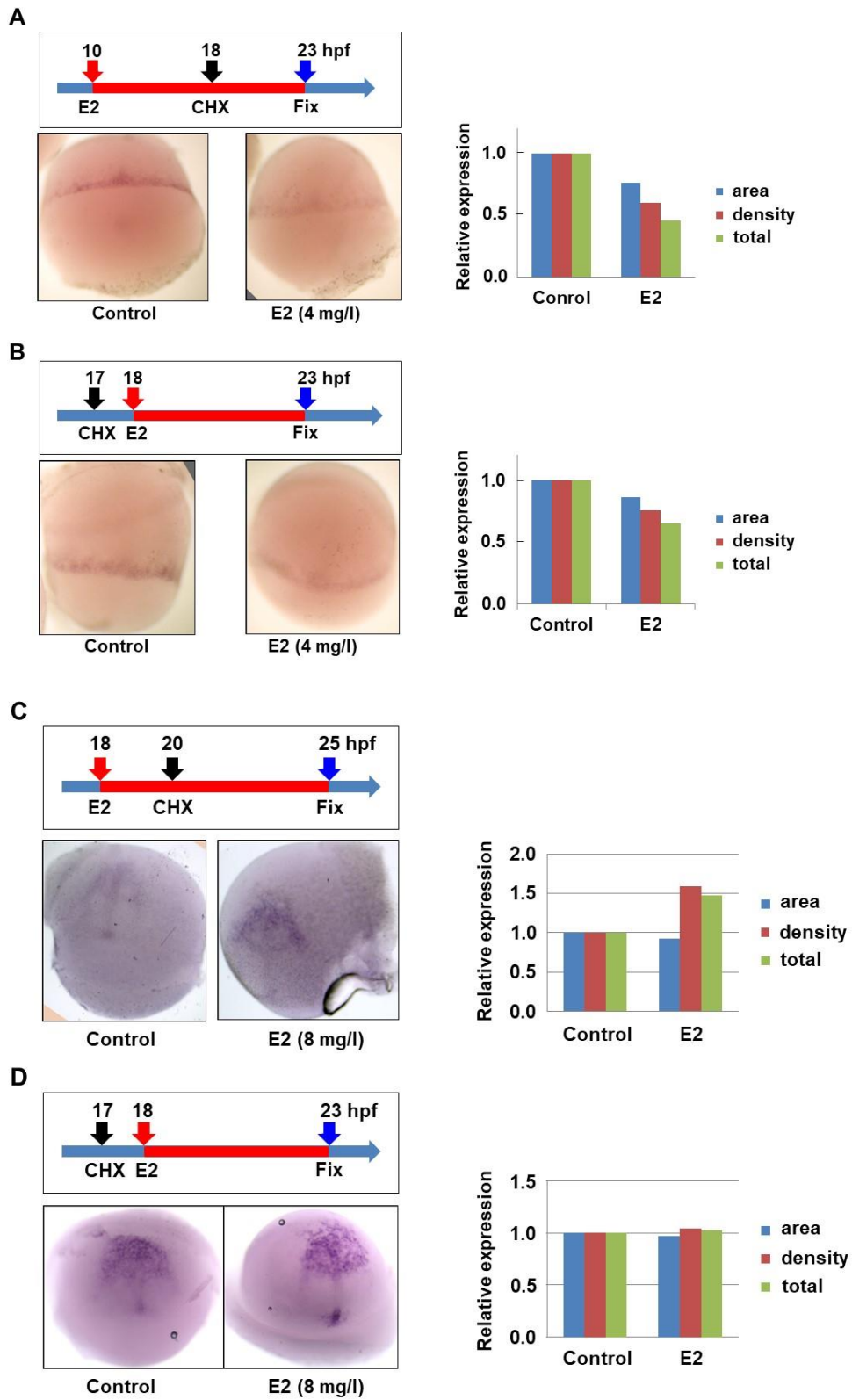




Figure 11. (continued)

D

*rara*

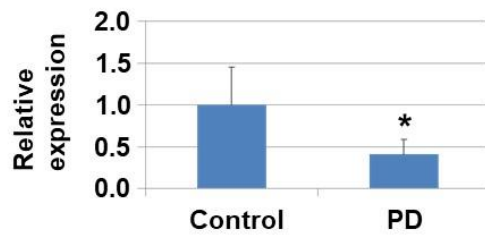
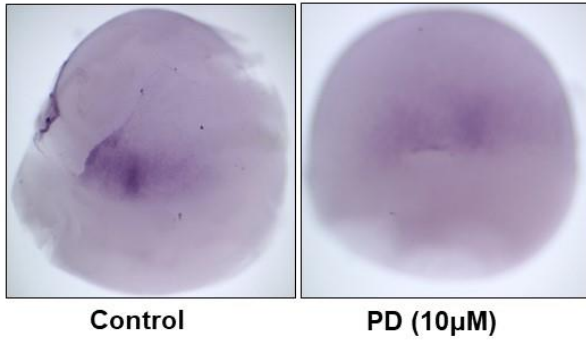


Figure 12. Effect of PD98059 on *raldh2* and *cyp26a1* expression.

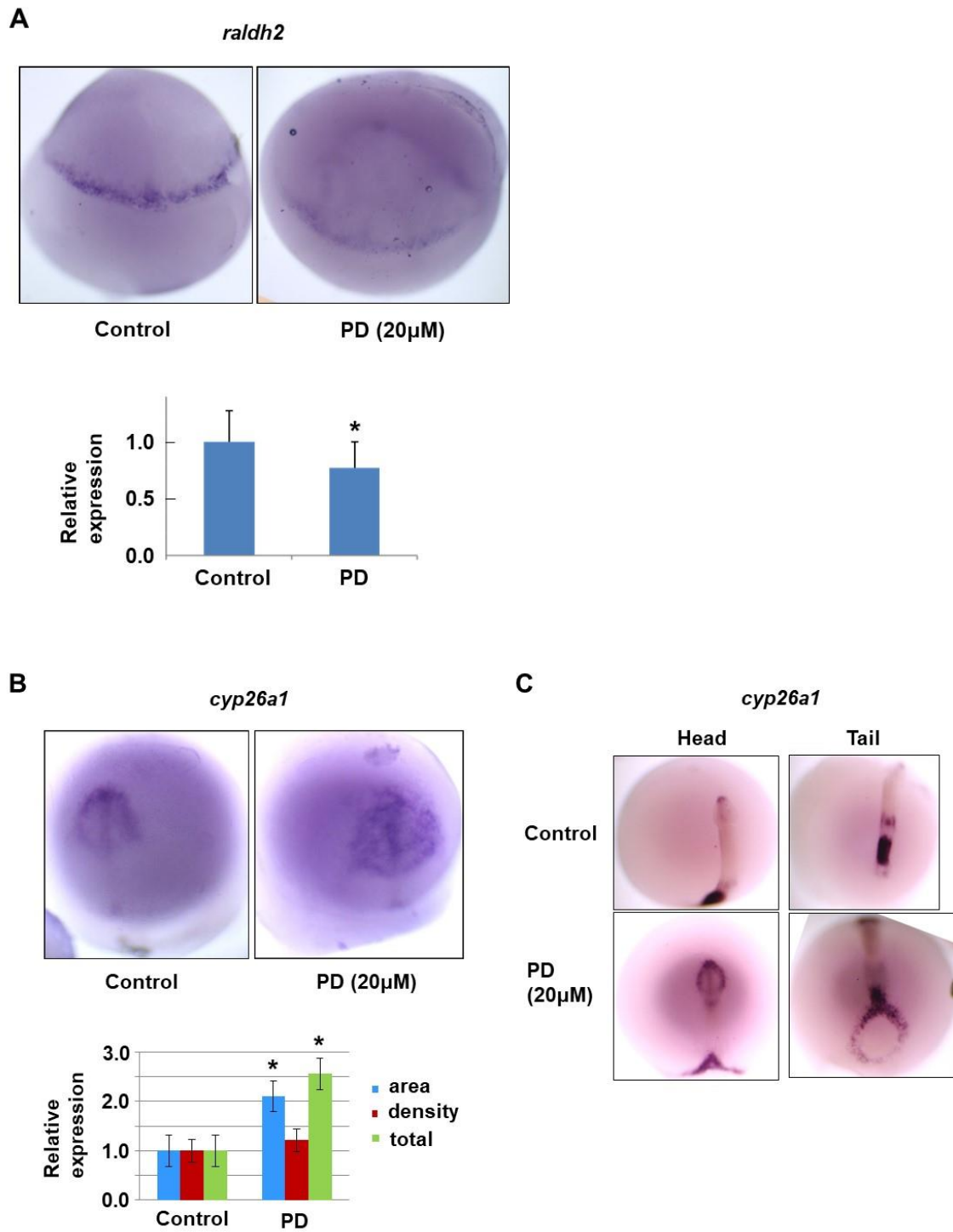
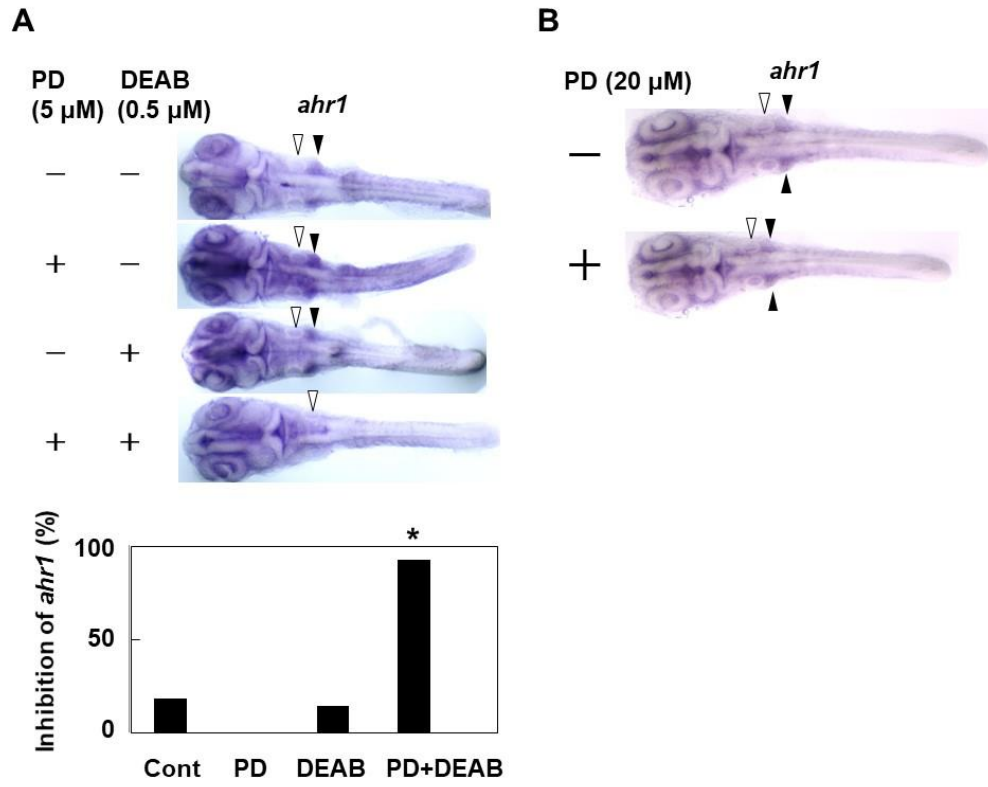


Figure 13. Effect of PD98059 on *ahr1* expression.



**Figure 14. Effect of E2 on FGF signaling.**

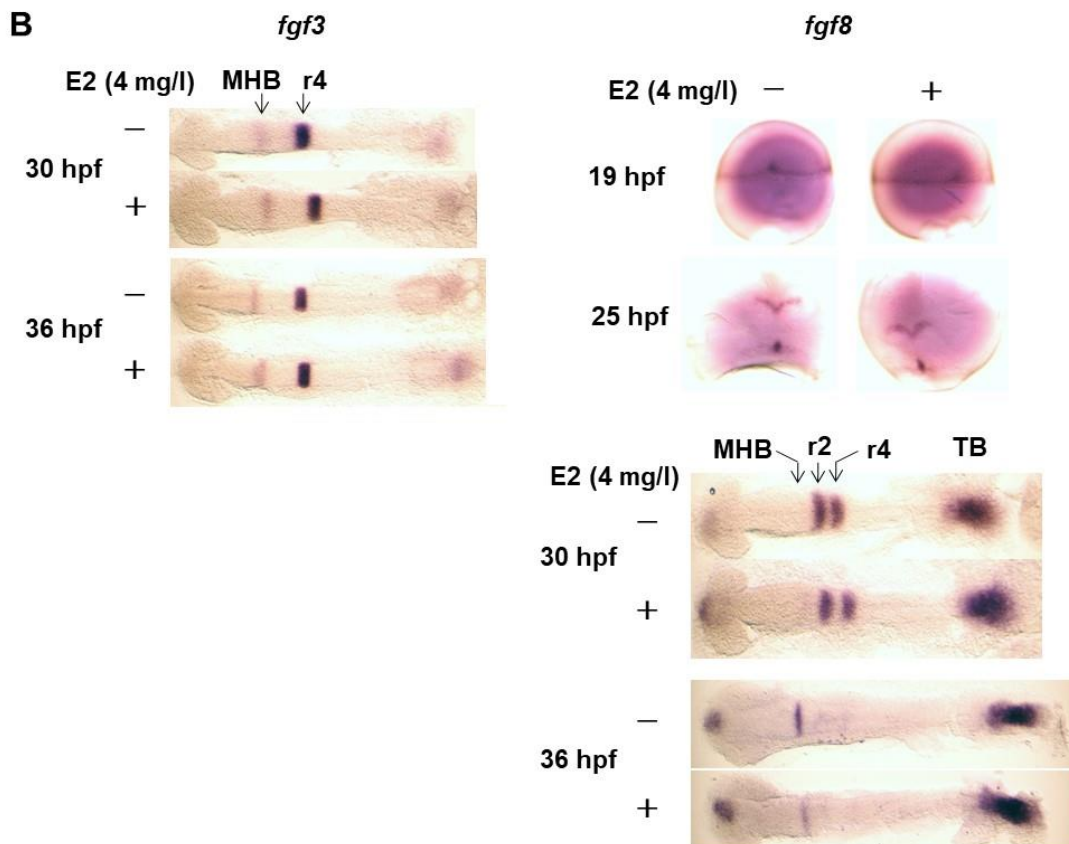
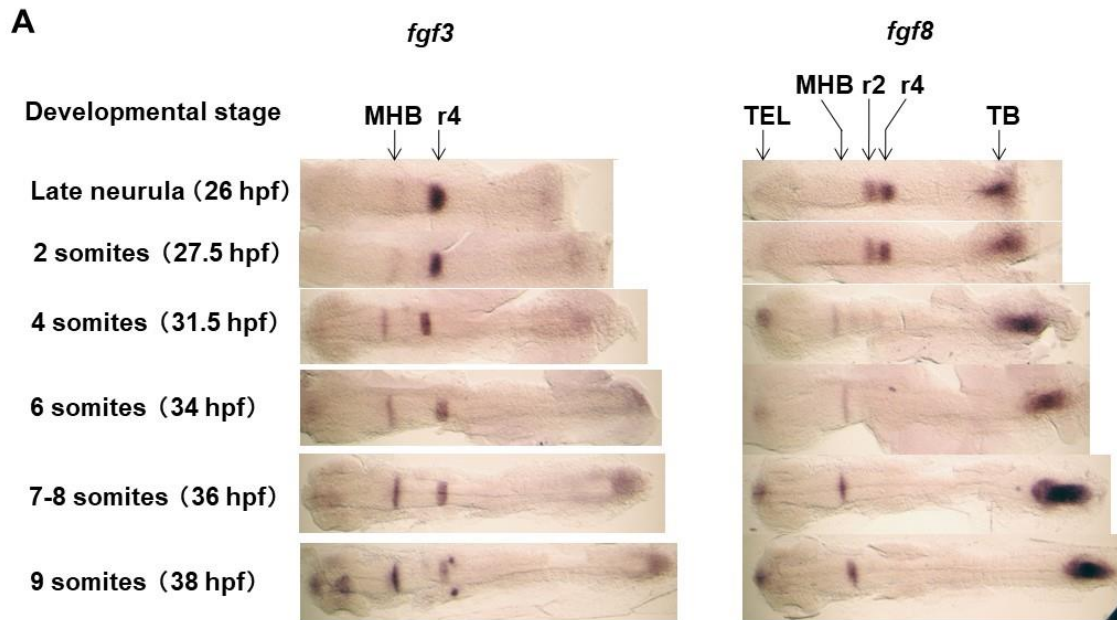


Figure 14. (continued)

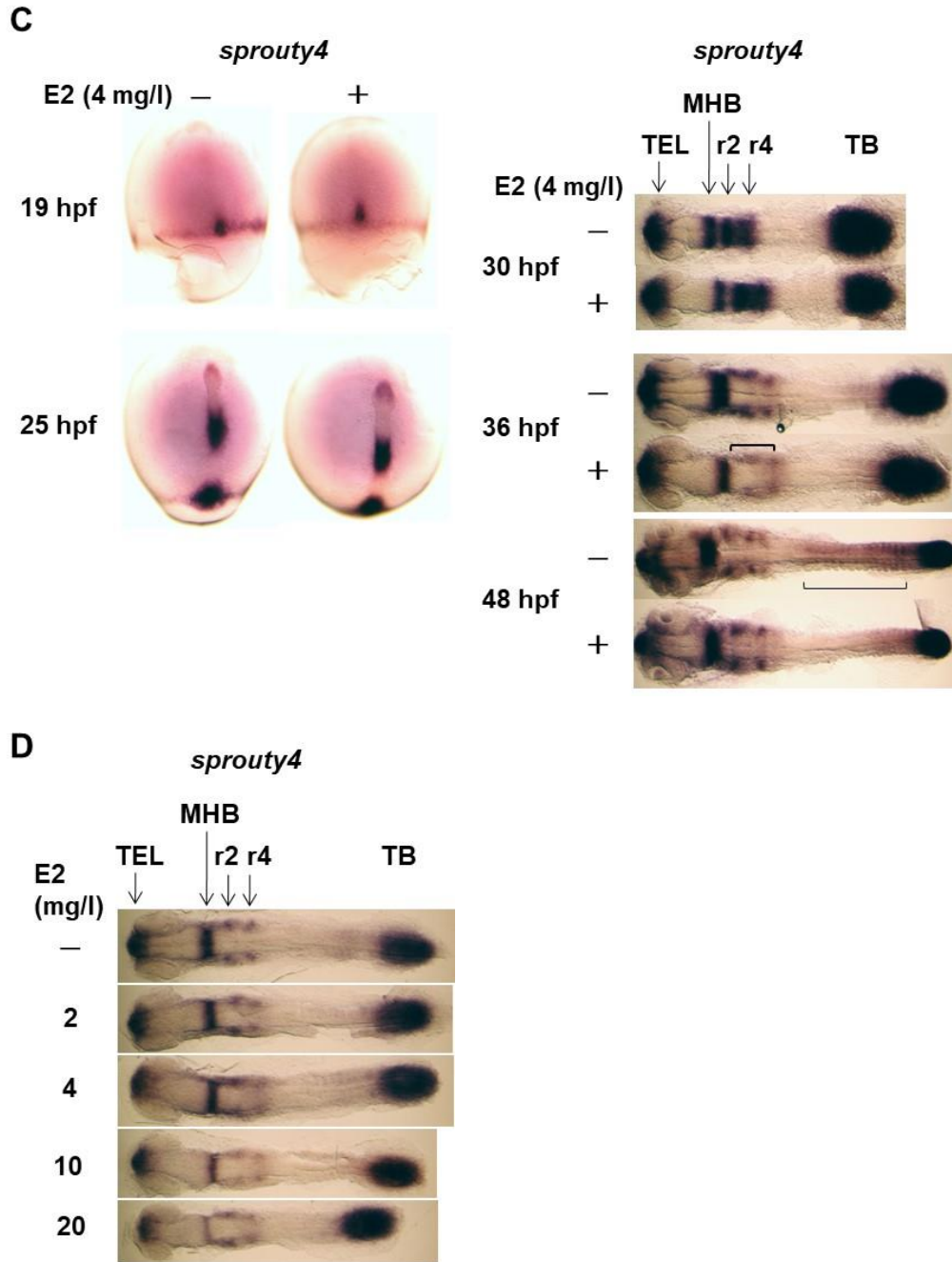


Figure 15. Effect of ER $\alpha$  overproduction on *fgf8* and *myoD* expression.

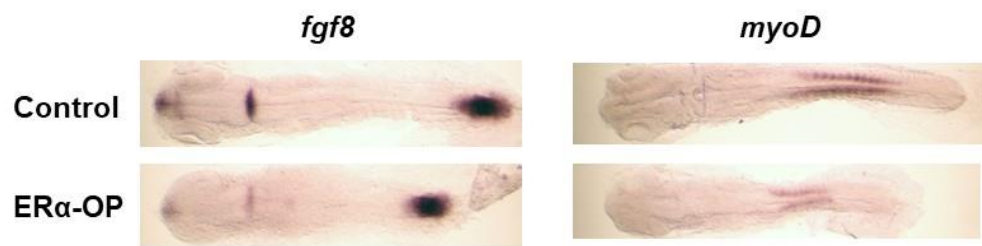


Figure 16. Effect of RA on *fgf8* and *sprouty4* expression.

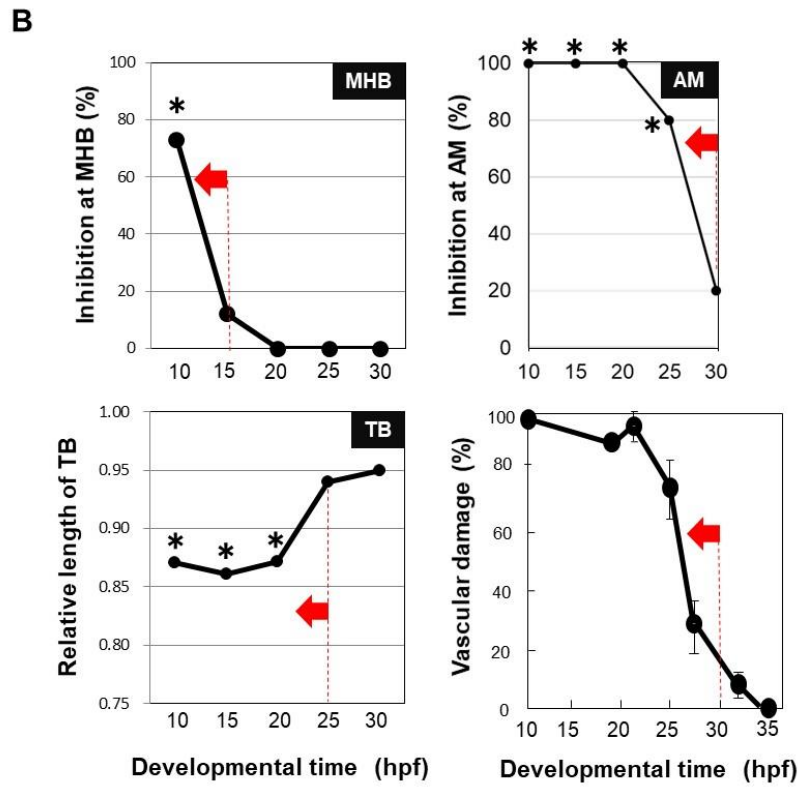
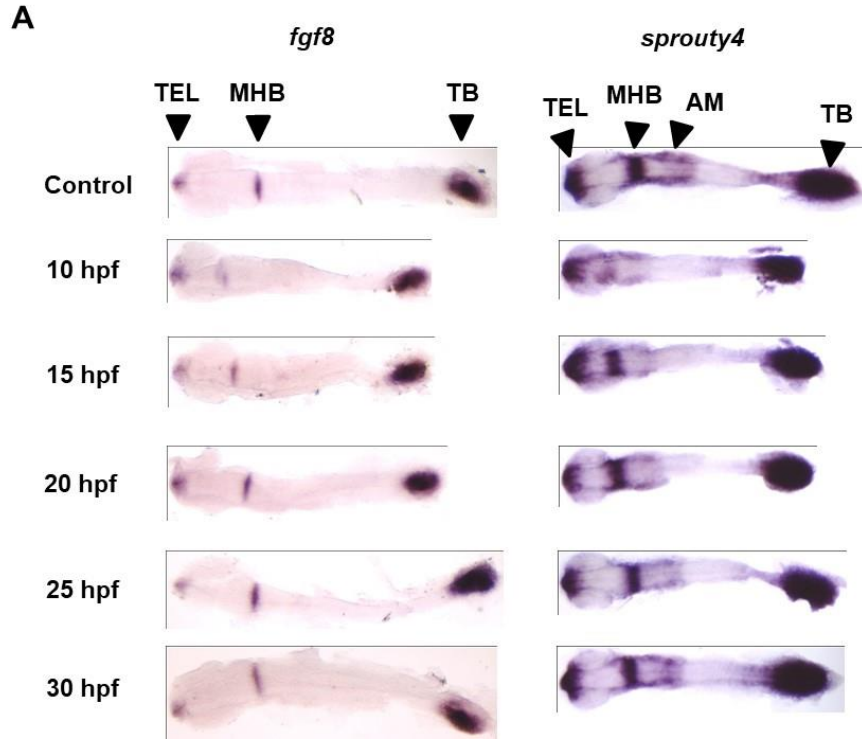
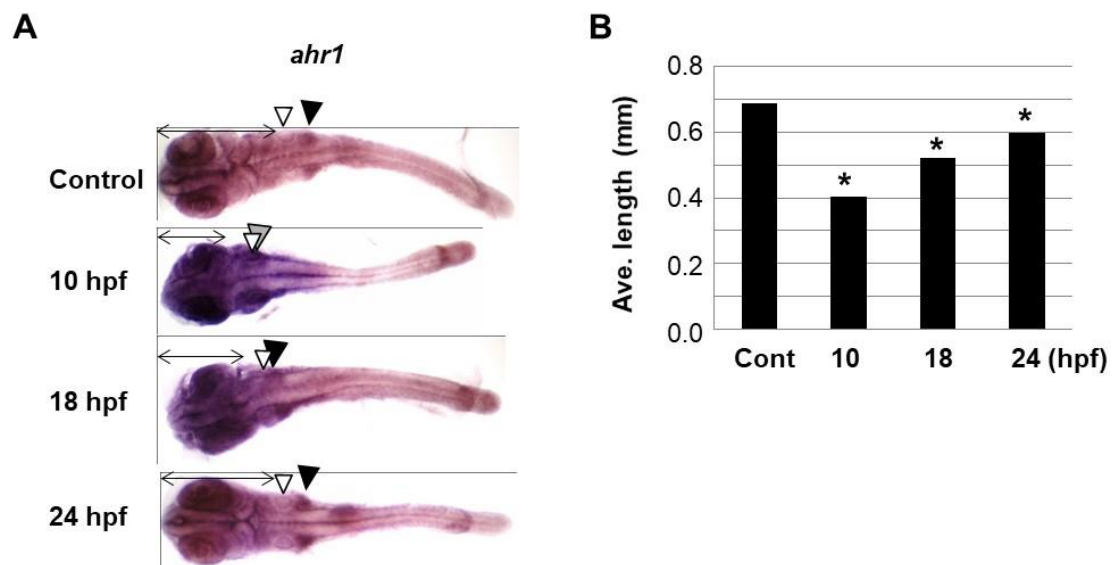
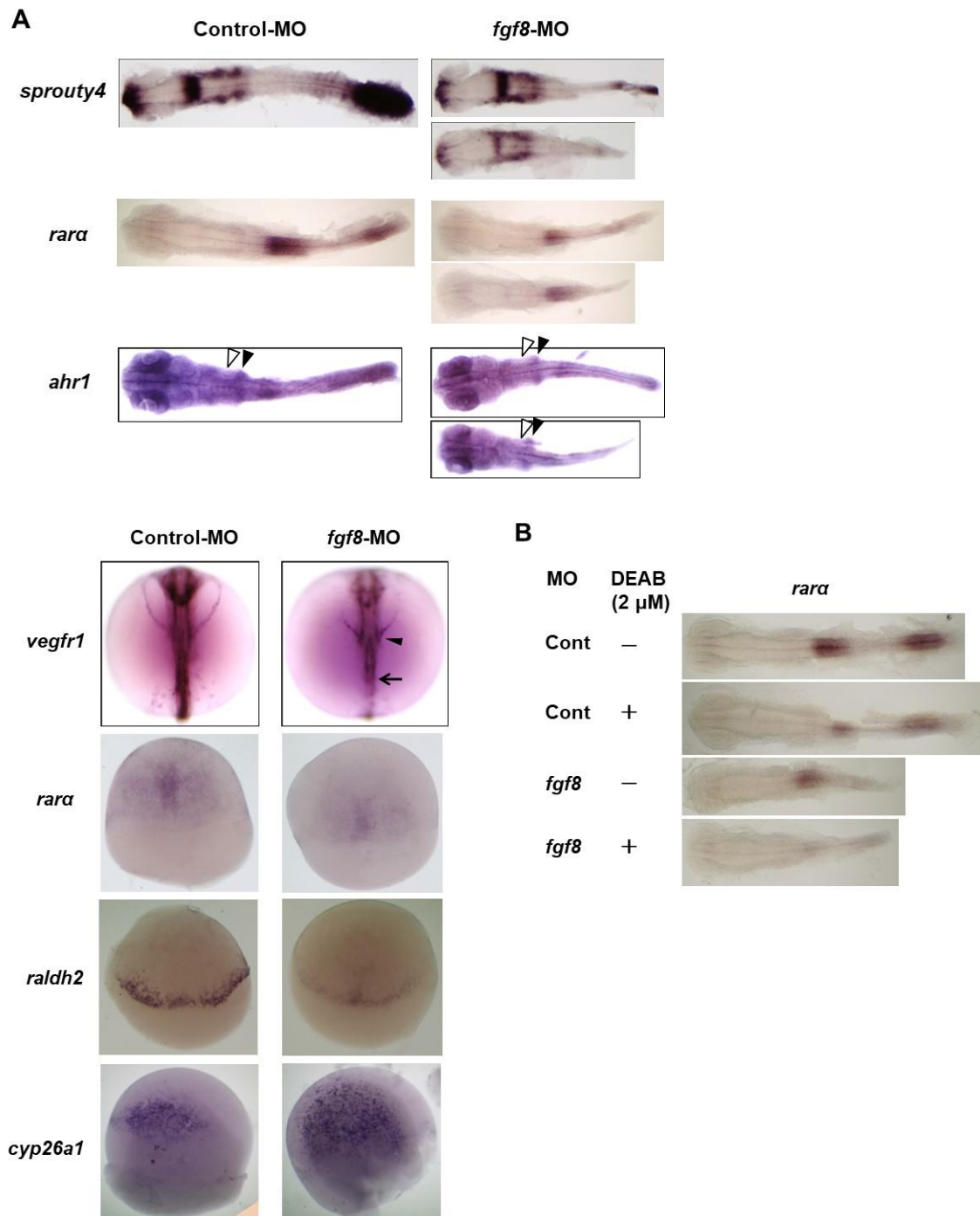


Figure 17. Effect of RA on *ahr1* expression.



**Figure 18. Effect of *fgf8* knockdown on CCV formation and RA metabolism and signaling.**



**Figure 19. Effect of antiestrogen on hindbrain formation.**

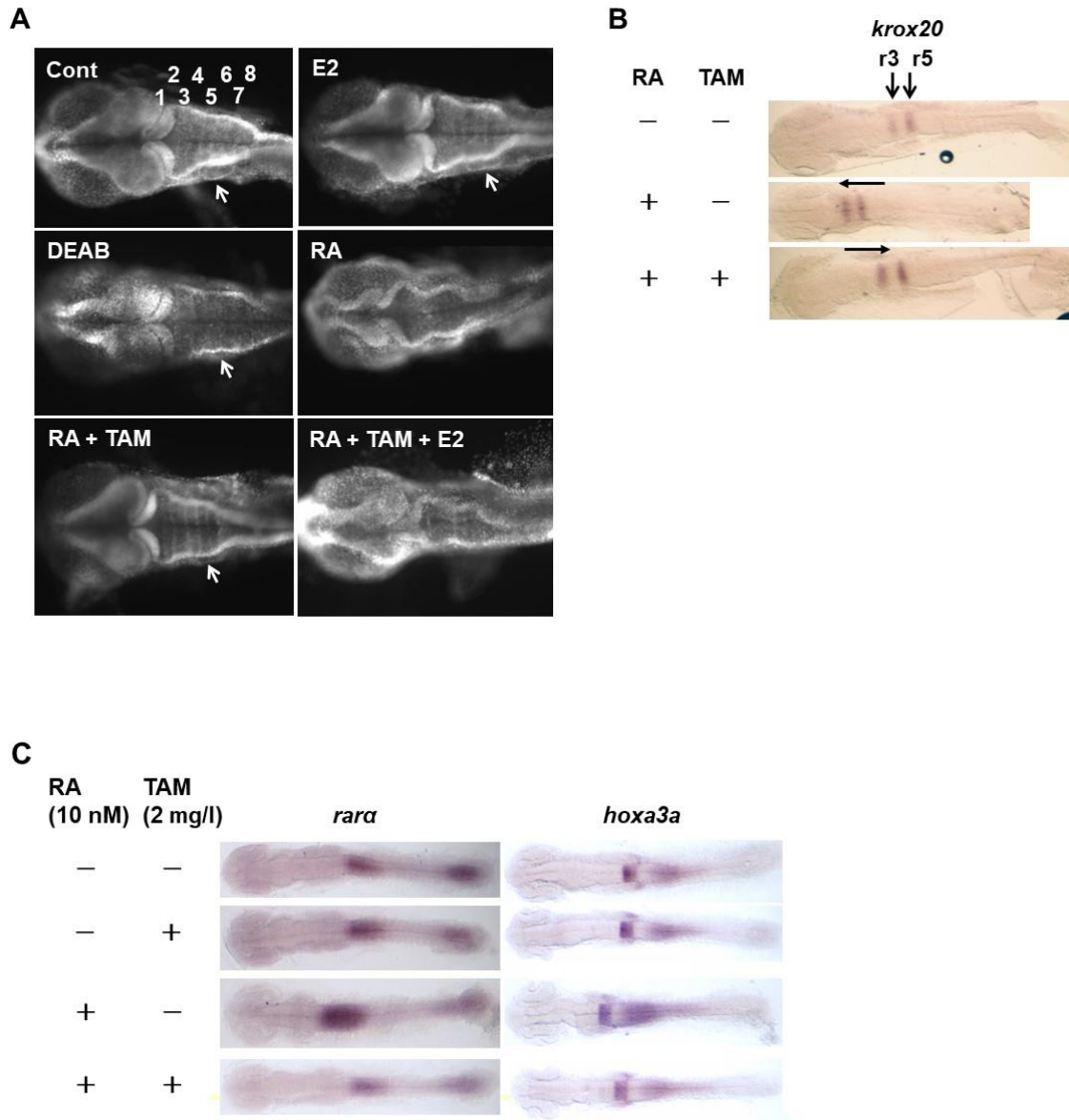


Figure 19. (continued)

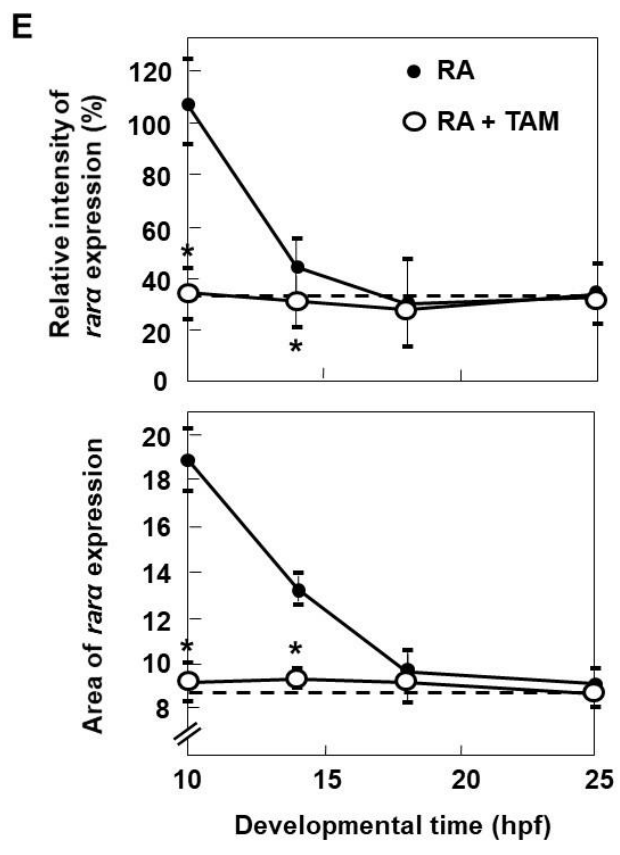
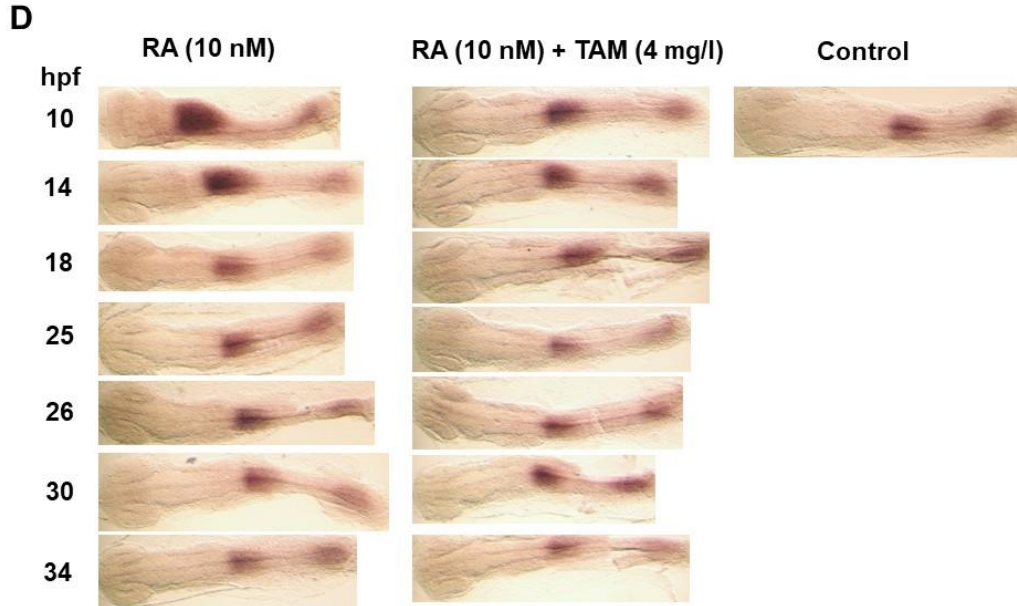


Figure 19. (continued)

F

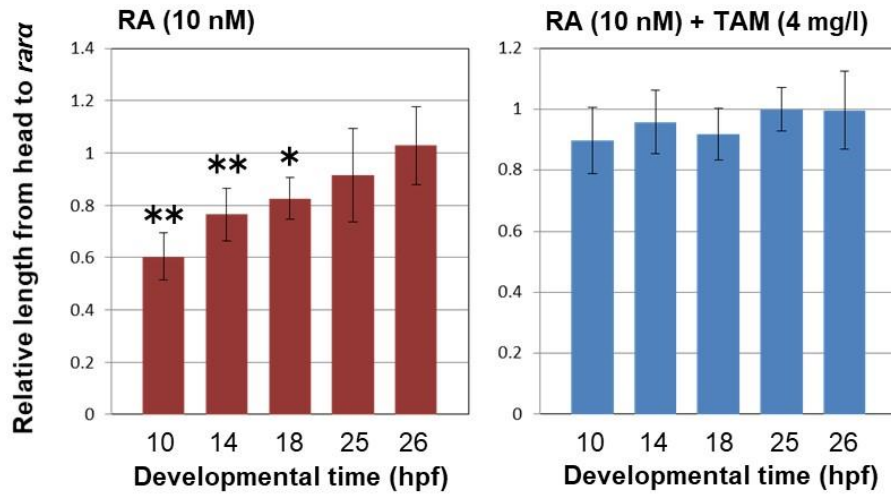
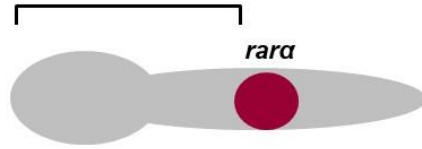


Figure 20. Effect of antiestrogen on *rara* expression during gastrula stage.

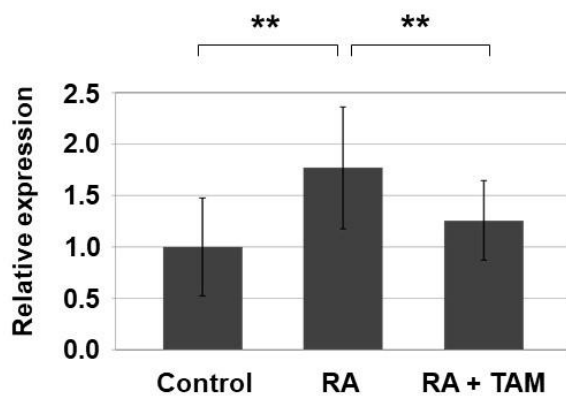
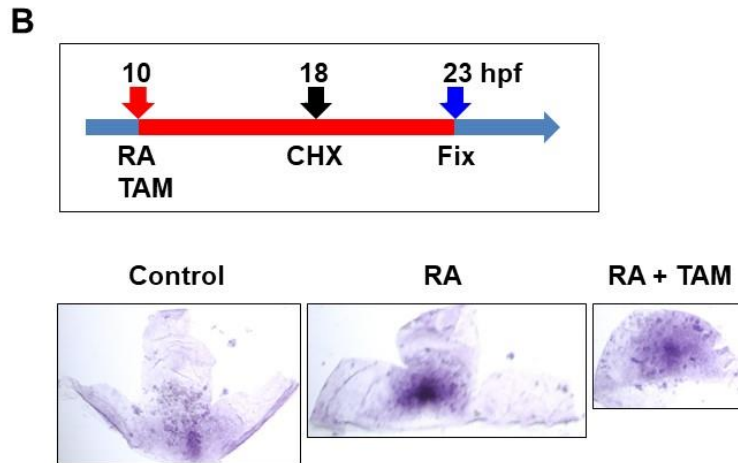
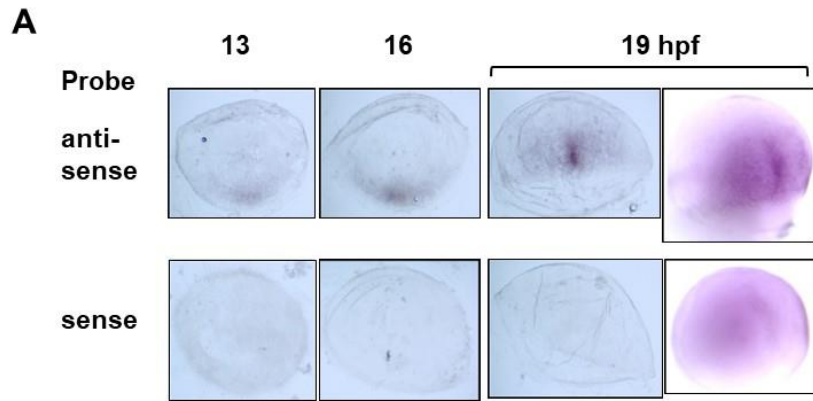


Figure 20. (continued)

C

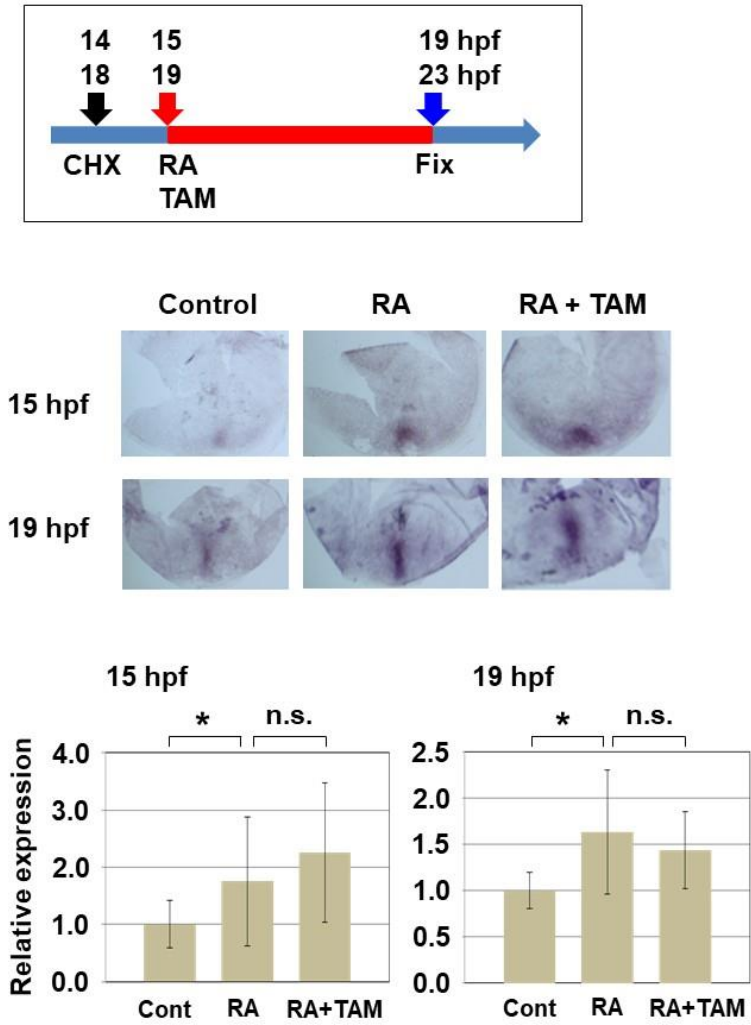
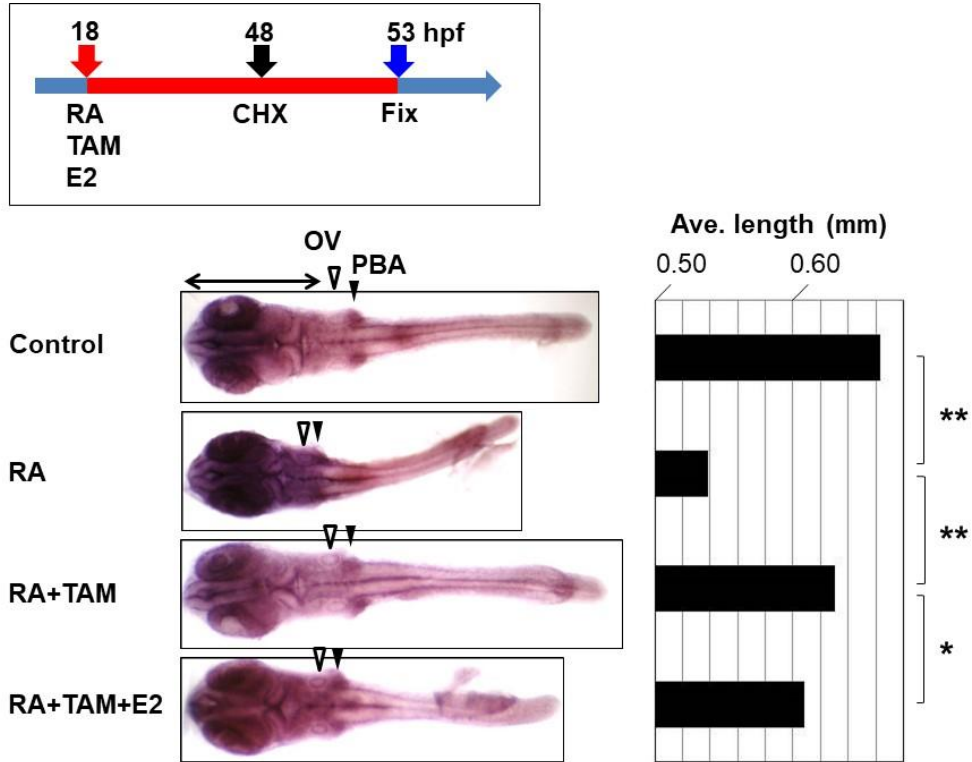


Figure 21. Effect of antiestrogen on *ahr1* expression.



**Figure 22. Effect of antiestrogen, ER $\alpha$ -KD, and RA on FGF signaling.**

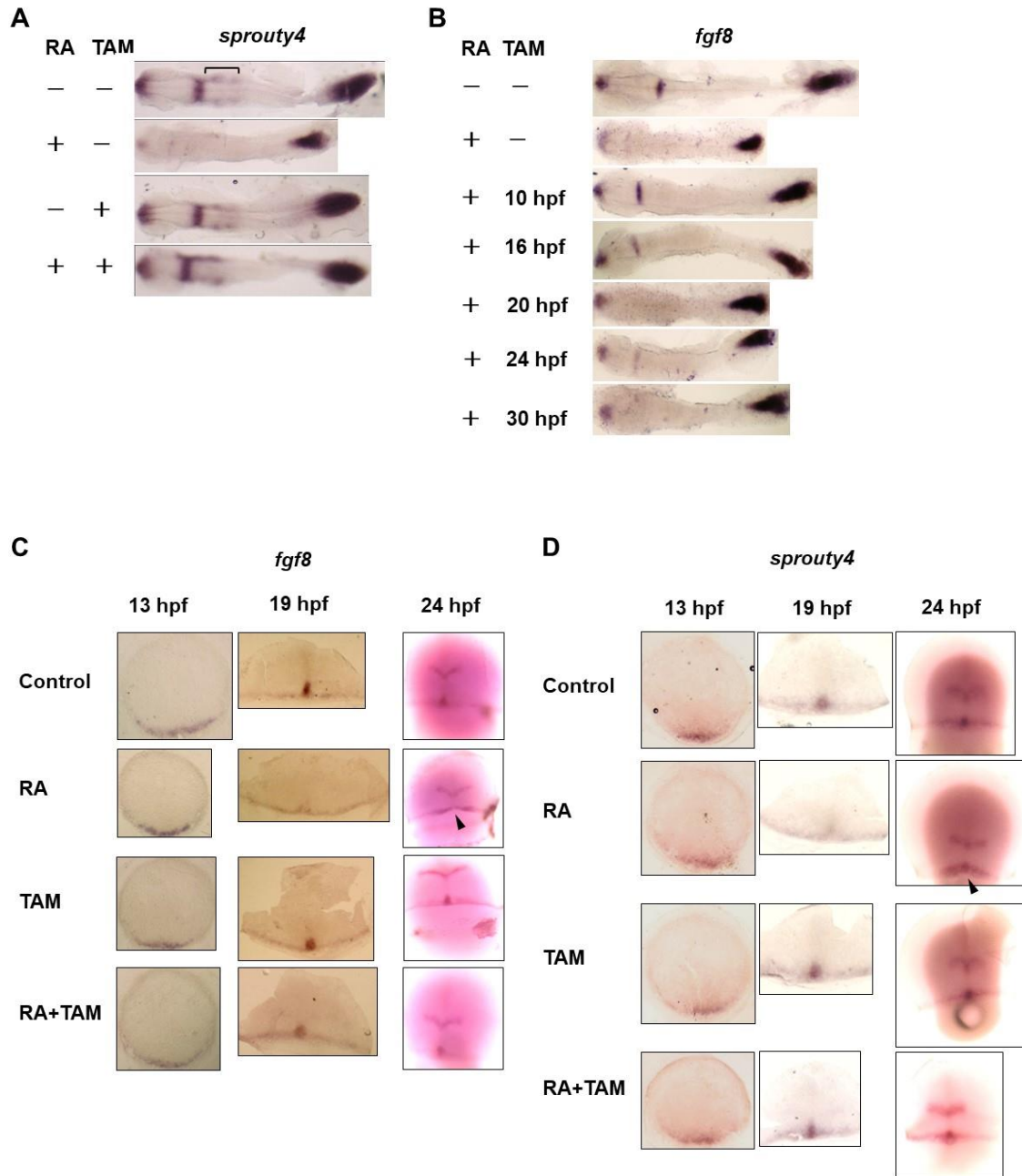


Figure 22. (continued)

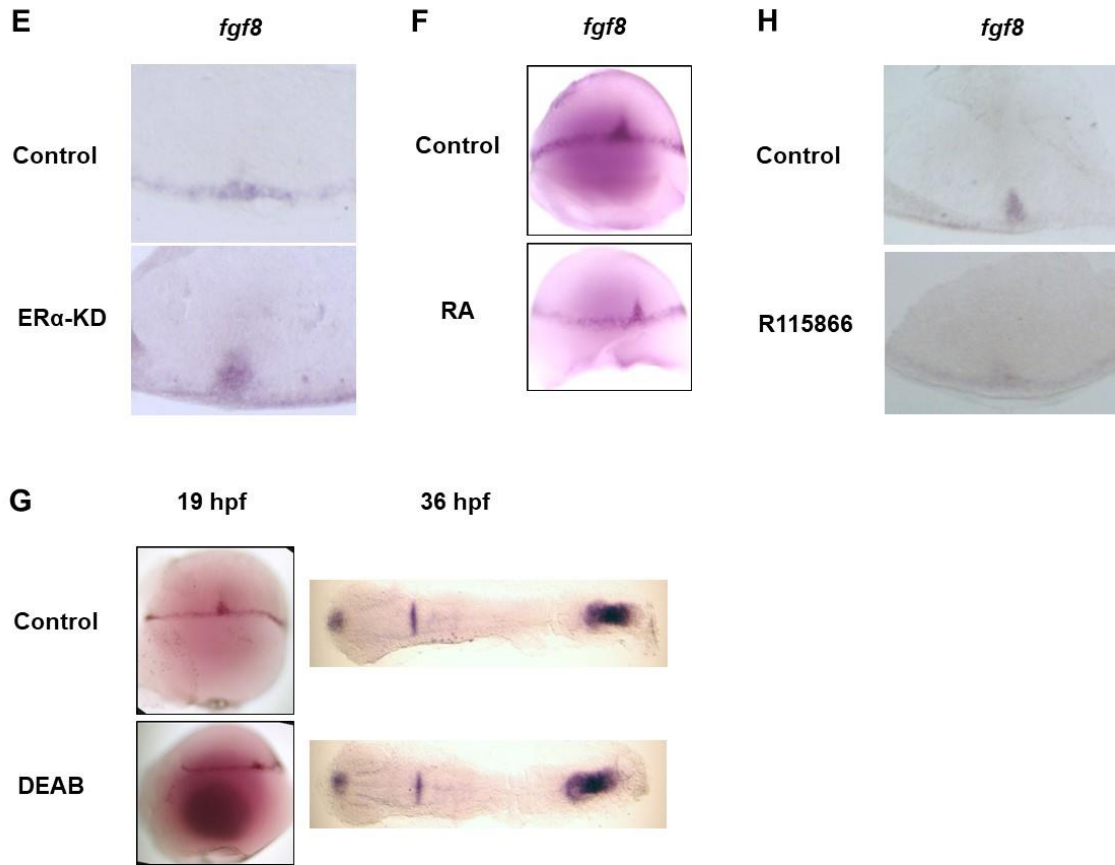


Figure 23. Effect of antiestrogen on vascular formation.

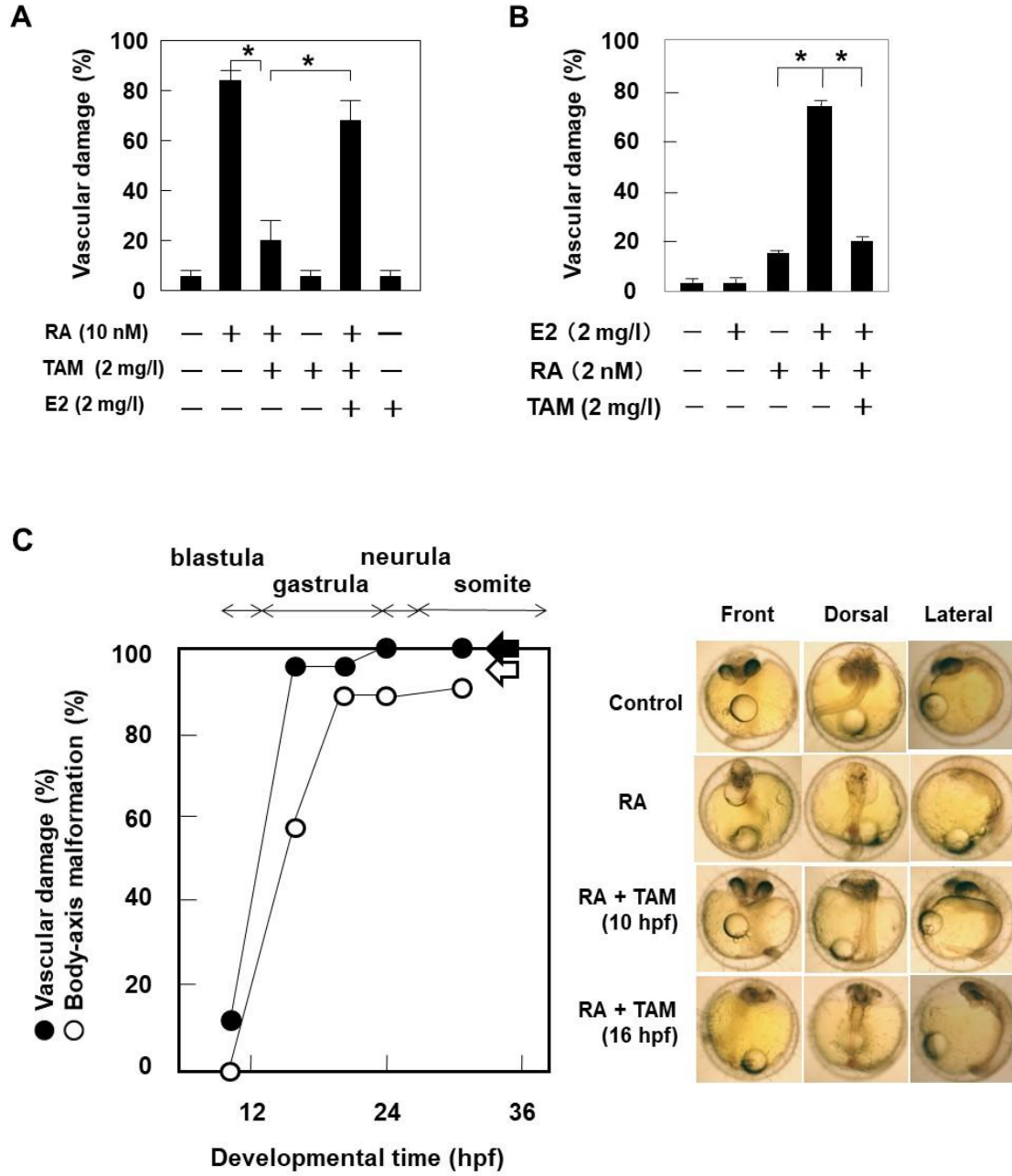


Figure 24. Synergistic inhibition of vascular formation by TAM and DEAB.

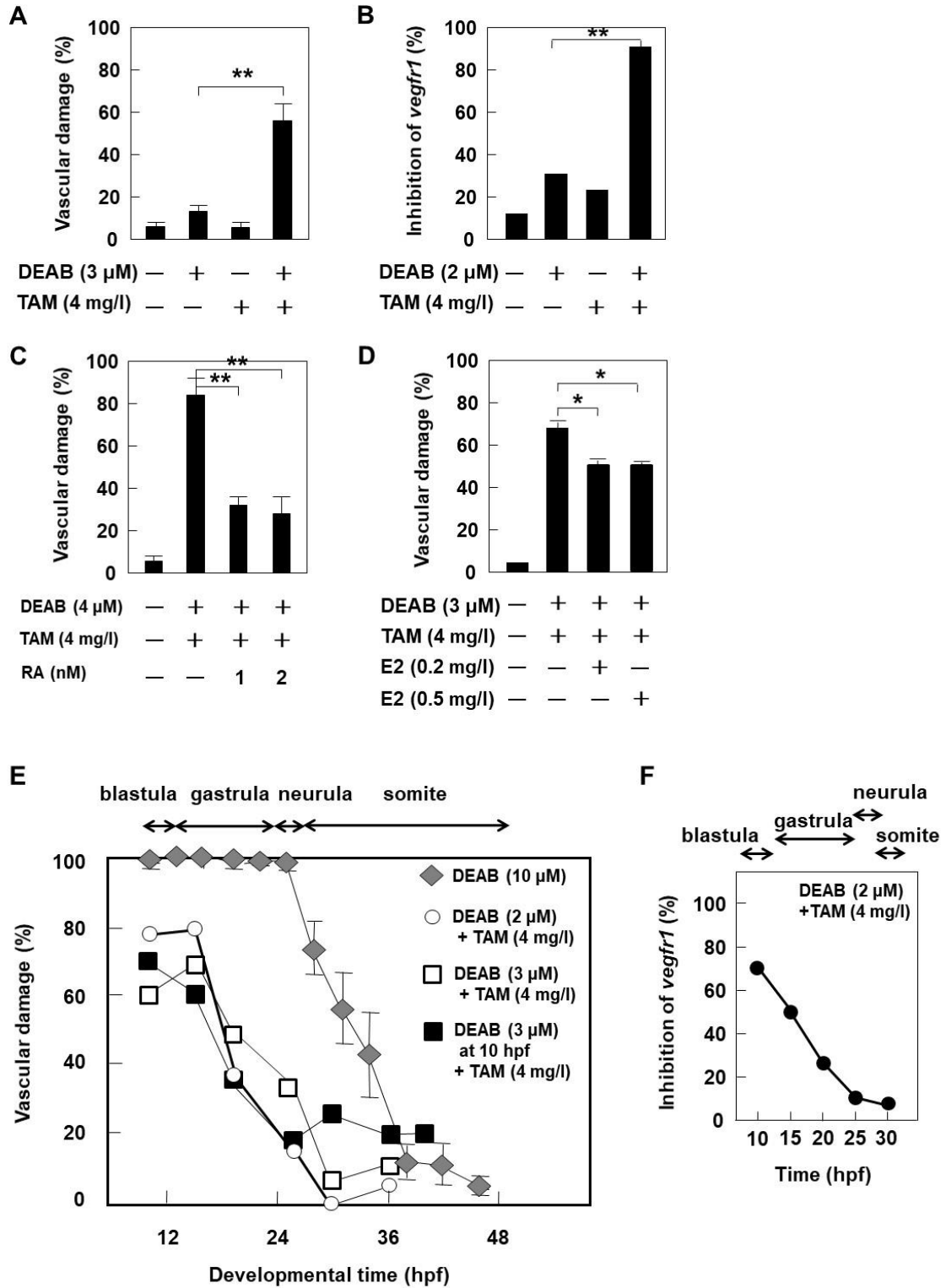


Figure 25. Control of *ahr1* transcript levels by RA and maternal estrogen.

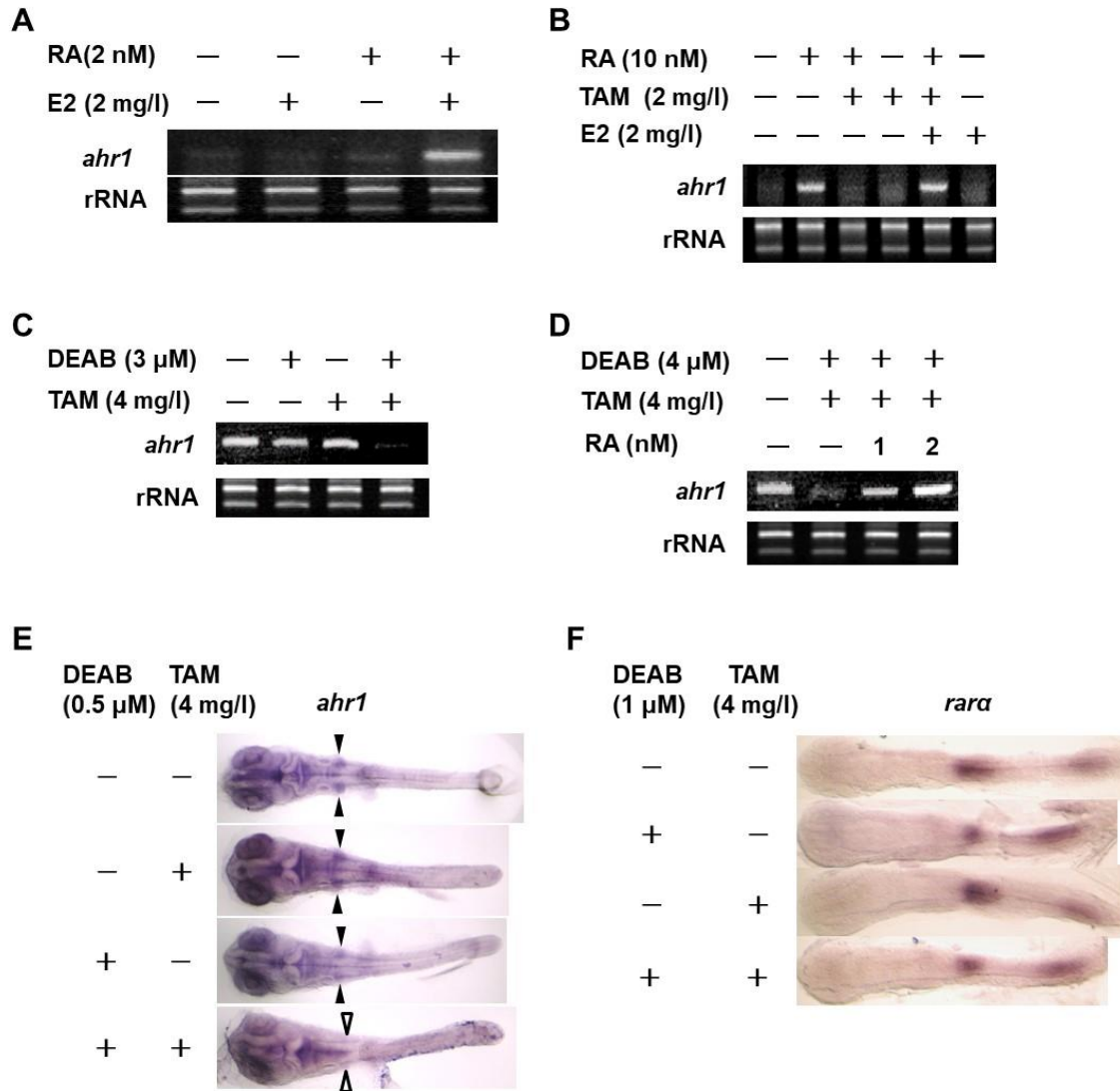


Figure 26. ER $\alpha$  is essential for *ahr1* expression and vascular formation.

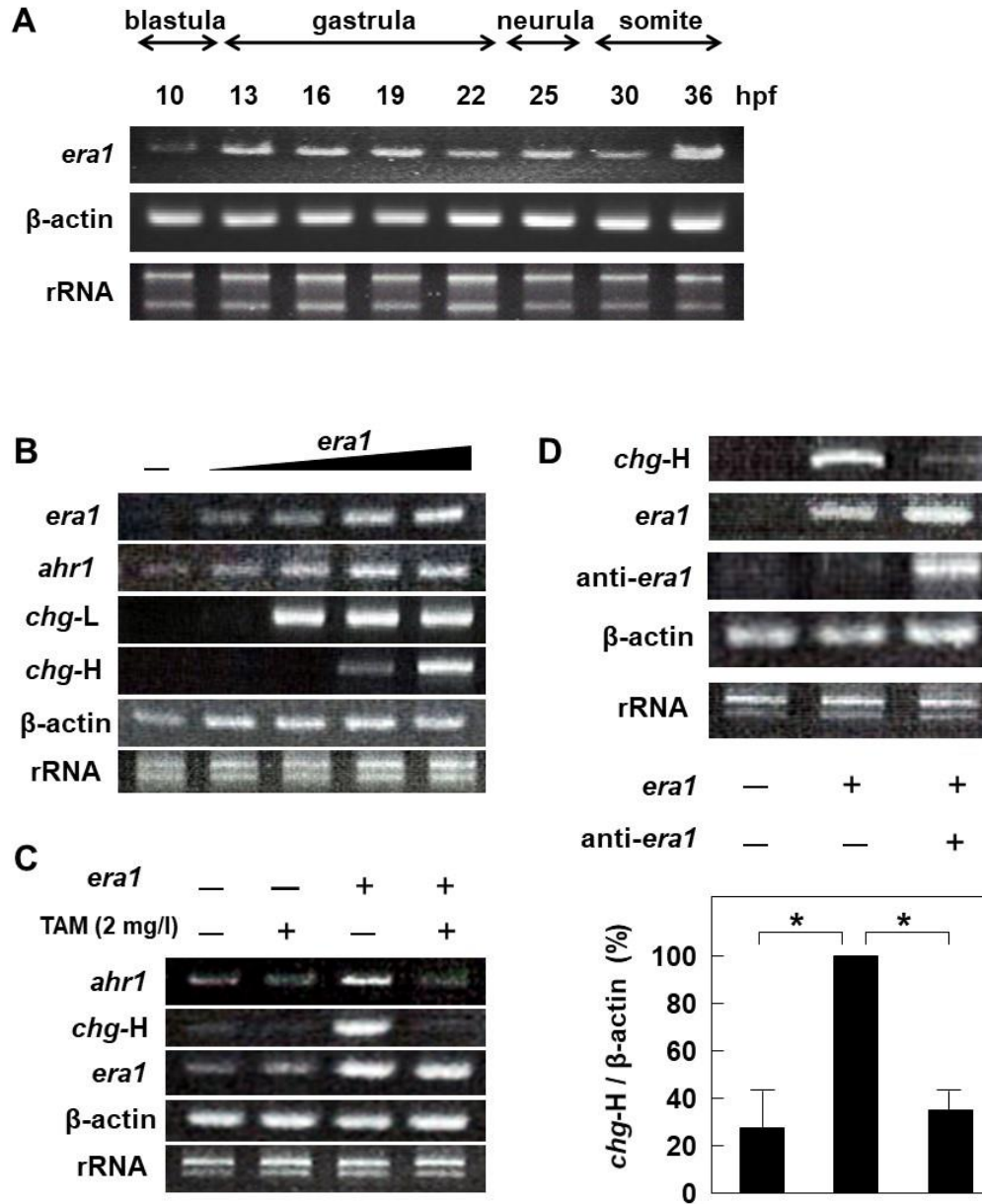


Figure 26. (continued)

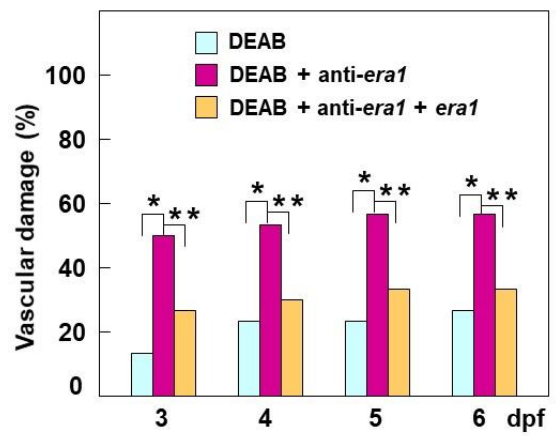
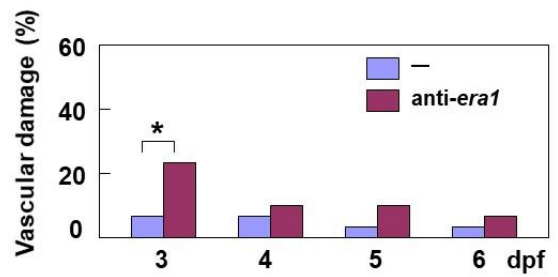
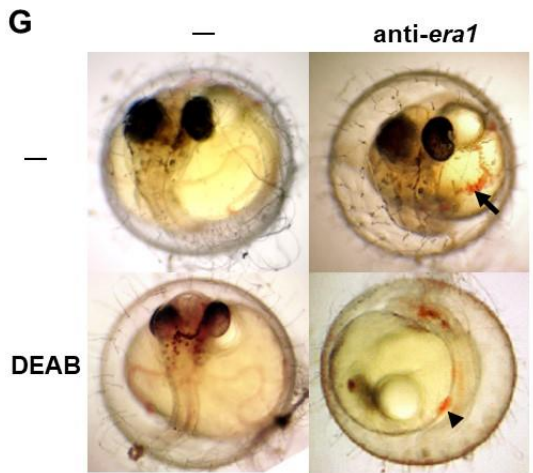
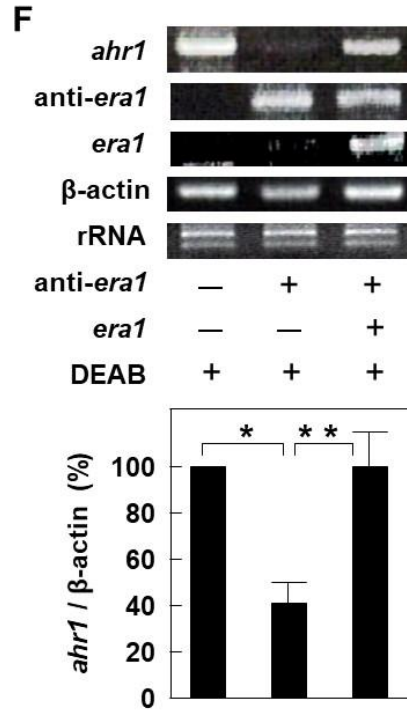
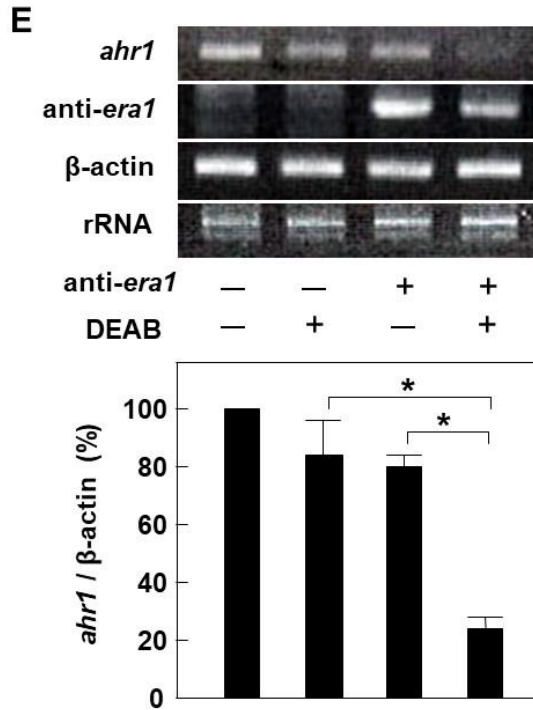
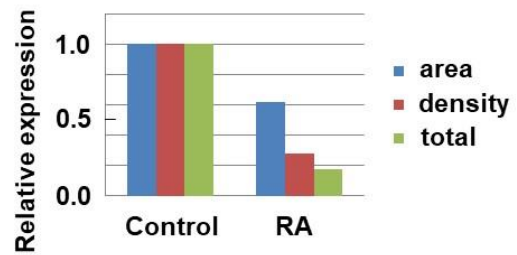
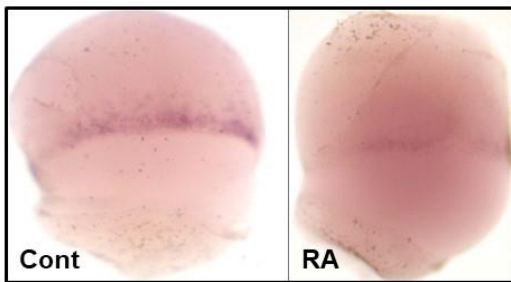
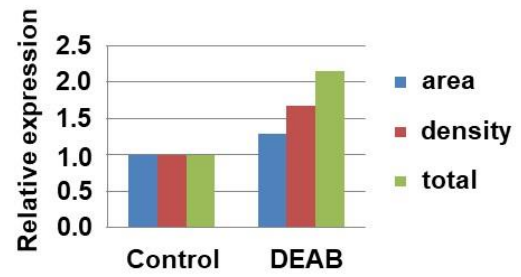
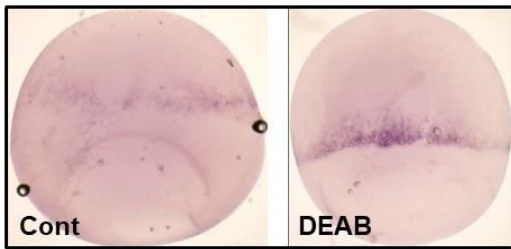
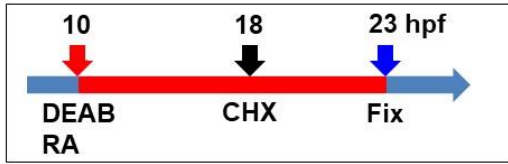


Figure 27. Control of *raldh2* expression by RA and maternal estrogen.

A



B

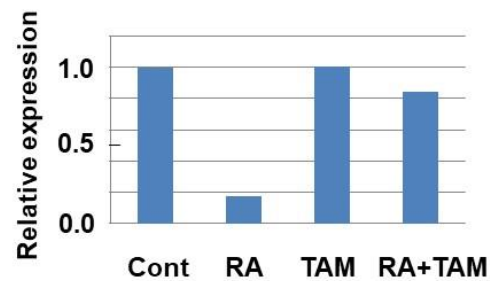
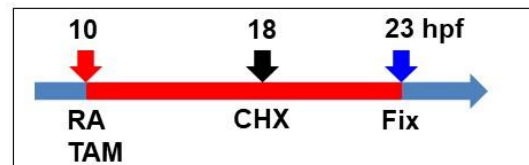
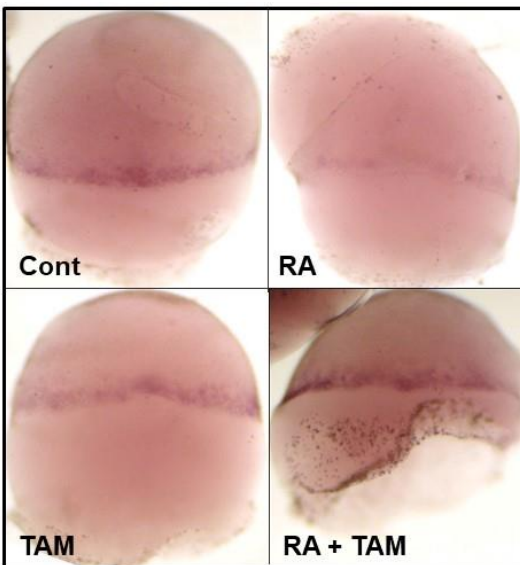


Figure 27. (continued)

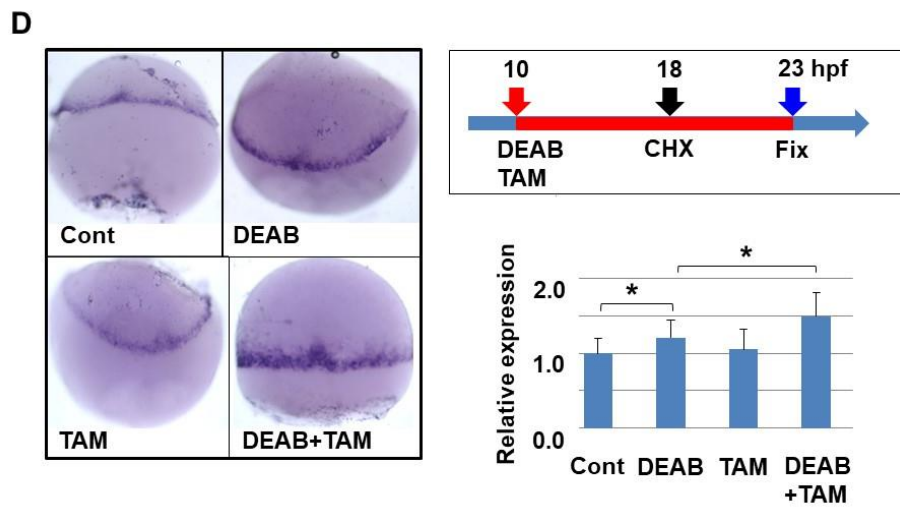
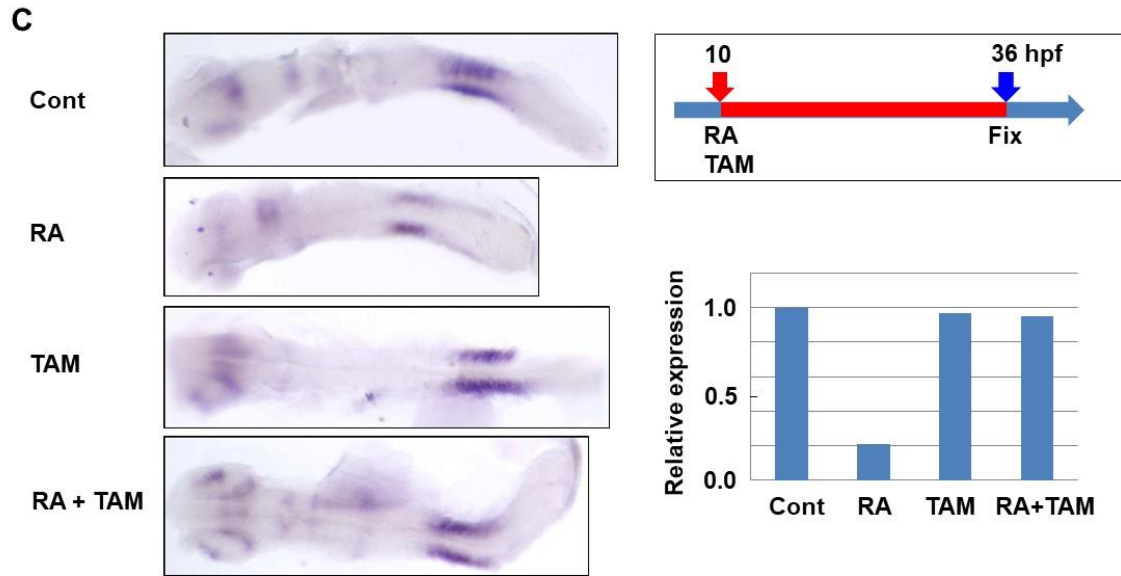
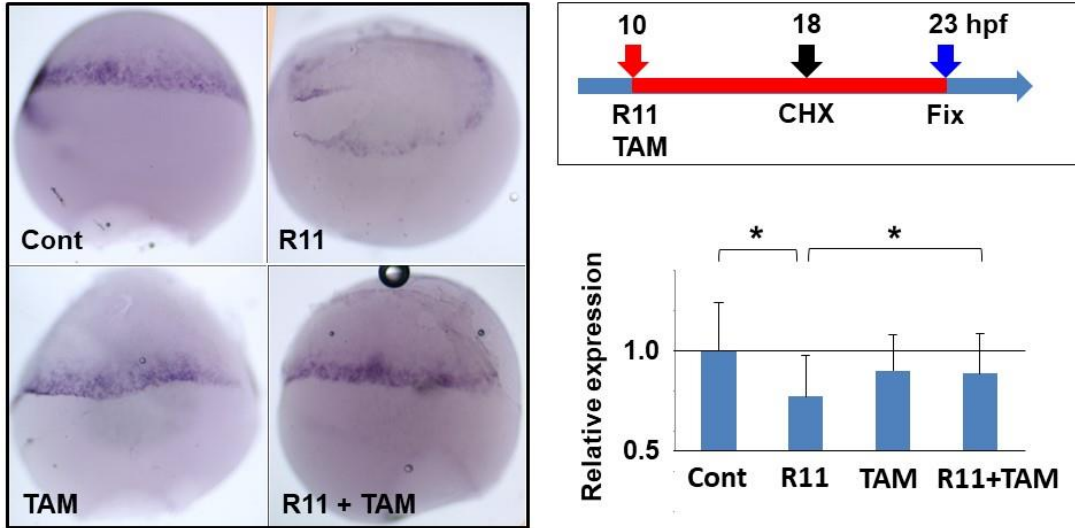


Figure 27. (continued)

E



F

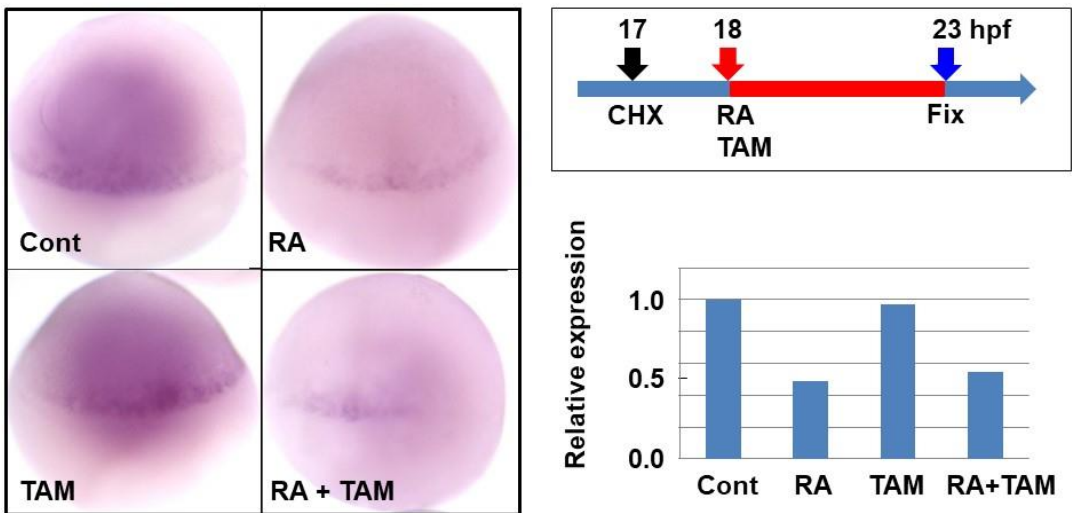
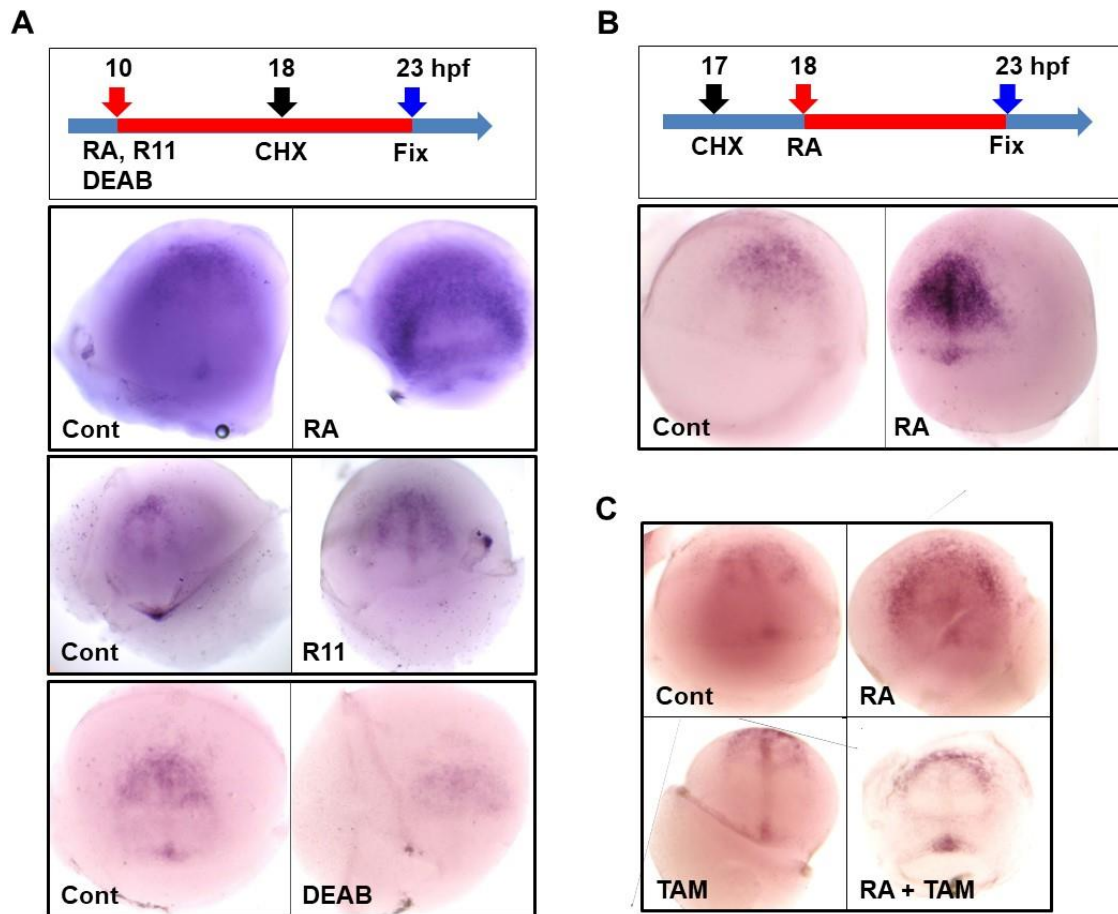
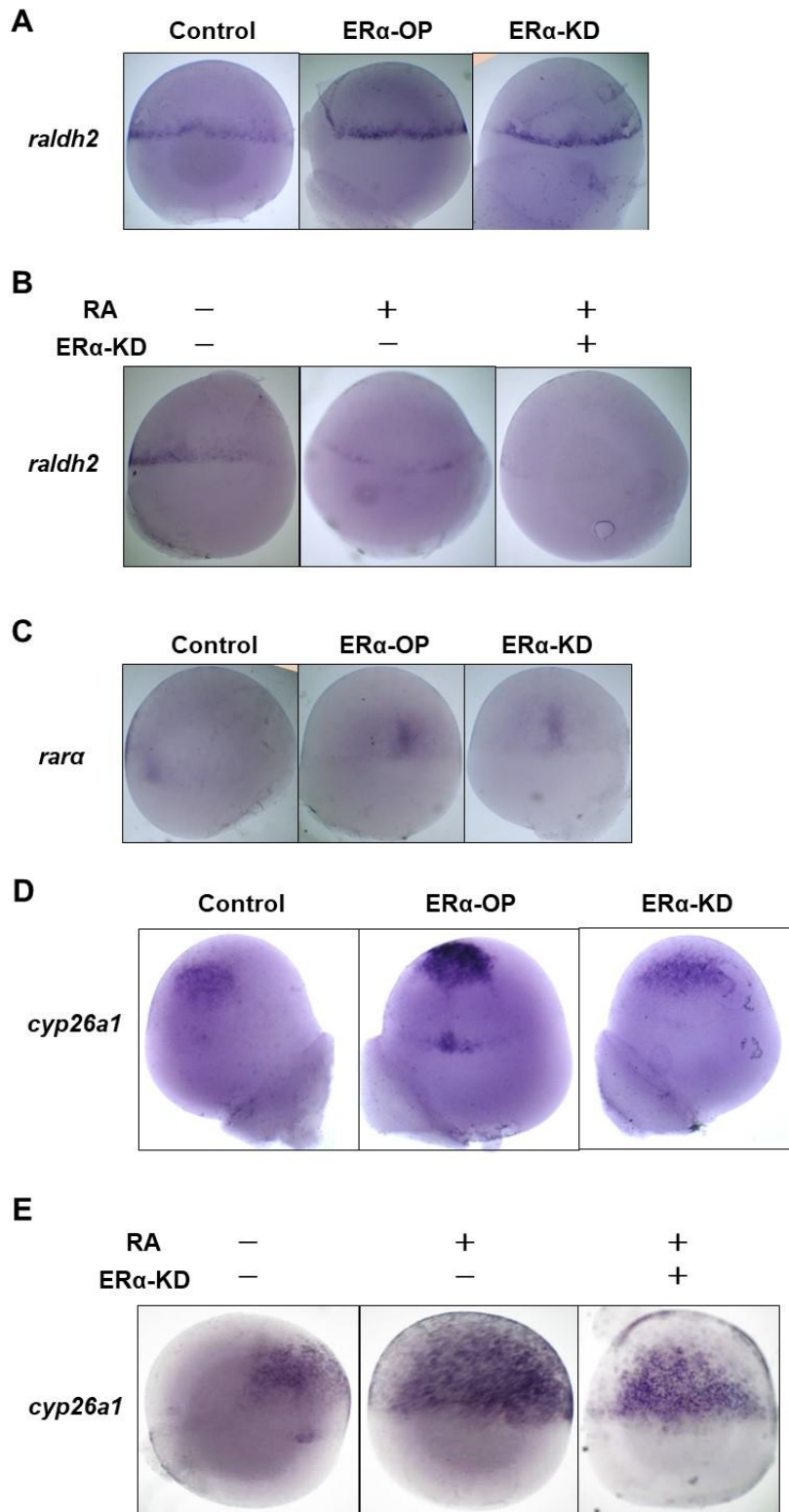


Figure 28. Control of *cyp26a1* expression by RA and maternal estrogen.



**Figure 29. Effects of overproduction and knockdown of ER $\alpha$  on expressions of *raldh2*, *rara*, and *cyp26a1*.**



**Figure 30. TAM advances RA-excess phenotypes.**

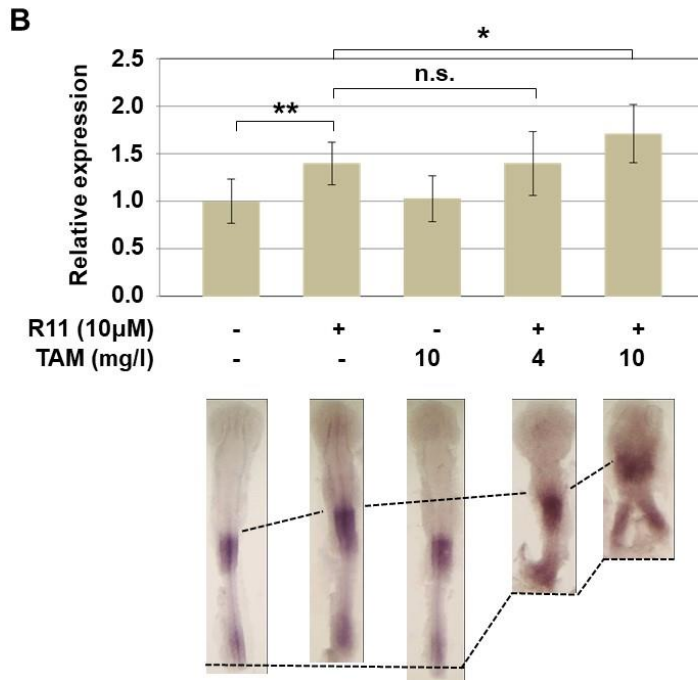
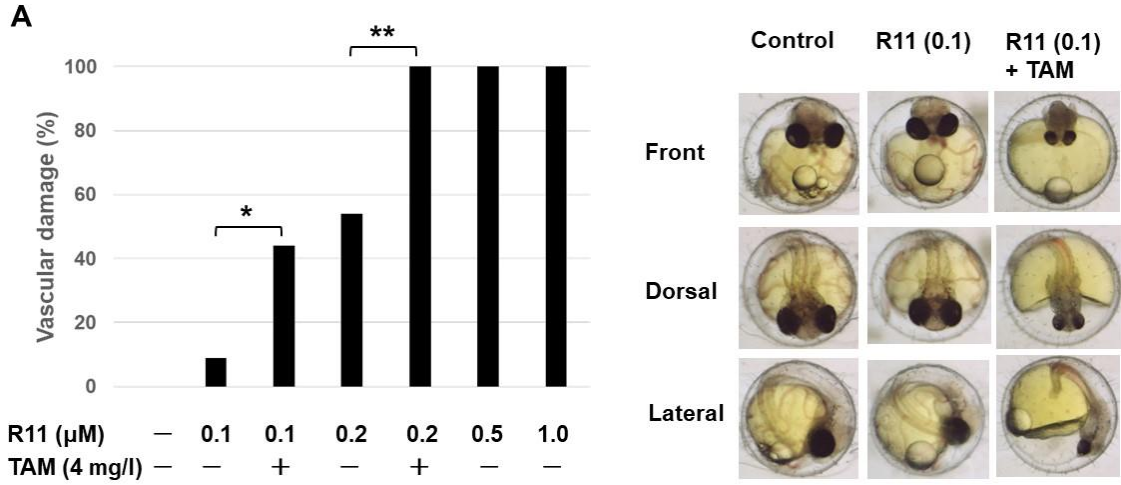


Figure 30. (continued)

